Physics – Uspekhi **49** (9) 905 – 936 (2006) ©2006 Uspekhi Fizicheskikh Nauk, Russian Academy of Sciences

REVIEWS OF TOPICAL PROBLEMS PACS numbers: 1**2.60. – i**, **13.15. + g**, 95.55.Vj, 95.85.Ry, 96.50.S –

Ultrahigh-energy neutrinos from astrophysical sources and superheavy particle decays

V A Ryabov

DOI: 10.1070/PU2006v049n09ABEH006052

Contents

Abstract. **Problems in the fields of neutrino astronomy and ultrahigh-energy astrophysics are reviewed. Neutrino fluxes produced in various astrophysical sources (*bottom-up* acceleration scenarios) and resulting from the decay of superheavy particles (*top-down* scenarios) are considered. Neutrino oscillation processes and the absorption and regeneration of neutrinos inside the earth are analyzed and some other factors affecting the intensity and flavor composition of astrophysical neutrino fluxes are discussed. Details of ultrahigh-energy neutrino interactions are discussed within the Standard Model, as well as using nonstandard scenarios predicting an anomalous increase in the inelastic neutrino – nucleon cross section. Ultrahigh-energy neutrino detection techniques currently in use in new-generation neutrino telescopes and cosmic ray detectors are also discussed.**

V A Ryabov Lebedev Physical Institute, Russian Academy of Sciences, Leninskii prosp. 53, 117924 Moscow, Russian Federation
Tel. (7-495) 135 24 52. Fax (7-495) 135 87 18
E-mail: ryabov@x4u.lebedev.ru; ryabov@fnal.gov

Received 25 January 2006, revised 30 March 2006
Uspekhi Fizicheskikh Nauk **176** (9) 931 – 963 (2006)
Translated by D B Pontekorvo; edited by A M Semikhatov

1. Introduction

For many years, the nature of cosmic rays (CRs) has remained one of the main open issues in astrophysics, while the uncertainty of their origin increases with their energy [1 – 3]. The neutrino is regarded as one of the possible candidates for the primary particle, which might have produced CR interaction events in Earth's atmosphere, involving ultrahigh-energy cosmic rays (UHECRs). This assumption pertains to the sort of hypotheses that, according to H Poincare's expression, "are introduced unconsciously, accepted tacitly, and for this reason we cannot get rid of them" [4].

There exist serious grounds for assuming the existence of various astrophysical and cosmological sources of neutrinos, although neutrinos of astrophysical origins have hitherto been registered only from two sources: the sun and the supernova SN 1987A. All other registered neutrinos are produced artificially (fluxes from nuclear reactors and beams, formed at proton accelerators), are products of primary CR interactions in the Earth's atmosphere, or are produced in the decays of radioactive elements.

On the whole, several dozen UHECR shower events have been registered in the Haverah Park [5], SUGAR [6], AGASA [8, 9], Fly's Eye [10] and HiRes [11, 12] experiments at energies

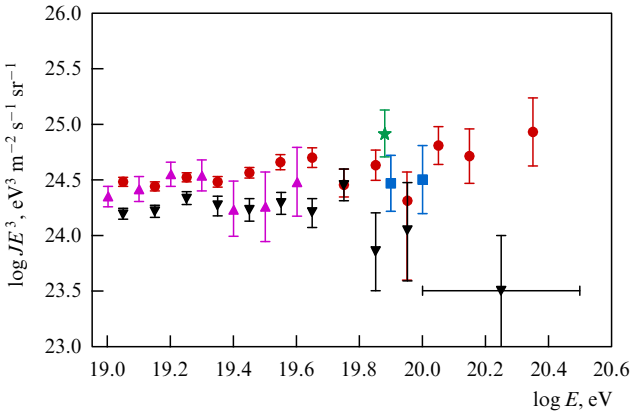

Figure 1. Ultrahigh-energy CR flux, measured in experiments: ★ — Haverah Park [5], ■ — SUGAR [6], ● — AGASA [8, 9], ▲— Fly's Eye (stereo) [10], ▼ — HiRes [11, 12].

$E_{\rm CR} > 5 \times 10^{19}$ eV (Fig. 1). In several of these, the reconstructed energy exceeded 10^{20} eV, which corresponds to an energy in the center-of-mass system $\sqrt{s} = \sqrt{2 m_{\rm N} E_{\rm CR}} \geqslant$ 800 TeV, where $m_{\rm N}$ is the nucleon mass. Interest in the particles that produced showers of such grandeur in the atmosphere is not restricted to the desire to reveal the sources at which they were produced, or the processes in which they were accelerated to such high energies. Their origin may be directly related to manifestations of new physics at an energy scale essentially exceeding the energies of modern accelerators.

From the traditional standpoint of physics, neither hadrons, nor photons, nor leptons (with the exception of neutrinos) could reach Earth with energies $E_{\rm CR} \geqslant 7 \times 10^{19}$ eV. This is not only related to the problem of generating particles of such high energies in an astrophysical source. The main complication consists in the particle retaining such energy in traveling through distances of a cosmological scale from the source where it was produced to Earth. With the exception of neutrinos, all other known elementary particles have sufficiently large interaction cross sections with the photon background at energies $E_{\rm CR} \geqslant 7 \times 10^{19}$ eV to lose a significant part of their energy on their way from extragalactic sources situated at distances $D \sim 30 - 50$ Mpc.

The propagation of protons of ultrahigh energies is restricted by pion photoproduction processes in the microwave background. This is the well-known Greisen – Zatsepin – Kuzmin (GZK) effect, which results in a cutoff of the primary CR spectrum [13,14]. Protons of energies above the Δ^*-resonance production threshold lose energy in each reaction

$$\mathrm{p} + \gamma_{\rm CMB} \to \Delta^* \to \mathrm{p} + \pi\,. \tag{1.1}$$

If Lorentz invariance is not violated, then the GZK-cutoff physics is indisputable: the threshold interaction energy of a proton with a photon from the microwave background in the 'laboratory' system is given by

$$E_{\rm p}^{\rm th} = \frac{m_\pi m_{\rm p}}{2\varepsilon_{\rm CMB}} \approx \frac{7 \times 10^{19}\ \text{eV}}{\varepsilon_{\rm CMB}/1\ \text{eV}}\,, \tag{1.2}$$

where $\varepsilon_{\rm CMB} = \varepsilon_{2.7\rm K} \approx 10^{-3}$ eV is the energy of the relic microwave photon. The proton interaction length $L_{\rm int}$ in reaction (1.1) can be estimated from the pion photoproduction cross section at energies close to the Δ^*-resonance production threshold ($\sigma(\mathrm{p}\gamma) \approx 135$ μb) and the relic photon density ($\rho = 410$ cm^{-3}):

$$L_{\rm int}(\mathrm{p} + \gamma_{\rm CMB} \to \Delta^* \to \mathrm{p} + \pi) = \big(\sigma(\mathrm{p}\gamma)\,\rho\big)^{-1} \approx 1.8 \times 10^{25}\ \text{cm} \approx 6\ \text{Mpc}. \tag{1.3}$$

At distances D, protons lose the energy $E_{\rm p} \propto E_0 \exp(-D/L_{\rm int})$ (Fig. 2) [15]. The microwave radiation spectrum is described by the Planck distribution with the temperature $T = (1 + z) \times 2.73$ K, where z is the redshift of the source. Protons of energies $E_{\rm p} \geqslant 10^{20}$ eV interact with nearly all background photons, while protons of lower energies only with photons at the end of the Planck spectrum. In the range of energies $5 \times 10^{19} \leqslant E_{\rm p} \leqslant 3 \times 10^{20}$ eV, the proton interaction length decreases rapidly (Fig. 2).

There exist no sources within the limits of our galaxy at distances ~ 10 kpc that are capable of generating particles with energies above the GZK-cutoff of the CR spectrum. Nor have such sources been observed on greater scales ($D \leqslant 50$ Mpc), although the possibility of their existence cannot be excluded in principle [16,17]. Most known sources, such as gamma-ray bursts (GRBs) or active galactic nuclei (AGNs), in which the acceleration of protons up to energies $E_{\rm GZK} \geqslant 7 \times 10^{19}$ eV is theoretically possible, are at distances $D \geqslant 100$ Mpc from Earth [18]. If events with energies $E_{\rm CR} \geqslant 10^{20}$ eV are registered by detectors on Earth, then the primary proton energy inside a source at such a distance should be at least 2 orders of magnitude greater than the registered energy.

The universe is also opaque to photons of energies above 10 TeV. Reactions of electron pair production due to the interaction of a photon of energy E_γ with a background photon of energy $\varepsilon_{\rm BG}$,

$$\gamma + \gamma_{\rm BG} \to \mathrm{e}^+ + \mathrm{e}^-\,, \tag{1.4}$$

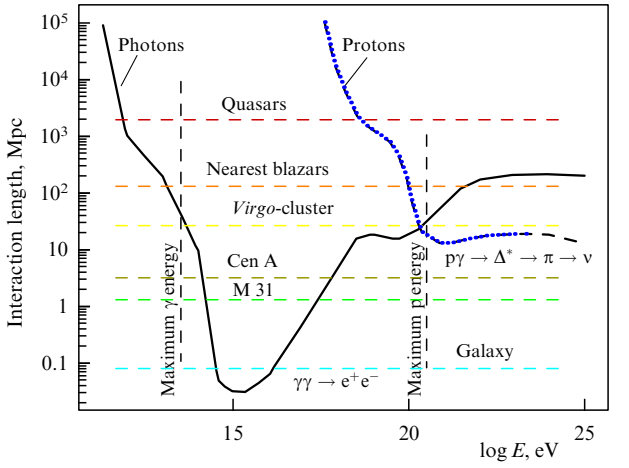

Figure 2. Interaction lengths of high-energy protons, $L_{\rm int}(\mathrm{p} + \gamma_{\rm CMB} \to \Delta^* \to \mathrm{p} + \pi)$, and of γ-quanta, $L_{\rm int}(\gamma + \gamma_{\rm IRB} \to \mathrm{e}^+ + \mathrm{e}^-)$, with microwave and infrared photon backgrounds, respectively [15]. The vertical lines show the maximum proton and γ-quantum energies observed on Earth. The horizontal lines (from top down) correspond to distances from the closest quasars, blasars, the Virgo-cluster, and the Cen A and M31 galaxies, as well as to the dimensions of our galaxy.

have the threshold

$$E_\gamma^{\rm th} \approx \frac{m_e^2}{\varepsilon_{\rm BG}}\,, \qquad (1.5)$$

where $m_e = 0.511$ MeV s^{-2} is the electron mass. Hence, it follows that photons of TeV energies are absorbed by the infrared background, of PeV energies by the microwave background, and of EeV energies by the radiobackground. The interaction length of a photon of energy $E_\gamma \approx 10$ TeV is $L_{\rm int}\,(\gamma + \gamma_{\rm BG} \to e^+ + e^-) \leqslant 100$ Mpc (see Fig. 2) and, consequently, photons from sources at cosmological distances, emitted with energies above 10 TeV, cannot reach Earth. Therefore, together with the UHECR observation, the observation of photons from the blazar Markarian 501 with energies above 20 TeV represents one more astrophysical paradox [19].

Evidently, the electron cannot serve as the particle causing the observed showers with energies above the GZK-cutoff of the CR spectrum either, since its energy losses during its propagation through the universe are great. Moreover, an electromagnetic cascade rapidly loses its energy owing to synchrotron radiation during its propagation in intergalactic magnetic fields.

At present, the only particle known to be capable of covering cosmological distances with virtually no absorption is the neutrino. The interaction lengths of neutrinos with TeV energies amount to 2.5×10^{11} g cm^{-2}; photons with the same energy cover distances of only about several hundred g cm^{-2}. In the case of neutrinos propagating in the universe, the background of relic neutrinos is essentially more important than the photon background. The UHECR formation mechanism, due to annihilation of high-energy neutrinos in the relic neutrino background, termed a 'Z-burst' [20, 21], assumes that the resonance production of the Z^0-boson occurs with its subsequent hadron decay. Characteristic neutrino energies in the region of the Z^0-resonance are

$$E_\nu \approx \frac{M_Z^2}{2\varepsilon_\nu} \approx 4.2 \times 10^{21}\ {\rm eV}\ \frac{\rm eV}{\varepsilon_\nu}\,, \qquad (1.6)$$

where ε_ν is the energy of relic neutrinos. The Z^0-boson decay products may contribute to the observed CR spectrum at energies $E_{\rm GZK} \geqslant 7 \times 10^{19}$ eV. Within the Z-burst scenario, any astrophysical objects generating neutrino fluxes with energies sufficient for the Z^0-boson production can serve as neutrino sources. The attractiveness of the Z-burst mechanism for the explanation of UHECR consists in the fact that the weak absorption of neutrinos provides the possibility of having a neutrino source situated as far away as desired, while the Z^0-boson may decay as close to Earth as necessary. On the other hand, to explain the observed flux of UHECR events in the framework of the Z-burst mechanism, gigantic neutrino fluxes emitted from the source are necessary.

Existing models of the formation of ultrahigh-energy neutrino fluxes are divided into *bottom-up* and *top-down* scenarios (Fig. 3). In astrophysics, the various mechanisms of particle acceleration from low to ultrahigh energies have been attributed the common term of 'bottom-up' mechanisms [22, 23]. The source of the acceleration process in such scenarios is the strong electromagnetic fields present in the vicinity of compact objects such as magnetized neutron stars or accretion disks of black holes. The particles receive higher energies in systems where shock waves are generated, which

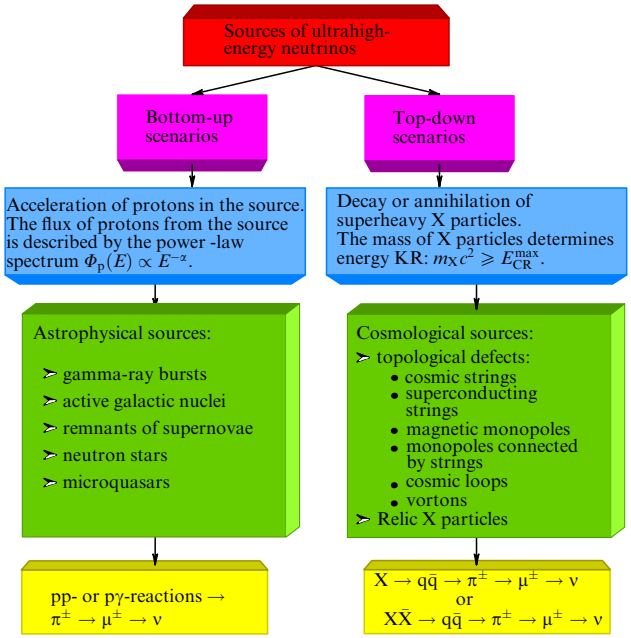

Figure 3. Scenarios for the production of ultrahigh-energy neutrinos.

propagate through the clouds of magnetized plasma. Pulsars, supernova remnants [24], and the most powerful sources of radiation in the universe, GRBs [25] and AGNs [26], may serve as such 'cosmic accelerators.' While protons in such systems can be accelerated up to energies above 10^{20} eV, pp- and pγ-interactions lead to the production of charged and neutral pions, whose decays result in neutrino and γ-quantum fluxes with the respective energies $E_\nu \leqslant 10^{19}$ eV and $E_\gamma \leqslant 10$ TeV [27].

An alternative to the acceleration mechanism of ultrahigh-energy particle production are 'top-down' scenarios, in which no acceleration mechanisms are required. These scenarios assume the existence of very heavy metastable particles of mass $m_X > 10^{21}$ eV that originated at the early stages of development of the universe and may be part of its 'dark matter.' The top-down mechanism implies physics beyond the Standard Model (SM) of elementary particles and their interactions. There are two ways of producing supermassive particles. The first is connected to nonthermal phase transitions in the early universe leading to the formation of topological defects (TDs): cosmic strings [28], superconducting strings [29], magnetic monopoles [30], monopoles connected to strings [31], cosmic loops [32], vortons [33], and bound monopole–antimonopole states [34]. The other possibility consists in the gravitational production of supermassive quasistable particles, first proposed by Zel'dovich and Starobinsky [35]. The production of such X particles, having survived until the present day, could be due to vacuum fluctuations at the inflation stage of the early universe [36, 37]. The decays and/or annihilations of X particles result in the production of the charged and neutral high-energy pions whose decays yield neutrino and γ-quantum fluxes. The specific characteristics of any of the top-down scenarios depend on the mass of the X particle m_X and on the cosmological time t characterizing the moment of their production [38].

The flavor composition of neutrino fluxes from the source in which the neutrinos are produced as a result of

pp- and pγ-interactions is independent of the type of the source itself. In these interactions, approximately equal amounts of π^+, π^0, and π^- are produced, which then decay into $\mu^+\nu_\mu$, $\gamma\gamma$, and $\mu^-\nu_\mu$, respectively. The further $\mu^- \to e^-\nu_\mu\bar{\nu}_e$ decay adds two more neutrinos for each pion decay. Thus, the initial mixture of pions $\pi^+ + \pi^0 + \pi^-$ becomes a mixture of photons and neutrinos with the relative compositions $2\gamma + 2\nu_\mu + 2\bar{\nu}_\mu + 1\nu_e + 1\bar{\nu}_e$. The resulting flavor composition of neutrino fluxes normalized to unity is given by

$$\Phi^0(\nu_e) : \Phi^0(\nu_\mu) : \Phi^0(\nu_\tau) = 1 : 2 : 0\,. \tag{1.7}$$

This relation between the fluxes is modified owing to neutrino oscillations. Along the way from the source to the detector, the neutrinos cover cosmological distances $L \approx 100-1000$ Mpc, which are much greater than the length of vacuum oscillations $L_{\rm osc} = 4\pi E_\nu/\Delta m_\nu^2$ and, consequently, they oscillate many times. The neutrino fluxes of flavor i, registered in the detector, are determined by the elements of the neutrino mixing matrix $|U_{\alpha i}|$:

$$\Phi^{\rm det}(\nu_i) = \sum_\alpha \Phi^0(\nu_\alpha)|U_{\alpha i}|^2\,. \tag{1.8}$$

For mixing matrices of different types with $|U_{e3}|^2 \ll 1$ and $|U_{\mu 3}| \approx |U_{\tau 3}|$, in agreement with the results of experimental studies of oscillations, the composition of astrophysical neutrino fluxes on the earth, at a distance $L \gg L_{\rm osc}$ from the source, is uniform with respect to flavors [39, 40]:

$$\Phi^{\rm det}(\nu_e) : \Phi^{\rm det}(\nu_\mu) : \Phi^{\rm det}(\nu_\tau) = 1 : 1 : 1\,. \tag{1.9}$$

The observation in detectors of such a flavor composition (or possibly differing from it) will provide a test of the neutrino oscillation scenarios and of various neutrino mass generation schemes. Because neutrinos can be observed arriving from sources beyond the boundaries of the observable universe, the level of sensitivity to oscillation parameters in experiments with astrophysical neutrinos may significantly exceed the limits obtained in experiments with solar, atmospheric, and acceleration neutrinos [41, 42].

The astronomy of cosmic ultrahigh-energy neutrinos (UHENs) occupies a unique place in modern science — at the meeting point of high-energy astrophysics and particle physics. On the one hand, measurements of UHEN spectra are especially important for determining the limit energies arising both in acceleration processes within superpowerful 'cosmic accelerators,' such as GRB or AGN, and in the decays of hypothetical supermassive particles. On the other hand, UHENs represent a natural laboratory for studying the interactions between elementary particles at energies exceeding those of the existing or even of planned accelerators. The interactions of cosmic neutrinos of energies $E_\nu \approx 10^{17}$ eV permit investigating processes of deep-inelastic νN scattering at equivalent energies in the center-of-mass system

$$\sqrt{s_{\nu N}} = \sqrt{2m_N E_\nu} \approx 14\left(\frac{E_\nu}{10^{17}\ {\rm eV}}\right)^{1/2}\ {\rm TeV}\,, \tag{1.10}$$

which are comparable to the expected energy in pp-interactions at the LHC collider, $\sqrt{s_{\rm pp}} \approx 14$ TeV.

The deep-inelastic νN-reaction cross sections have been measured at the FNAL accelerator up to maximum energies $E_\nu \approx 400$ GeV in the NuTeV experiment [43]. For estimation of the cross sections at higher energies, one must use calculations requiring the knowledge of the parton distribution functions (PDFs) depending on the squared transferred momentum Q^2 and of the Bjorken variable x. The higher the energy of the neutrino interacting with a nucleus, the more important role is played by contributions to the νN cross section corresponding to smaller and smaller x values. At present, record measurements of the PDF down to $x \sim 10^{-5}$ for the values $Q_0^2 \approx 1$ GeV^2 have been performed in ep-interactions at the HERA accelerator [44 – 46]. Calculations of the cross sections at high energies are based on different approaches to the PDF description for large values of $Q_0^2 \to Q^2 \approx M_W^2$, where $M_W \approx 82$ GeV is the W-boson mass, and for small values of $x \to 10^{-8}$. Deep-inelastic νN cross sections have been calculated for energies up to 10^{12} GeV in many works [47 – 55]. It may seem paradoxical, but in spite of different phenomenological approaches to accounting for nonlinear QCD effects, the calculated cross sections reported in all the above references practically coincide. Thus, at the energy $E_\nu = 10^{21}$ eV, the cross sections calculated in Refs [48, 51, 53, 55] differ from the value $\sigma_{\nu N}(E_\nu = 10^{21}\ {\rm eV}) \approx 10^{-4}$ mb by less than a factor of 2.

If the neutrino is considered a candidate for the primary particle serving as a source of UHECRs, then it is necessary to assume that neutrinos (by analogy with protons) start to undergo interactions high up in the atmosphere. For this to happen, cross sections of the order of hadron cross sections are necessary, $\sigma_{\nu N}(E_\nu) \geqslant 1$ mb. The possibility of neutrinos interacting strongly at high energies was discussed nearly 40 years ago by Berezinsky and Zatsepin [56]. At present, the idea of strongly interacting neutrinos no longer seems so exotic. Even within the SM framework, neutrino cross sections for a certain class of nonperturbative electroweak processes induced by instantons are predicted to be of the order of a millibarn [57, 58].

A new wave of interest in neutrino interactions with anomalously large cross sections arose in connection with the development of quantum gravity theories involving a TeV scale of unification of interactions and large (∼ 1 mm) extra dimensions of space – time. Within this approach, all SM particles and fields exist in the ordinary $(3+1)$-dimensional space, while gravity propagates in a space of extra n dimensions and becomes strong not on the Planck scale $M_{\rm Pl} \approx 10^{28}$ eV but on the fundamental scale of unification $M_{4+n} \approx 1$ TeV [59 – 62]. In all gravitational models with extra dimensions on the $\sqrt{s} \approx 1$ TeV scale in the center-of-mass system, the exchange of a massive spin-2 graviton (Kaluza – Klein excitations) provides additional contributions to any two-particle cross section. Therefore, the cross sections of νN interactions in the vicinity of $M_{4+n} \approx \sqrt{s} \approx 1$ TeV (which corresponds to the energy $E_\nu \approx 10^{15}$ eV in the nucleon center-of-mass system) increase by several orders of magnitude compared to the standard SM calculations. Thus, for $E_\nu \approx 10^{20}$ GeV, the νN cross section may amount to 1 – 100 mb in the case of the asymptotic behavior $\sigma_{\nu N} \sim s^1$, or even larger values if $\sigma_{\nu N} \sim s^2$ [63, 64].

In the case of UHEN interactions in the atmosphere, with the collision energy $\sqrt{s} \approx M_{\rm BH} > M_{4+n}$, strong gravity on the TeV scale could manifest itself in the formation of exotic objects such as microscopic black holes [65]. If $E_\nu \approx 10^{12}$ GeV, then the additional contributions from black hole production processes to the total νN cross section may amount to 10^{-2} mb [66]. At the same time as the production of black holes, the production of specific p-dimensional states, *p-branes*, is possible on the TeV gravity scale [67].

The *p-brane* production cross section may be greater than the production cross section of black holes of the same mass and may amount to 100 mb at energies $E_\nu \approx 10^{11}$ GeV [67, 68].

Registration of UHENs that may reach us from distant sources will serve as a valuable instrument of high-energy astrophysics and will simultaneously permit us to investigate the physics of the microworld beyond the SM. Even quite rough estimates of νN cross sections for energies not available to accelerators will provide a test of the laws of fundamental physics close to the TeV scale. The number of neutrino events registered in a detector is proportional to the integral flux times the cross section,

$$N_\nu \propto \int \Phi_\nu(E_\nu)\, \sigma_{\nu N}(E_\nu)\, \mathrm{d}E_\nu\,, \tag{1.11}$$

and therefore detectors with volumes exceeding 1 km^3 are needed in order to 'feel' the cross section at the SM level ($\sigma_{\nu N} \sim 10^{-4}$ mb). This is related to the neutrino fluxes generated both in the bottom-up and top-down scenarios being small.

For estimating the neutrino fluxes reaching Earth, one first of all uses the flux of so-called cosmogenic, or GZK, neutrinos as a reference point. Such neutrinos are certain to originate in the case of propagation of ultrahigh-energy protons produced in sources of any kind owing to their interactions with the microwave background. For the most realistic proton generation spectrum $\sim E_p^{-2}$ in isotropically distributed sources, the calculated flux of cosmogenic neutrinos is given by [69]

$$E_\nu^2 \Phi_\nu^{\mathrm{GZK}}(E_\nu) \leqslant 3 \times 10^1 \text{ eV cm}^{-2}\,\text{s}^{-1}\,\text{sr}^{-1}\,. \tag{1.12}$$

Large target volumes for neutrino interactions can be provided for in detectors using natural volumes of pure water or ice, which simultaneously serve as a radiator for generating Cherenkov radiation by secondary particles resulting from neutrino interactions. The idea to use large volumes of oceanic water for the registration of muons and neutrinos was proposed by Markov [70], while the first muons from νN interactions in a natural water volume were observed with the aid of optical Cherenkov radiation in Lake Baikal in the NT-200 detector [71]. At present, the best experimental bound on the diffuse neutrino flux, obtained in the experiment ALANDA in the range $5 \times 10^{13} - 5 \times 10^{15}$ eV [72], amounts to

$$E_\nu^2 \Phi_\nu^{\mathrm{AMANDA}}(E_\nu) \leqslant 8.4 \times 10^2 \text{ eV cm}^{-2}\,\text{s}^{-1}\,\text{sr}^{-1}\,, \tag{1.13}$$

which is more than an order of magnitude lower than the sensitivity necessary for revealing the flux of cosmogenic neutrinos.

It will be possible to achieve the necessary sensitivity to cosmogenic fluxes in the new generation of underwater neutrino telescopes, NESTOR [73] and ANTARES [74], and to essentially surpass it in the IceCube telescope [75], built in the ice at the South Pole, Antarctica, which will register fluxes at the level

$$E_\nu^2 \Phi_\nu^{\mathrm{IceCube}}(E_\nu) \leqslant 4 \times 10^0 \text{ eV cm}^{-2}\,\text{s}^{-1}\,\text{sr}^{-1}\,. \tag{1.14}$$

A very promising line of UHEN studies is based on the construction of devices capable of registering radiowaves from showers produced by neutrinos originating in condensed media. However, it was not possible to achieve the required sensitivity to cosmogenic fluxes in the first experiments of this type, RICE [76], FORTE [77], and GLUE [79]. In new ambitious projects using the radiomethod, it will be possible to investigate neutrino fluxes of EeV energies at a level significantly inferior to cosmogenic levels. For this, it has been proposed to probe gigantic rock salt mines using the SALSA [78] setup, and in the experiment ANITA [80], to survey a large volume of the antarctic ice shield during a long flight of an aerostat and to monitor a significant part of the moon's surface from a satellite orbiting the moon in the LORD experiment [81, 82].

Besides dedicated neutrino detectors, high-energy neutrinos can also be registered by setups used in UHECR studies. The registration method is based on the observation of deeply penetrating quasihorizontal showers in the atmosphere and was applied in the AGASA and HiRes setups for determining the upper bound for the νN cross section. The new ground-based detectors with large apertures, Telescope Array [83] and Auger [84], are soon to be commissioned. The next step in the development of UHECR detectors is connected with the experiments on satellites, EUSO [85] and OWL [86], which in the EeV energy range will be capable of registering UHEN-initiated showers developing deep in the atmosphere. The sensitivity of these experiments will be sufficient for a reliable determination of cosmogenic neutrino fluxes.

One can hope that the information obtained by new experiments registering UHENs will contribute to the resolution of numerous mysteries related to the fundamental laws describing nature in a unique manner.

2. The propagation of neutrinos through the universe

2.1 The interaction of neutrinos with the relic photon background

Unlike protons and photons, neutrinos can cover cosmological distances in the universe with virtually no absorption. Their interaction cross sections with the microwave background are too small to play any significant role in astrophysics.

At energies $\sqrt{s} \approx 2m_e$, the elastic scattering reaction cross section

$$\nu + \gamma_{\mathrm{CMB}} \to \nu + \gamma \tag{2.1}$$

amounts to only [87]

$$\sigma(\nu + \gamma \to \nu + \gamma) \approx 10^{-66}\ \text{cm}^2\,. \tag{2.2}$$

At the same energies, the three-particle inelastic processes

$$\nu + \gamma_{\mathrm{CMB}} \to \nu + \gamma + \gamma \tag{2.3}$$

exhibit cross sections

$$\sigma(\nu + \gamma \to \nu + \gamma + \gamma) \approx 10^{-52}\ \text{cm}^2\,. \tag{2.4}$$

Starting from energies $\sqrt{s} \approx m_e$, the reactions

$$\nu + \gamma_{\mathrm{CMB}} \to \nu + e^+ + e^- \tag{2.5}$$

may occur, with cross sections exceeding (2.4) by several orders of magnitude [88]:

$$\sigma(\nu + \gamma \to \nu + e^+ + e^-) \approx 10^{-47}\ \text{cm}^2\,. \tag{2.6}$$

At energies in the center-of-mass system above the $W^{\pm}$-boson production threshold, significant contributions to the cross section of high-energy neutrino absorption on the microwave γ-background are due to the reactions [89]

$$\nu + \gamma_{\text{CMB}} \to l^- + W^+\,, \tag{2.7}$$

where $l = e,\ \mu,\ \tau$. For the electron neutrino, characteristic cross sections of reactions (2.7) at energies $\sqrt{s} \approx M_W$ reach the values

$$\sigma(\nu_e + \gamma_{\text{CMB}} \to e^- + W^+) \approx 8 \times 10^{-34}\ \text{cm}^2 \tag{2.8}$$

and somewhat lower values in the case of reactions $\nu_\mu + \gamma_{\text{CMB}}$ and $\nu_\tau + \gamma_{\text{CMB}}$.

2.2 Interactions with the relic neutrino background

UHEN propagation is influenced more significantly by the cosmological background of relic neutrinos, predicted by Big Bang cosmology. After relic photons, such neutrinos, being stable, may be the most abundant particles in the universe. The mean square energy in the center-of-mass system for a neutrino of ultrahigh energy E_ν interacting with a relic neutrino of energy ε_ν is given by [90]

$$\langle s \rangle \approx (45\ \text{GeV})^2 \left(\frac{\varepsilon_\nu}{10^{-3}\ \text{eV}}\right)\left(\frac{E_\nu}{10^{15}\ \text{GeV}}\right). \tag{2.9}$$

If the relic neutrino is relativistic, then $\varepsilon_\nu \approx 3T_\nu(1 + \eta/4)$, where $T_\nu \approx 1.9(1+z)\,\text{K} = 1.6\times10^{-4}(1+z)$ eV is the temperature of the relic neutrino background for a redshift z, and $\eta \leqslant 50$ is a dimensionless chemical potential. If, on the contrary, the neutrinos are nonrelativistic, then $\varepsilon_\nu = \max\{3T_\nu, m_\nu\}$. In Eqn (2.9), the quantity $\sqrt{s}$ at $E_\nu < 10^{15}$ GeV does not exceed the SM gauge boson masses. Therefore, in this energy region, the cross sections of neutrino interaction processes with the relic neutrino background are determined within the SM framework.

In $\nu\bar{\nu}$-interactions at high energies and sufficiently small masses of the relic neutrinos, direct production of high-energy γ-quanta is possible:

$$\nu + \bar{\nu} \to \gamma + \gamma\,. \tag{2.10}$$

This process, however, proceeds via loop diagrams and is suppressed owing to the Yang theorem, and therefore its cross section [91]

$$\sigma(\nu + \bar{\nu} \to \gamma + \gamma) = 5.6 \times 10^{-42}\left[\left(\frac{m_\nu}{1\ \text{eV}}\right)\left(\frac{E_\nu}{10^{21}\ \text{eV}}\right)\right]^3 \text{cm}^2 \tag{2.11}$$

does not exceed values $\sim 10^{-41}$ cm^2 even at ultrahigh neutrino energies $E_\nu \approx 10^{21}$ eV and neutrino masses $m_\nu \approx 1$ eV.

References [20, 21, 90, 92] deal with the main interaction modes of high-energy neutrinos with the relic neutrino background:

a) the t-channel of a Z^0-boson exchange in the reactions

$$\nu_i + \bar{\nu}_j \to \nu_i + \bar{\nu}_j\,; \tag{2.12}$$

b) the t-channel of a $W^{\pm}$-boson exchange in the reactions

$$\nu_i + \bar{\nu}_j \to l_i + \bar{l}_j\,, \tag{2.13}$$

for example, $\nu_\mu + \bar{\nu}_\tau \to \mu + \tau$;

c) the s-channel of a Z^0-boson exchange in the reactions

$$\nu_i + \bar{\nu}_j \to f_i + \bar{f}_j \tag{2.14}$$

such as $\nu_\mu + \bar{\nu}_\tau \to$ hadrons. Here, i and j are neutrino states of any of the e-, μ-, τ-flavors, with $i \neq j$; l_i, l_j and f_i, f_j are respectively any charged leptons and fermions. If these fermions are quarks, they fragment into hadrons.

Scattering reaction (2.12) does not affect the neutrino propagation significantly, since no charged particles are produced in it.

The cross sections of $\nu\bar{\nu}$-reactions involving $W^{\pm}$-boson exchange (2.13) increase linearly with energy up to $s \cong M_W^2$ [90]:

$$\frac{\mathrm{d}\sigma(\nu_i\bar{\nu}_j \to l_i\bar{l}_j)}{\mathrm{d}\cos\theta^*} = \frac{G_F^2 s}{4\pi}\ M_W^2(1+\cos\theta^*)^2\left[\frac{s}{2}(1-\cos\theta^*) + M_W^2\right]^{-2}, \tag{2.15}$$

where θ^* is the scattering angle in the center-of-mass system and M_W is the $W^{\pm}$-boson mass. In the ultrarelativistic limit, this cross section at energies

$$s(\text{asym}) = 2E_\nu m_\nu = 2 \times 10^{23}\,\frac{E_\nu}{10^{22}\ \text{eV}}\,\frac{m_\nu}{10\ \text{eV}}\ \text{eV}^2 \gg M_W^2 \tag{2.16}$$

tends to the constant value

$$\sigma_{\text{asym}}(\nu_i + \bar{\nu}_j \to l_i + \bar{l}_j) \approx \frac{\pi\alpha^2}{2\sin^4\theta_W M_W^2} \approx 10^{-34}\ \text{cm}^2\,, \tag{2.17}$$

where α is the fine structure constant and θ_W is the Weinberg angle.

The behavior of the cross sections of $\nu\bar{\nu}$-reactions involving production of the Z^0-boson, Eqn (2.14), has a resonance character [92]:

$$\frac{\mathrm{d}\sigma(\nu_i\bar{\nu}_j \to Z^0 \to f_i\bar{f}_j)}{\mathrm{d}\cos\theta^*} = \frac{G_F^2 s}{4\pi}\,\frac{M_Z^2}{(s-M_Z)^2 + M_Z^2\Gamma_Z^2} \times \left[g_L^2(1+\cos\theta^*)^2 + g_R^2(1-\cos\theta^*)^2\right], \tag{2.18}$$

where $M_Z \approx 91.2$ GeV and $\Gamma_Z \approx 2.5$ GeV are the Z^0-boson mass and decay width and g_L and g_R are the dimensionless left and right coupling constants. The resonance sets in close to the energy

$$E_\nu^{\text{res}} = \frac{M_Z^2}{2m_\nu} = 4.2 \times 10^{21}\left(\frac{m_\nu}{1\ \text{eV}}\right)^{-1}\text{eV}\,, \tag{2.19}$$

when $\sqrt{s} = M_Z$. The resonance energy width is $\delta E_\nu(\text{res})/E_\nu(\text{res}) \approx 2\delta M_Z/M_Z \approx 2\Gamma_Z/M_Z = 0.06$. The annihilation cross section averaged over energy amounts to [21]

$$\left\langle\sigma(\nu_i + \bar{\nu}_j \to Z^0 \to f_i + \bar{f}_j)\right\rangle \approx \frac{4\pi G_F}{\sqrt{2}} = 4.2 \times 10^{-32}\ \text{cm}^2\,. \tag{2.20}$$

When $s \gg M_Z^2$, the asymptotic behavior of the cross section becomes

$$\sigma_{\text{asym}}(\nu_i + \bar{\nu}_j \to Z^0 \to f_i + \bar{f}_j) \propto \frac{1}{s}\,. \tag{2.21}$$

At energies $\sqrt{s} > 2M_W$, the W-boson pair production channel $\nu_i + \bar{\nu}_j \to W^+ + W^-$ [93] starts playing a significant role. At energies $\sqrt{s} \gg 2M_W$, the cross section tends to the value

$$\sigma_{\text{asym}}(\nu_i + \bar{\nu}_j \to W^+ + W^-) \propto \frac{M_W^2}{s}\,\ln\frac{s}{M_W^2}\,. \tag{2.22}$$

The behavior of all the $\nu\bar{\nu}$ cross sections considered is shown in Fig. 4 [20]. It follows that the most optimistic estimates of the $\nu\bar{\nu}$- and $\nu\gamma$-reaction cross sections do not exceed 10^{-32} cm^2, even in the case of ultrahigh-energy neutrinos.

We now estimate the interaction probability of a neutrino propagating through the relic neutrino background. The density of the number of light states ($m_\nu < 1$ MeV) in the universe at present is given by [94]

$$n_\nu^0 + n_{\bar{\nu}}^0 \approx \frac{3}{4}\left(\frac{T_\nu^0}{T_\gamma^0}\right)^3 n_\gamma^0 \approx 112\ \text{cm}^{-3}, \quad n_\nu^0 = n_{\bar{\nu}}^0\,, \tag{2.23}$$

where $(T_\nu^0/T_\gamma^0)^3 \approx 4/11$ and $n_\gamma^0 \approx 400$ cm^{-3}. The maximum possible contribution of relic neutrinos to the energy density of the universe is [94]

$$\Omega_\nu H^2 = \frac{\sum_i m_{\nu_i}}{94\ \text{eV}}\,, \tag{2.24}$$

where $H = 0.7$ is the Hubble constant in units of 100 km Mpc^{-1}. For neutrinos with masses $m_\nu \approx 0.07$ eV, this contribution merely amounts to $\Omega_\nu H^2 = 0.8 \times 10^{-3}$. The interaction probability of a neutrino having covered cosmological distances $L_{\text{cosm}} \approx 1000$ Mpc $\approx 3 \times 10^{27}$ cm through the relic neutrino background is then given by

$$P_{\text{cosm}}(\nu\bar{\nu}) = \max\{\sigma(\nu\bar{\nu})\}(n_\nu^0 + n_{\bar{\nu}}^0)\,L_{\text{cosm}} \approx 10^{-32}\ \text{cm}^2 \times 112\ \text{cm}^{-3} \times 3 \times 10^{27}\ \text{cm} = 3.3 \times 10^{-3}\,. \tag{2.25}$$

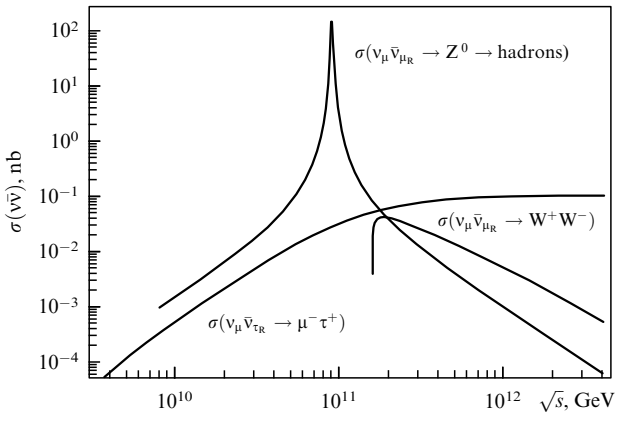

Figure 4. Cross sections of $\nu\bar{\nu}$ processes of high-energy neutrino interactions with the neutrino relic background versus energy in the center-of-mass system [20].

Even if we consider neutrino sources beyond the boundary of the cosmological event horizon $L_{\text{horiz}} \approx 5$ Gpc, the probability in (2.25) does not exceed 5%. A neutrino may therefore reach Earth practically without absorption, even if it originated in the most distant regions of the universe.

In Section 7, a detailed discussion is presented of the possibility for the deep-inelastic neutrino–nuclear cross section to undergo significant enhancement within the theories with n extra space–time dimensions and a TeV scale of quantum gravity. Here, also, it is necessary to note that the new physics in extra dimensions will introduce additional contributions to the cross sections of $\nu\bar{\nu}$- and $\nu\gamma$-processes, considered above within the SM framework [95]. This is, first and foremost, connected with the new annihilation channel of ultrahigh neutrinos in the relic background neutrinos

$$\nu\bar{\nu} \to G_{KK}\,, \tag{2.26}$$

in which massive spin-2 Kaluza–Klein gravitons are produced. The cross section of this process [96]

$$\sigma(\nu\bar{\nu} \to G_{KK}) \approx 4 \times 10^{-33-3n/2} \times 2^{n/2}\left(\frac{m_\nu}{1\ \text{eV}}\right)^{n/2}\left(\frac{E_\nu}{10^{21}\ \text{eV}}\right)\left(\frac{1\ \text{TeV}}{M_{4+n}}\right)^{n+2}\ \text{cm}^2 \tag{2.27}$$

increases rapidly with the energy. However, even at energies $E_\nu \approx 10^{21}$ GeV, cross section (2.27) is in any case smaller than at the Z^0-resonance peak (2.20).

2.3 Neutrino fluxes required for the Z-burst scenario of UHECR production

The UHECR production models based on ultrahigh-energy neutrinos being capable of producing Z^0-bosons when propagating through the relic neutrino background are known by the common term 'Z-burst' [20, 21]. The neutrino energy required for the Z^0-resonance production is determined by expression (2.19). The Z^0-bosons produced in each act of neutrino annihilation decay very rapidly (the lifetime of the Z^0-boson in its rest frame is $\sim 3 \times 10^{-25}$ s). About 70% of the Z^0s decay via hadron channels involving the production, on the average, of one baryon–antibaryon pair, and $\sim 10\,\pi^0$ two-particle decays of the latter yield ~ 20 γ-quanta [97]. The energies of hadrons and γ-quanta resulting from Z^0-boson decays are

$$\langle E_p \rangle \approx \frac{E_\nu(\text{Z-res})}{30} \approx 1.3\left(\frac{\text{eV}}{m_{\nu_j}}\right) \times 10^{20}\ \text{eV}\,, \tag{2.28}$$

$$\langle E_\gamma \rangle \approx \frac{E_\nu(\text{Z-res})}{60} \approx 0.7\left(\frac{\text{eV}}{m_{\nu_j}}\right) \times 10^{20}\ \text{eV}\,. \tag{2.29}$$

In UHECR production models involving Z-bursts, any astrophysical objects emitting neutrinos with energies sufficient for producing the Z^0-resonance may serve as sources of neutrinos. Because neutrinos are very weakly absorbed during their propagation in the universe, the neutrino sources may be at arbitrarily large distances, while the Z^0-boson decay products determine the CR spectrum beyond the GZK-cutoff. Actually, the Z-burst model demonstrates the possibility to avoid the GZK-cutoff without introducing new physics beyond the SM. The limit CR energies in this model are determined by relation (2.28). As follows from this expression, a resonance in the vicinity of the Z^0-boson

production threshold is to be observed at energies E_ν, increasing as the mass of the heaviest neutrino decreases. Correspondingly, at higher energies, both secondary protons and γ-quanta must be produced. Thus, neutrino annihilation provides a unique chance not only to register the relic neutrino background but also to determine the absolute mass value of the heaviest neutrino component [98 – 101]. Moreover, if large neutrino fluxes do exist in nature with energies close to the Z^0-resonance, then future neutrino telescopes will allow studying the neutrino absorption spectrum, which carries information on absolute neutrino masses, on the flavor composition of neutrino mass states, and on cosmological parameters determining the evolution of the universe [102, 103].

If the flux of CR particles observed in detectors with energies above the GZK-cutoff is assumed to be due to the decay products of Z^0-bosons originating in UHEN interactions with the relic neutrino background, then it is possible to estimate the primary neutrino flux necessary for realization of this scenario. For resolving the multiparametric problem of reconstructing the primary neutrino spectrum, approximation of the general form is applied,

$$\Phi_\nu(E_\nu, z) \propto E_\nu^{-\alpha}\,(1+z)^m\,. \tag{2.30}$$

Expression (2.30), being simple at first sight, contains a number of free parameters. First, the neutrino generation spectrum at the source $\propto E_\nu^{-\alpha}$ and the maximum possible energies $E_\nu^{\max}$ are not known. Second, the neutrino mass m_ν determining the energy (2.19) required for Z^0-resonance production is quite arbitrary. Finally, the interval of redshifts $z^{\min} - z^{\max}$, where the neutrino sources are situated, and the power m determining the evolution of the source $\propto (1+z)^m$ are also unknown parameters. Therefore, in order to calculate the primary neutrino flux, some of the unknown parameters present in (2.30) have necessarily to be fixed, while the others varied within the admissible region of their values.

As calculations reveal [99, 100, 104 – 107], if the observed UHECR spectrum is related to Z^0 decay products, then gigantic primary neutrino fluxes are needed for the realization of such a scenario. This is illustrated by the primary neutrino flux calculated for the Z-burst model in Ref. [107] and presented in Fig. 5. It can be seen that at the resonance energy (2.19), the neutrino flux reaches the value

$$E_\nu^2 \Phi_\nu^{\text{Z-burst}}(E_\nu^{\text{res}}) \approx 10^5 \text{ eV cm}^{-2}\,\text{s}^{-1}\,\text{sr}^{-1}\,. \tag{2.31}$$

The requirement that there exist gigantic neutrino fluxes, whose origin cannot be explained within the framework of standard astrophysics, is one of the main difficulties encountered by the Z-burst model. In a universe with uniformly distributed nonrelativistic background neutrinos, the average UHEN annihilation length at the Z^0-resonance production energies is given by [21]

$$L_{\text{ann}} = \left(\langle\sigma_{\text{ann}}\rangle\langle n_\nu\rangle\right)^{-1} \approx (4.2\times 10^{-32}\ \text{cm}^2 \times 56\ \text{cm}^{-3})^{-1} \approx 4.3\times 10^{29}\ \text{cm}. \tag{2.32}$$

Consequently, the probability of neutrinos of energies close to the resonance energy annihilating into a Z^0-boson at distances ~ 50 Mpc from Earth is

$$P(\nu\bar{\nu} \to Z^0) \approx \frac{50\ \text{Mpc}}{L_{\text{ann}}} = 3.6\times 10^{-4}\,. \tag{2.33}$$

With the fraction of decays producing hadrons Br ($Z^0 \to$ hadrons) = 70%, the probability of annihilation with subsequent decays into hadrons amounts to

$$P(\nu\bar{\nu} \to Z^0 \to \text{hadrons}) \approx 2.5\times 10^{-4}\,. \tag{2.34}$$

This means that only one out of 4000 primary neutrinos with resonance energies produces a Z-burst to be observed on Earth as hadron and electromagnetic cascades.

The efficiency of event generation in Z-burst scenarios increases if gravitational clusterization of relic neutrinos occurs in local regions of the universe on scales of the GZK zone (of the order of 50 Mpc): in galactic halos, local groups, galactic clusters, and superclusters [20, 21, 104, 105, 108, 109]. In this case, the neutrino densities in such regions may significantly exceed the average neutrino density (2.23) in the universe by a factor f_ν reaching values from 10 – 1000 [21, 105, 108, 109] up to $10^5 - 10^7$ [20]. Correspondingly, probability (2.34) increases by the same factor, and the requirements for the neutrino flux intensities are reduced. The local relic neutrino density could reach even higher values ($10^{10} - 10^{16}$ cm^{-3}) in the specific objects proposed in Ref. [110] and termed 'neutrino clouds' by the authors.

The density of relic neutrinos may be higher than average density (2.23) if CP-violation occurs in the neutrino sector [111]. Density (2.23) corresponds to the existence of a rigorous $\nu - \bar{\nu}$ symmetry $L_\nu = (n_\nu - n_{\bar{\nu}})/n_\gamma = 0$. If, on the contrary, a $\nu - \bar{\nu}$ asymmetry exists and $L_\nu \neq 0$, then an additional contribution appears in the energy density of the universe [111]. Thus, for the asymmetry factor $L_\nu \approx 4$, with four neutrinos for each relic photon, the density of the neutrino background may achieve values $n_\nu \sim 1700$ cm^{-3}. Consequently, the Z-burst production probability (2.36) may be 30 times higher.

It is shown in Refs [99, 100, 106, 107] that the high-energy part of the CR spectrum can be made consistent with the Z-burst scenario in the case of an exotic source, opaque to

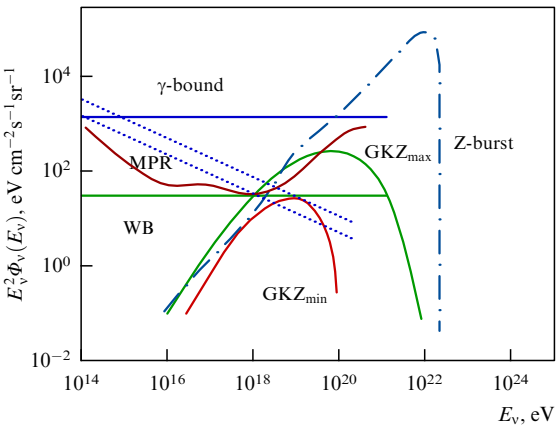

Figure 5. Neutrino fluxes calculated for different models: cosmogenic fluxes GKZ$_{\min}$ [69] and GKZ$_{\max}$ [107, 116]; the fluxes required for the Z-burst scenario [100, 106, 107]. Theoretical bounds for the fluxes (WB [142, 143] and MPR [145 – 147]) and the experimental γ-bound corresponding to EGRET measurements [113]. Tilted dotted lines are the extension of the WB bound for neutrino fluxes normalized at the observed KL flux in AGASA (upper line) and HiRes (lower line) experiments [144].

protons and high-energy photons, exclusively generating neutrino fluxes. An example of such a source is an unstable superheavy relic particle that decays mainly into neutrinos [112]. However, even if the source emits only neutrinos, the γ-quanta resulting from Z-bursts scatter in the relic photon background. Electromagnetic cascades then result in a corresponding contribution to the flux of diffuse γ-quanta. Therefore, the fluxes of photons with energies in the GeV–TeV range, measured in the EGRET experiment [113], impose strong restrictions on the diffuse flux of ultrahigh-energy neutrinos:

$$E_\nu^2 \Phi_\nu(E_\nu) \leqslant E_\nu^2 \Phi_\nu^{\mathrm{EGRET}}(E_\nu) \leqslant 6 \times 10^2 \text{ eV m}^{-2}\,\text{s}^{-1}\,\text{sr}^{-1}\,, \quad (2.35)$$

and, correspondingly, on the Z-burst scenario.

Besides enormous fluxes, Z-bursts require the existence of sources capable of generating neutrinos of energies $E_\nu \geqslant 10^{21}$ eV. If such neutrinos are produced in $\pi^\pm$-decays, then pion photoproduction requires protons of even higher energies $\sim 20\,E_{\mathrm{res}} \approx 8.4 \times 10^{22}$ eV (eV m_ν^{-1}). The nature of sources capable of generating protons of such energies is not known but, ultimately, the production of any particles with energies above the GZK-cutoff remains an unresolved problem of astrophysics.

2.4 Fluxes of cosmogenic, or GZK, neutrinos

Before dealing directly with neutrino fluxes from various astrophysical and cosmological sources, it is necessary to examine the neutrino fluxes originating during the propagation of ultrahigh-energy protons produced in these sources. Such protons may not reach the detectors on Earth, owing to the GZK-cutoff [13, 14]. Their interaction with the microwave background produces pions, whose decays produce so-called cosmogenic (i.e., produced by particles pertaining to CR) or GZK neutrinos. The main processes are the reactions

$$\mathrm{p}\gamma_{\mathrm{CMB}} \to \Delta^* \to \mathrm{n}\pi^+\,, \quad \mathrm{p}\gamma_{\mathrm{CMB}} \to \Delta^* \to \mathrm{p}\pi^0\,. \quad (2.36)$$

Subsequent decay chains of charged pions result in the neutrino flux:

$$\pi^+ \to \mu^+ + \nu_\mu\,, \quad \mu^+ \to \mathrm{e}^+ + \bar{\nu}_\mu + \nu_\mathrm{e}\,, \quad (2.37)$$

and the decays of neutral pions into the flux of γ-quanta

$$\pi^0 \to \gamma\gamma\,. \quad (2.38)$$

Also possible are the reactions

$$\mathrm{p}\gamma_{\mathrm{CMB}} \to \mathrm{n} + \pi^+ + \pi^+ + \pi^-\,, \quad (2.39)$$

whose cross sections are smaller than in reactions involving the Δ^*-resonance production, but whose final states contain a significant number of pions, the decays of which contribute essentially to the generation of neutrino fluxes.

The fluxes of cosmogenic neutrinos are calculated in Refs [69, 92, 107, 114–117]. The general method of calculation is as follows. The neutrino spectrum is taken to be a power-law spectrum of the proton source, which has the exponent α and an exponential cutoff,

$$\frac{\mathrm{d}N_\mathrm{p}}{\mathrm{d}E_\mathrm{p}} \propto E_\mathrm{p}^{-\alpha} \exp\left(-\frac{E_\mathrm{p}}{E_{\max}}\right). \quad (2.40)$$

The flux of neutrinos of flavor i, produced in proton interactions with the microwave background, is determined as an integral over the redshifts z and proton energies E_p [69]:

$$\Phi_{\nu_i}(E_{\nu_i}) = \frac{c}{4\pi E_{\nu_i}} \int\int L(z, E_\mathrm{p})\, Y(E_\mathrm{p}, E_{\nu_i}, z)\, \frac{\mathrm{d}E_\mathrm{p}}{E_\mathrm{p}}\, \mathrm{d}z, \quad (2.41)$$

where

$$Y(E_\mathrm{p}, E_{\nu_i}, z) = E_\nu\, \frac{\mathrm{d}^2 N_{\nu_i}}{\mathrm{d}N_\mathrm{p}\, \mathrm{d}E_{\nu_i}}$$

is a function describing neutrino production in decays of pions from pγ reactions and $L(z, E_\mathrm{p})$ is a function parameterizing the distribution of proton sources over the redshifts z and their evolution.

The ambiguity in the calculations of cosmogenic neutrino fluxes is related to the uncertainty in the parameters α, $E_{\max}$, z, and m, which vary within broad limits in different works. Figure 5 presents the minimum and maximum cosmogenic neutrino fluxes.

In calculations of the minimum flux [69],

$$E_\nu^2 \Phi_\nu^{\mathrm{GZK}_{\min}}(E_\nu) \leqslant 3 \times 10^1 \text{ eV cm}^{-2}\,\text{s}^{-1}\,\text{sr}^{-1} \quad (2.42)$$

a power-law spectrum with $\alpha = 2$ is assumed for the proton source, together with its exponential cutoff (2.40) with $E_{\max} = 10^{21.5}$ eV. The neutrino fluxes obtained in Refs [92, 114, 115] and the lower bound in [116] are in agreement with (2.42).

Calculation of the maximum flux [107, 117]

$$E_\nu^2 \Phi_\nu^{\mathrm{GZK}_{\max}}(E_\nu) \leqslant 10^3 \text{ eV cm}^{-2}\,\text{s}^{-1}\,\text{sr}^{-1} \quad (2.43)$$

is based on the proton spectrum with $\alpha = 1$ extending up to energies $E_{\max} = 3 \times 10^{22}$ eV at $z_{\max} = 2$ and $m = 3$. The upper bound for the cosmogenic flux, obtained in Ref. [116], is consistent with the value in (2.43). It can be seen from Fig. 5 that the maximum cosmogenic neutrino fluxes are at least two orders of magnitude smaller than required for Z-burst scenarios.

Cosmogenic neutrino fluxes are also caused by CR proton interactions with the infrared background radiation (an analog of reactions (2.38) with the substitution $\mathrm{p}\gamma_{\mathrm{CMB}} \to \to \mathrm{p}\gamma_{\mathrm{IBG}}$). Their values

$$E^2 \Phi_\nu^{\mathrm{GZK\text{-}IRB}}(E_\nu) \leqslant 10^0 \text{ eV cm}^{-2}\,\text{s}^{-1}\,\text{sr}^{-1}\,, \quad (2.44)$$

calculated in Refs [118, 119] are an order of magnitude smaller than the minimum fluxes due to the interaction of protons with the microwave background in (2.42).

2.5 Influence of neutrino oscillations on the propagation of neutrinos in the universe

In all astrophysical sources inside which neutrinos are produced in pγ and pp interactions, their initial flavor composition is

$$\Phi^0(\nu_\mathrm{e}) : \Phi^0(\nu_\mu) : \Phi^0(\nu_\tau) = 1 : 2 : 0\,. \quad (2.45)$$

In the three-flavor scenario of neutrino oscillations, the relation between the electroweak neutrino states $\nu_\alpha = \nu_e, \nu_\mu, \nu_\tau$ and the mass eigenstates $\nu_i = \nu_1, \nu_2, \nu_3$

$$\nu_\alpha = \sum_i U_{\alpha i}\, \nu_i \tag{2.46}$$

is expressed via the mixing matrix

$$U_{\alpha i} = \begin{pmatrix} U_{e1} & U_{e2} & U_{e3} \\ U_{\mu 1} & U_{\mu 2} & U_{\mu 3} \\ U_{\tau 1} & U_{\tau 2} & U_{\tau 3} \end{pmatrix}, \tag{2.47}$$

which satisfies the unitarity condition $\sum_i |U_{\alpha i}|^2 = 1$.

In the general case of mixing involving an arbitrary number of massive (including sterile) neutrinos, the probability of vacuum oscillations [120]

$$P(\nu_\alpha \to \nu_\beta) = \sum_j |U_{\alpha j}|^2 |U_{\beta j}|^2 + 2 \sum_{k>j} \mathrm{Re}\left[U_{\alpha j}\, U^*_{\beta j}\, U^*_{\alpha k}\, U_{\beta k}\right] \cos \frac{\Delta m^2_{ij} L}{2E_\nu} \tag{2.48}$$

in the limit as $L \to \infty$ for sources at cosmological distances $L \approx 100-1000$ Mpc retains only the first term

$$P(\nu_\alpha \to \nu_\beta) = \sum_j |U_{\alpha j}|^2 |U_{\beta j}|^2 . \tag{2.49}$$

Within a broad range of energies $10^3 \leqslant E_\nu \leqslant 10^{11}$ GeV and squared mass differences $10^{-10} \leqslant \Delta m^2_\nu \leqslant 1$ eV^2, the vacuum oscillation length is

$$L_{\mathrm{osc}} \approx \frac{E_\nu}{\Delta m^2_\nu} \ll L , \tag{2.50}$$

and therefore neutrinos oscillate many times on the way from the source to Earth. This is readily shown, e.g., by considering neutrino fluxes produced in the AGN sources Mkn421 and Mkn501, which are at distances of about 140 Mpc from Earth. If we set $\Delta m^2 = 10^{-5}$ eV, then the oscillation length $L_{\mathrm{osc}} \approx 2.5 \times 10^{-24}$ Mpc$(E_\nu\,\mathrm{eV}^{-1})$, and hence even for neutrinos of the energy 10^{21} eV, the length $L_{\mathrm{osc}} \approx 2.5 \times 10^{-4}$ Mpc. Thus, owing to oscillations arriving at Earth, the flux $\Phi^{\mathrm{det}} = \left(\Phi^{\mathrm{det}}(\nu_e), \Phi^{\mathrm{det}}(\nu_\mu), \Phi^{\mathrm{det}}(\nu_\tau)\right)$ does not coincide with the primary flux from the source $\Phi^0 = \left(\Phi^0(\nu_e), \Phi^0(\nu_\mu), \Phi^0(\nu_\tau)\right)$. The effects due to matter do not affect the final result, as was shown in Ref. [121], where the background of relic neutrinos was considered as the only essential matter on the way of UHENs produced at a distant astrophysical source.

The flavor composition of neutrino fluxes in a detector

$$\begin{pmatrix} \Phi^{\mathrm{det}}(\nu_e) \\ \Phi^{\mathrm{det}}(\nu_\mu) \\ \Phi^{\mathrm{det}}(\nu_\tau) \end{pmatrix} = P_{\alpha\beta} \begin{pmatrix} \Phi^0(\nu_e) \\ \Phi^0(\nu_\mu) \\ \Phi^0(\nu_\tau) \end{pmatrix} \tag{2.51}$$

is determined by probability matrix (2.49), which depends on the elements of mixing matrix (2.47). In Ref. [39], it is shown that in the case of a normal neutrino mass hierarchy $|\Delta m^2_{21}| < |\Delta m^2_{32}| < |\Delta m^2_{31}|$ (with $\Delta m^2_{21} \approx \Delta m^2_{\mathrm{sun}}$ and $\Delta m^2_{32} \approx \Delta m^2_{\mathrm{atm}}$), in accordance with the data of SuperKamiokande on atmospheric neutrinos [122–125], of the accelerator experiment K2K [126], and of the reactor experiment CHOOZ [127], the mixing matrix elements can be chosen such that

$$|U_{e3}|^2 \ll 1 \quad \text{and} \quad |U_{\mu 3}| \approx |U_{\tau 3}| . \tag{2.52}$$

Substituting probability matrix (2.49) in (2.51) and taking (2.52) into account, we obtain the following flavor composition of astrophysical neutrino fluxes in the detector:

$$\begin{aligned} \begin{pmatrix} \Phi^{\mathrm{det}}(\nu_e) \\ \Phi^{\mathrm{det}}(\nu_\mu) \\ \Phi^{\mathrm{det}}(\nu_\tau) \end{pmatrix} &= \begin{pmatrix} |U_{e1}|^2 & |U_{e2}|^2 & |U_{e3}|^2 \\ |U_{\mu 1}|^2 & |U_{\mu 2}|^2 & |U_{\mu 3}|^2 \\ |U_{\tau 1}|^2 & |U_{\tau 2}|^2 & |U_{\tau 3}|^2 \end{pmatrix} \\ &\times \begin{pmatrix} |U_{e1}|^2 & |U_{\mu 1}|^2 & |U_{\tau 1}|^2 \\ |U_{e2}|^2 & |U_{\mu 2}|^2 & |U_{\tau 2}|^2 \\ |U_{e3}|^2 & |U_{\mu 3}|^2 & |U_{\tau 3}|^2 \end{pmatrix} \begin{pmatrix} 1 \\ 2 \\ 0 \end{pmatrix} \Phi^0(\nu_e) \\ &= \begin{pmatrix} |U_{e1}|^2 & |U_{e2}|^2 & |U_{e3}|^2 \\ |U_{\mu 1}|^2 & |U_{\mu 2}|^2 & |U_{\mu 3}|^2 \\ |U_{\tau 1}|^2 & |U_{\tau 2}|^2 & |U_{\tau 3}|^2 \end{pmatrix} \\ &\times \left[\begin{pmatrix} 1 \\ 1 \\ 1 \end{pmatrix} \Phi^0(\nu_e) + \begin{pmatrix} |U_{\mu 1}|^2 - |U_{\tau 1}|^2 \\ |U_{\mu 2}|^2 - |U_{\tau 2}|^2 \\ |U_{\mu 3}|^2 - |U_{\tau 3}|^2 \end{pmatrix} \Phi^0(\nu_e) \right] \cong \begin{pmatrix} 1 \\ 1 \\ 1 \end{pmatrix} \Phi^0(\nu_e). \end{aligned} \tag{2.53}$$

With the unitarity condition and the condition $\left||U_{\mu j}|^2 - |U_{\tau j}|^2\right| \ll 1$ applied, the second term in the square brackets vanishes. Neutrino oscillations alter the initial flavor composition (2.45), and the ratios between the neutrino fluxes reaching Earth are

$$\Phi^{\mathrm{det}}(\nu_e) : \Phi^{\mathrm{det}}(\nu_\mu) : \Phi^{\mathrm{det}}(\nu_\tau) = 1 : 1 : 1 . \tag{2.54}$$

This relation is determined exclusively by conditions (2.52), is independent of the neutrino energy, and holds for any form of the parameterization of the three-flavor mixing matrix [40].

Recently, a series of publications has appeared in which possible deviations from (2.54), presently known as the standard relation, are discussed. Such deviations may be caused by the mixing of active and sterile neutrino states [128–130], by massive neutrinos having magnetic moments [131], by the heavier neutrinos ν_i decaying into a light stable or sterile state ν_j [132–135], or by CPT-symmetry breaking [136–139].

As was recently shown in Ref. 140], the initial composition of neutrino fluxes in the source at high energies may differ from (2.45). By analogy with the energy dependence of the flavor composition of atmospheric neutrinos, such an effect may also occur for neutrino fluxes in astrophysical sources. Because the lifetime of the pion is less than that of the muon, at sufficiently high energies the probability of the pion decaying before it loses a significant fraction of its energy in interactions with the surrounding radiation exceeds the probability of its μ-decay. In other words, at high energies, the relative contribution of μ-decays may be suppressed, and hence the flavor relation of neutrino fluxes in the source, (2.45), is modified: $\Phi^0(\nu_e) : \Phi^0(\nu_\mu) : \Phi^0(\nu_\tau) = 0 : 1 : 0$. This, in turn, also results in the ratios between the fluxes on the earth differing from (2.54): $\Phi^{\mathrm{det}}(\nu_e) : \Phi^{\mathrm{det}}(\nu_\mu) : \Phi^{\mathrm{det}}(\nu_\tau) = 0 : 1.8 : 1.8$ [140].

The indicated diversity of admissible theoretical schemes describing the distortion of neutrino fluxes may create

difficulties in interpreting experimental results of measurements of the flavor composition of astrophysical neutrinos in future neutrino telescopes [139, 141].

3. Astrophysical sources of ultrahigh-energy neutrinos: bottom-up scenarios

3.1 Theoretical limits for neutrino fluxes from astrophysical sources

The sources of photons of energies up to several TeV have been well studied by methods of gamma-astronomy. If there exist sources in which proton acceleration occurs, then the production of photons should be accompanied by the production of neutrinos. At present, however, there exist no experimental indications pointing to the existence of correlations between pointlike sources of photons and neutrinos.

There do exist theoretical, model, bounds for neutrino fluxes from astrophysical sources of any nature, in which neutrinos originate in the decays of $\pi^{\pm}$ resulting from pp and $p\gamma$ interactions. The best known bounds of astrophysical neutrino fluxes are the Waxman – Bahcall (WB) [142, 143] and Mannheim – Protheroe – Rachen (MPR) [145 – 147] bounds.

The WB bound is based on the observed UHECR flux and on the assumption of a power-law spectrum of ultrahigh-energy proton generation in the source, proportional to E_p^{-2}. Such a generation spectrum is consistent with the Fermi mechanism of proton acceleration at the fronts of shock waves. If the protons produced in astrophysical sources with an energy E_p lose part of their energy in pion photoproduction before leaving the source, then the spectrum of neutrinos from $\pi^{\pm}$-decays must reflect the proton spectrum, $E_\nu^2\,\mathrm{d}N_\nu/\mathrm{d}E_\nu \propto E_p^2\,\mathrm{d}N_p/\mathrm{d}E_p$. The fraction of the proton energy transferred to the neutrinos in $p\gamma$ interactions is energy-independent and amounts to $E_\nu \approx 0.05 \times E_p$ [27]. Waxman and Bahcall, assuming proton sources to be isotropically distributed in the observable universe and transparent to protons, normalized the calculated proton spectrum to the cosmic ray flux observed at energies $E_p \approx 10^{19} - 10^{20}$ eV and obtained the upper bound for the neutrino flux [142, 143] (see Fig. 5)

$$E_\nu^2 \Phi_\nu(E_\nu) \leqslant E_\nu^2 \Phi_\nu^{\mathrm{WB}}(E_\nu) \approx 1.5 \times 10^1 (1+z)^m \ \text{eV cm}^{-2}\,\text{s}^{-1}\,\text{sr}^{-1}\,. \quad (3.1)$$

An extended WB bound was recently proposed in Ref. [144]. It was obtained under the assumption that the extragalactic CR component starts to dominate at energies $E_p \approx 10^{17.6}$ GeV. Moreover, the integral power-law spectrum changes with energy and the exponent of the spectrum $\alpha \neq 2$. In Fig. 5, the extended WB bound for neutrino fluxes from sources transparent to protons is shown with tilted lines, normalized to the CR flux observed in the AGASA and HiRes experiments.

The MPR limit was obtained under the assumption that the extragalactic proton fluxes are due to all the sources with generation spectrum (2.40) and that $\alpha = 1$. The maximum proton energies in such sources were varied within broad limits: $E_{\max} = 10^{15} - 3 \times 10^{22}$ eV. The proton emission spectra $\propto E_p^{-1}$ and their exponential cutoff, together with the varying energies $E_{\max}$, were required by the authors of Refs [145 – 147] in order to reproduce the effect of superposition of neutrino spectra from different sources. Such hard emission spectra allow normalizing neutrino fluxes in accordance with the experimental upper bound for the extragalactic CR proton component

$$N_p(E_p) = 0.8\left(\frac{E_p}{1\ \text{GeV}}\right)^{-2.75} \text{cm}^{-2}\,\text{s}^{-1}\,\text{sr}^{-1}\ \text{GeV}^{-1}\,, \quad 3 \times 10^{15} < E_p < 10^{21}\ \text{eV}\,. \quad (3.2)$$

In the MPR approach, the sources generating protons with energies $E_{\max} \geqslant 10^{20}$ eV make a small contribution to the observed UHECR flux owing to the GZK cutoff of the spectrum. On the other hand, neutrino fluxes from such sources may be very significant and by two orders of magnitude greater than the WB limit (see Fig. 5):

$$E_\nu^2 \Phi_\nu(E_\nu) \leqslant E_\nu^2 \Phi_\nu^{\mathrm{MPR}}(E_\nu \approx 10^{21}\ \text{eV}) \approx 10^3\ \text{eV cm}^{-2}\,\text{s}^{-1}\,\text{sr}^{-1}\,. \quad (3.3)$$

It is shown in Refs [107, 117] that for any astrophysical source where γ-quanta and neutrinos are the decay products of pions produced in photoproduction reactions, the resulting neutrino fluxes may exceed not only the WB bound but also the MPR bound. This is true for sources with emission spectra that are harder than $\propto E_p^{-1.5}$ found at large redshifts ($z \geqslant 2$) with a strong evolution dependence ($m \geqslant 3$), in which protons are accelerated to maximum energies $E_{\max} \geqslant 10^{22}$ eV. At first sight, the probability for sources with such parameters to exist seems small: objects with an emission spectrum exhibiting such a gentle slope have not been observed yet, while the physical principles of proton acceleration up to such energies are not known. On the other hand, to explain the UHECR spectra by protons from extragalactic sources, even harder initial conditions are needed.

3.2 Gamma-ray bursts

Gamma-ray bursts (GRBs) are sources in the universe that generate powerful bursts of photons from fractions of a second to several hundred seconds long. The nature of GRBs has become better understood as a result of studies performed during the past decade within a series of experiments on satellites (BATSE, BeppoSAX, Hubble, HETE, Conus, Integral) and at ground-based observatories. Apparently, GRBs result from the collapses of supernovae, as a consequence of which compact sources are formed with characteristic dimensions $r_0 \approx 10^7$ cm and colossal luminosities $L_{\mathrm{GRB}} \approx 10^{52}$ egr s^{-1}. Such events are accompanied by afterglows in the radio, optical, and X-ray ranges [148]. The energy spectra of different GRBs differ from each other. In the main, the spectrum has a maximum in the region 0.1 – 1 MeV, which in many cases extends up to GeV energies [25, 149]. Recently, the Milagro collaboration presented the results of observations of γ-quanta of energies 100 GeV – 21 TeV [150] arriving from directions pointing to certain GRBs.

The GRB behavior is described by various models, such as the model of a relativistic fireball — a mixture of protons, neutrons, and $e^{\pm}$ and γ-quanta in a magnetic field, which expands in volume and is characterized by Lorentz factors $\Gamma_{\mathrm{GRB}} = 10^2 - 10^3$ [151, 152]. The acceleration of particles up to ultrahigh energies occurs in shock waves propagating within either the internal [151] or the external [152] regions of a fireball. The electrons that are accelerated in the case of relativistic expansion of the internal regions of the fireball produce an observable photon flux, owing to synchrotron or

inverse Compton radiation. In the region where the kinetic energy of the expanding fireball is diffused, shock acceleration of protons is also expected up to energies $E_p \approx 10^{20}$ eV [151, 152].

A natural consequence of the acceleration of protons up to high energies is their photomeson reactions with the participation of γ-quanta inside the expanding fireball. These interactions result in the production of charged pions, whose decays are accompanied by the emission of neutrinos of energies $E_\nu > 10^{14}$ eV [153]. This energy is determined from the relation between the energy E_γ and the energy of the accelerated proton E_p at the Δ-resonance production threshold (in the laboratory system)

$$E_\gamma E_p = 0.2\ \mathrm{GeV}^2 \times \Gamma_{\mathrm{GRB}}^2 . \tag{3.4}$$

For the γ-quanta observed with characteristic energies $E_\gamma \approx 1$ MeV at the values $\Gamma_{\mathrm{GRB}} \approx 10^2$, the proton energy required for pion production is $E_p > 10^{16}$ eV. Since the neutrinos produced in pion decays carry away ≈ 5% of the proton energy, their expected energy $E_\nu^{\mathrm{GRB}} > 10^{14}$ eV [142, 143, 153].

The neutrino flux from GRBs can be estimated assuming the CRs observed with energies exceeding 10^{19} eV to be composed of protons from cosmologically distributed sources exhibiting a spectrum typical of the Fermi acceleration mechanism, $\mathrm{d}N_{\mathrm{CR}}/\mathrm{d}E_{\mathrm{CR}} \propto E_{\mathrm{CR}}^{-2}$ [154]. Calculations [155] reveal that even higher exponents of the spectrum inclination are admissible without contradicting the observable data from AGASA and HiRes. In any case, the neutrino spectrum $\mathrm{d}N/\mathrm{d}E_\nu \propto E^{-\alpha}$ must reflect the behavior of the proton spectrum, while the luminosities of the neutrino and γ-fluxes produced in photonuclear reactions must satisfy the relation $L_\nu : L_\gamma \approx 1 : 3$ [156]. Then, the maximum neutrino flux from GRBs can be estimated as [142, 157]

$$E_\nu^2 \Phi_{\nu_\mu}^{\mathrm{GRB}} \approx 10^1 \frac{f_\pi}{0.2}\ \mathrm{eV\ cm^{-2}\ s^{-1}\ sr^{-1}} , \tag{3.5}$$

where $f_\pi \approx 0.1$ is the proton energy fraction transferred to the pion produced and $\Phi_{\nu_\mu}^{\mathrm{GRB}} \approx \Phi_{\nu_e}^{\mathrm{GRB}}$. This neutrino spectrum extends from $E_\nu^{\mathrm{GRB}} \approx 10^{14}$ eV to energies $E_\nu^{\mathrm{GRB}} \approx 10^{16}$ eV. Further, the spectrum rapidly decreases owing to significant pion energy losses.

Neutrinos of large energies (so-called 'halo' neutrinos) are produced at the early stages of the expanding fireball interaction with the surrounding gas. They are emitted ∼ 10 s after the main burst during a similar time interval. The source of such a neutrino 'afterglow' is due to return shock waves propagating inside the fireball [158, 159]. The electrons accelerated within the return shock waves emit γ-quanta of the visible and ultraviolet ranges (10 eV – 1 keV). Protons may be accelerated in such shock waves up to $E_p \approx 10^{21}$ eV. Interactions between low-energy photons and ultrahigh-energy protons produce 'halo' neutrinos with energies $E_\nu^{\mathrm{GRB\text{-}afterglow}} \approx 10^{17} - 10^{19}$ eV. If the fireball expands into a medium of density $\sim 10^4$ cm^{-3}, as in the case of a collapsing massive star, then the 'halo' neutrino flux is given by [157]

$$E_\nu^2 \Phi_{\nu_\mu}^{\mathrm{GRB\text{-}afterglow}} \approx 10^1 \min\left(1, \frac{E_\nu}{10^{17}\ \mathrm{eV}}\right) \mathrm{eV\ cm^{-2}\ s^{-1}\ sr^{-1}} . \tag{3.6}$$

Because no protons with energies $E_p \gg 10^{20}$ eV are expected to be produced in the GRB scenario, the neutrino fluxes with energies $E_\nu > 10^{19}$ eV must also be strongly suppressed.

Besides the neutrino 'halo' following a GR burst, neutrino fluxes preceding all the γ and ν from the main burst may be observed. Depending on the source of GRB production, these neutrino precursors of a burst exhibit varying energetics. Two main models of GRB production are being considered: the Collapsar [160, 161] and Supranova [162] models.

The Collapsar model assumes the progenitor of a GRB to be the prompt collapse of a massive star to a black hole. The collapse results in the formation of relativistic jets, which either penetrate the star's shell or, in the case of very slow-rotating stars, go out, heating the star plasma up to keV temperatures. In both cases, protons in jets may be accelerated up to energies $\geqslant 10^{14}$ eV, and their interactions with photons in the cavities of the jets lead to the production of neutrinos with energies $E_\nu \geqslant 5 \times 10^{12}$ eV [163].

In the Supranova model [162], GRB production is a result of the explosion of a supernova with the subsequent origination of a neutron star (pulsar) of the mass $\approx 2.5 - 3\ M_{\mathrm{sun}}$. In a time from several days up to months, the neutron star loses energy, emitting the so-called pulsar wind. Eventually, the neutron star collapses to a black hole, resulting in the observation of a GRB. In this scenario, neutrinos are emitted during the entire period, from the supernova explosion to the GRB [164]. Neutrinos are produced in either pp or pγ interactions, when the supernova remnant shell being ejected represents, respectively, either a proton or a photon target for relativistic protons of the pulsar wind. In the first case, the neutrinos have energies $E_\nu \geqslant 10^{13}$ eV and in the second case, $E_\nu \geqslant 10^{16}$ eV [165 – 167].

Neutrino fluxes from GRBs are presented in Fig. 6. Such fluxes can be registered by new-generation neutrino telescopes and by CR detectors [168 – 172].

3.3 Active galactic nuclei

Active galactic nuclei (AGN) are powerful sources of radiation in the universe, being sustained by the gravitational energy of mutter falling into a black hole. Although the AGN

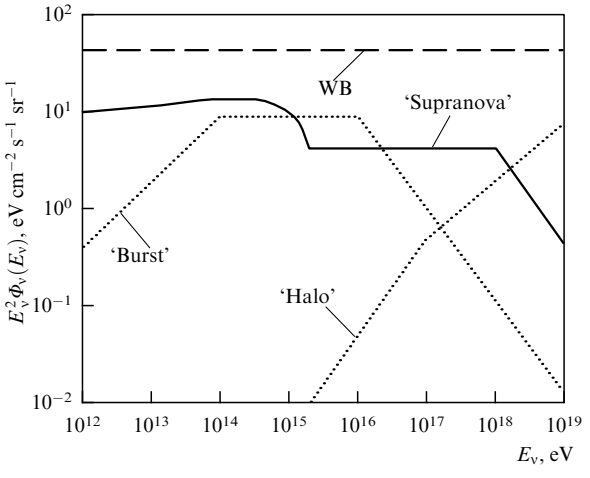

Figure 6. Neutrino fluxes from GRBs. The dotted lines correspond to a 'burst,' i.e., to the neutrino flux from the main burst and to the neutrino 'halo' [165]. Shown also are the neutrino flux in the Supranova model and the WB bound.

luminosity is less than that of a GRB, $L_{\rm AGN} \approx 10^{45} - 10^{49}$ erg s^{-1}, they shine for a much longer period of time involving regular bursts several days long [24, 173]. Such an energetics requires the existence of a black hole with an enormous mass ($M_{\rm BH} \approx 10^9\, M_{\rm sun}$). That they are observed to be at shorter distances than GRBs is only related to their lower luminosity in the gamma range. In recent years, about 70 AGNs have been registered in the satellite experiments EGRET [173], BeppoSAX [175], Whipple/Veritas [176, 177], and HESS [178]. Among AGNs, there is a certain class of objects called blazar, sources emitting γ-quanta in the form of collimated jets. Photons of TeV energies have been observed from the blazars Markarian 421, H 1426+428, 1 ES 2344+514, and 1 ES 1959+650. Photons with energies above 20 TeV were registered from the source Markarian 501.

Two main AGN models are considered in which significant ultrahigh-energy neutrino fluxes are predicted: the 'hidden-core' and 'jet' models, describing blazars.

In the hidden-core model [179, 180], protons are accelerated up to ultrahigh energies within the internal AGN regions and cannot leave the source owing to the very large thickness for pγ and pp interactions. Such a thick and opaque source with a hypothetical accelerator in the form of a black hole serves as a natural neutrino factory with quite a high luminosity. This is the model of a purely neutrino source, in which the observed high-energy CR and γ-quantum fluxes impose no restrictions on the neutrino fluxes. Therefore, the WB bound cannot be applied in the case of the hidden-core model, and the neutrino fluxes $\Phi_\nu^{\rm AGN\text{-}core} \propto E_\nu^{-2}$, calculated in Refs [179, 180] and shown in Fig. 7, exceed it by more than two orders of magnitude. It must be noted that these calculations were recently corrected [181] such that the neutrino flux expected in the hidden-core model should be 20 times smaller than the fluxes calculated in Refs [179, 180].

Most AGN jet models [156, 182–184] are based on the assumption that the spectrum of γ-quanta observed in the TeV energy region is related to the decays of the π^0 produced in interactions of protons accelerated within jets, with the gas and radiation surrounding the black hole. In these models, the neutrino emission spectrum $\mathrm{d}N_\nu/\mathrm{d}E_\nu \propto E_\nu^{-1}$ is predicted to extend up to energies $E_\nu^{\max} \approx 0.05 E_{\rm p}^{\max}$. In the case of such emission spectra, the calculated neutrino fluxes (Fig. 7) may significantly exceed the WB bound:

$$E_\nu^2 \Phi_\nu^{\rm AGN}(E_\nu) \leqslant (1-4) \times 10^3 \text{ eV cm}^{-2}\,\text{s}^{-1}\,\text{sr}^{-1}\,. \qquad (3.7)$$

The blazar model, in which the origin of TeV γ-quanta is explained by the synchrotron radiation of accelerated protons [185], served as a development of the hadron scenarios. The synchrotron energy losses of protons lead to the γ-flux significantly exceeding the neutrino flux. Therefore, here, unlike in the jet models discussed above, the neutrino flux is smaller by two orders of magnitude and satisfies the WB bound (see Fig. 7).

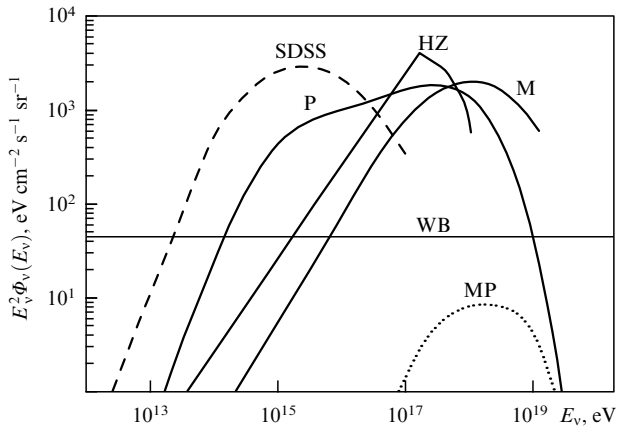

Figure 7. Neutrino fluxes in AGN scenarios: hidden-core — SDSS [179]; for jet models of sources of the blazar type — P [184], HZ [156], M [183], MP [185]. The WB bound is shown for comparison.

3.4 Other astrophysical sources of neutrinos

Having dealt with ultrahigh-energy neutrino fluxes from GRBs and AGNs, we must note that a number of sources capable of generating neutrinos with energies 1–10 TeV exist in the universe. The following are considered to be such sources [186].

Supernova explosions. These are collapse processes of a massive star. A collapse should result in the observation, over approximately an hour, of a large flux of neutrinos of TeV energies [187], which appears 10 hours after the ejection of 10 MeV neutrinos due to the cooling of the neutron star. In the model of a supernova containing an energetic pulsar, the maximum flux is

$$\frac{\mathrm{d}N_\nu^{\text{supernova explosion}}}{\mathrm{d}E_\nu} \approx 10^3 \left(\frac{E_\nu}{1\text{ GeV}}\right)^{-3.6} \text{GeV}^{-1}\,\text{m}^{-2}\,\text{s}^{-1}\,. \qquad (3.8)$$

Supernova remnants. Of the supernova remnants, the best studied objects are Crab [188, 189], Cassiopeia A [190], RXJ1713.7-3946 [191], and SN 1987 A [192]. γ-quanta from these sources have been observed with energies up to dozens of TeVs. If the origin of the γ-quanta is connected with π^0-decays, then the charged pions produced together with them in photonuclear interactions must decay, resulting in a flux of neutrinos with energies $E_\nu \approx 10$ TeV [193],

$$\frac{\mathrm{d}N_\nu^{\text{supernova remnant}}}{\mathrm{d}E_\nu} \approx 10^{-4} \left(\frac{E_\nu}{1\text{ GeV}}\right)^{-2} \text{GeV}^{-1}\,\text{m}^{-2}\,\text{s}^{-1}. \qquad (3.9)$$

Strongly magnetized neutron stars (*magnetars*). In the magnetospheres of such stars, protons are accelerated and interact with thermal photons via Δ-resonance production. This leads to neutrino fluxes with energies $E_\nu \approx 1-2$ TeV, which for sources such as SGR 1900+14 and 1E1048-5937 are estimated [194] to be

$$\frac{\mathrm{d}N_\nu^{\text{magnetar}}}{\mathrm{d}E_\nu} \approx 10^0 \left(\frac{E_\nu}{1\text{ TeV}}\right)^{-1} \text{TeV}^{-1}\,\text{cm}^{-2}\,\text{s}^{-1}\,. \qquad (3.10)$$

Double-star systems. These consist of a magnetized neutron star rotating about a massive star and can be sources of neutrinos of energies 300 GeV $\leqslant E_\nu \leqslant$ 1 TeV. Their flux is estimated on the basis of the observed flux of γ-quanta from the well-studied double system A0535+26 [195] and is given by

$$\frac{\mathrm{d}N_\nu^{\text{double system}}}{\mathrm{d}E_\nu} \approx 10^{-3} \left(\frac{E_\nu}{1\text{ GeV}}\right)^{-2.35} \text{GeV}^{-1}\,\text{m}^{-2}\,\text{s}^{-1}. \qquad (3.11)$$

Microquasars. These are objects associated with the class of double systems including a neutron star and a black hole.

They are sources of jets within which protons are accelerated and interact with synchrotron γ-quanta. During the active stage of a microquasar, (several-hour long) photomeson reactions result in neutrino fluxes with energies 1 – 100 TeV, estimated for systems such as CygnusX3, GX339-4, SS433 [196, 197] to be

$$\frac{\mathrm{d}N_{\nu}^{\mathrm{microquasar}}}{\mathrm{d}E_{\nu}} \approx 10^{-3}\left(\frac{E_{\nu}}{1\ \mathrm{Gev}}\right)^{-2}\ \mathrm{GeV}^{-1}\ \ \mathrm{m}^{-2}\,\mathrm{s}^{-1}. \tag{3.12}$$

Spiral galaxies. As a result of hadron processes, spiral galaxies can emit high-energy γ-quanta and neutrinos. The registered flux of γ-quanta with TeV energies, arriving from a region of a radius above 10 kpc in the direction of the spiral galaxy NGC253 [198], permits estimating the neutrino flux as [199]

$$\frac{\mathrm{d}N_{\nu}^{\mathrm{starburst}}}{\mathrm{d}E_{\nu}} \approx 10^{-12}\left(\frac{E_{\nu}}{1\ \mathrm{TeV}}\right)^{-1.85}\ \mathrm{TeV}^{-1}\,\mathrm{sm}^{-2}\,\mathrm{s}^{-1}. \tag{3.13}$$

All the presented estimates of neutrino fluxes are based either on recalculation of γ-quantum fluxes of TeV energies observed arriving from astrophysical sources such as supernova remnants or on model scenarios of proton acceleration in the vicinity of compact objects such as neutron stars. The latter scenarios result in quite a significant arbitrariness in the estimates of neutrino fluxes, related to the uncertainty in the fraction of energy carried away by relativistic hadrons from the concrete source.

4. Top-down decay scenario for the production of cosmological neutrinos

4.1 Production and decays of superheavy X-particles

The decays of superheavy X-particles serve as an alternative to the acceleration scenario for UHECR and UHEN production. The X-particles may be heavy gauge bosons, Higgs bosons, or superheavy fermions. With masses of the order of the scale of the Grand Unification Theory (GUT), undoubtedly exceeding 10^{21} eV, such particles should decay into leptons and quarks. Quark hadronization must then result in hadron jets that become UHECR and UHEN sources. X-particles are not connected with any astrophysical objects. They can decay at distances $\leqslant 50$ Mpc from Earth, for example, within the halo of our galaxy. Therefore, the CR spectrum GZK-cutoff problem does not exist in the top-down scenario. Nucleons, γ-quanta, and neutrinos produced in X-particle decays can retain a significant part of their energy up to the moment when they are registered in a detector.

One of the possibilities for X-particle production is related to their continuous radiation due to specific physical processes such as collapse or annihilation with respect to relatively stable topological defects (TDs). TD formation could have occurred in the early universe during cosmological phase transitions associated with spontaneous symmetry breaking on the GUT scale. Several types of such relic phenomena are considered.

Cosmic strings can liberate part of their energy in the form of X-particles as the result of a collapse occurring when two separated string segments approach each other at a distance of the order of the string width [28].

Superconducting cosmic strings moving in extragalactic magnetic fields initiate electric currents that achieve a critical value, resulting in the production of an X-particle [29, 200].

Vortons represent a variety of superconducting string loops that can gradually lose their energy owing to subbarrier quantum transitions, by emitting X-particles [33, 201, 202].

Magnetic monopoles can exist in the form of bound metastable monopole – antimonopole states, whose annihilation produces X-particles [30].

Hybrid topological defects represent states of monopoles connected by strings. Falling into this category are phenomena such as monopole – antimonopole pairs $\mathrm{M}-\overline{\mathrm{M}}$ connected by strings [31], or cosmic loops (*necklaces*) — chains of monopoles connected by two strings attached to each monopole [32]. Annihilation of $\mathrm{M}-\overline{\mathrm{M}}$ pairs and loops may produce X-particles.

Mirror topological defects may be the source of mirror X-particles, whose decay products are invisible in the ordinary world. The only exception are mirror neutrinos, which may become observable as a result of oscillations into usual neutrinos [203]. The averaged X-particle emission rate (the number of particles per unit volume and per unit time) depends only on their mass m_{X} and cosmological time t:

$$\frac{\mathrm{d}N_{\mathrm{X}}}{\mathrm{d}t} = k m_{\mathrm{X}}^{p} t^{-4+p}, \tag{4.1}$$

where k and p are dimensionless constants whose values depend on the sort of superheavy particle [38]. If the UHECR flux observed by AGASA [8, 9] and HiRes [11, 12] is assumed to be caused by nucleons from high-energy jets produced in X-particle decays, then for the above to be true the necessary value is $\mathrm{d}N_{\mathrm{X}}/\mathrm{d}t \approx (1.5-2.5)\times 10^{-37}\ \mathrm{m}^{-1}\,\mathrm{s}^{-1}$.

Another possibility could be that superheavy quasistable X-particles are relic remnants of the Big Bang epoch, and have still not decayed. Such particles could have been produced in the early universe via gravity from vacuum fluctuations during the inflation stage of expansion [36, 37]. At present, X-particles may compose a significant part of the cold dark matter of the universe [204 – 206, 214]. X-particle masses may be of the order of the mass of the inflanton — a special scalar field of the inflation theory [36, 37]:

$$m_{\mathrm{X}} \geqslant m_{\phi} \approx 10^{22}\ \mathrm{eV}. \tag{4.2}$$

In this scenario, the existence of an unknown symmetry and of a mechanism for its dynamic breaking are necessary to ensure the very long lifetime of X-particles:

$$\tau_{\mathrm{X}} \approx 10^{10} - 10^{22}\ \mathrm{years}, \tag{4.3}$$

at least comparable to the age of the universe. As candidates for superheavy X-particles,e.g., WIMPZILLA [207] and SIMPZILLA [208] are considered.

4.2 Neutrino fluxes from X-particle decays

Calculation of neutrino spectra in the top-down scenario is based on quark hadronization processes described by quantum chromodynamics (QCD). The decays of X-particles of any kind result in quark and lepton production. In quark hadronization, hadron jets originate together with unstable leptons. Pion decays produce fluxes of high-energy photons, light leptons, and neutrinos. A small admixture of protons and neutrons is also present. The complete function

of fragmentation into a hadron jet, initiated by a quark, is described in QCD by the expression [29, 90, 209]

$$\frac{\mathrm{d}N_\mathrm{h}(x)}{\mathrm{d}x} \approx \frac{15}{16}\, x^{-3/2}(1-x)^2 . \tag{4.4}$$

If $x = 2E/m_\mathrm{X} \ll 1$, then expression (4.4) is well approximated by the power law

$$\frac{\mathrm{d}N_\mathrm{h}(E)}{\mathrm{d}x} \propto E^{-1.5} . \tag{4.5}$$

If an X-particle is assumed to decay into N_q quarks and N_l leptons and the energy m_X to be uniformly distributed among them, then the nucleon spectrum from the decay of an X-particle of any nature can be described by the expression [90, 209]

$$\Phi_\mathrm{N}(E_i, t_i) = \frac{\mathrm{d}N_\mathrm{X}(t_i)}{\mathrm{d}t}\, N_\mathrm{q} f_\mathrm{N}\, \frac{N_\mathrm{q}+N_\mathrm{l}}{m_\mathrm{X}}\, \frac{\mathrm{d}N_\mathrm{h}}{\mathrm{d}x} , \tag{4.6}$$

where E_i is the energy of the emitted hadron, f_N is the fraction of energy attributed to nucleons in the hadron jet, and $x = (N_\mathrm{q}+N_\mathrm{l})\, E_i/m_\mathrm{X}$.

The spectrum of γ-quanta from neutral pion decays $\pi^0 \to 2\gamma$ in the jet has the form [90]

$$\Phi_\gamma(E_i, t_i) \approx 2 \int_{E_i}^{m_\mathrm{X}/(N_\mathrm{q}+N_\mathrm{l})} \Phi_{\pi^0}(E, t_i)\, \frac{\mathrm{d}E}{E} , \tag{4.7}$$

where

$$\Phi_{\pi^0}(E, t_i) \approx \frac{1}{3}\, \frac{1-f_\mathrm{N}}{f_\mathrm{N}}\, \Phi_\mathrm{N}(E, t_i)$$

represents the spectrum of neutral pions in the jet.

Finally, the neutrino spectrum from charged pion decays $\pi^\pm \to \mu^\pm \nu_\mu(\bar\nu_\mu)$ in the jet is given by [38, 90]

$$\Phi^{\pi\to\mu\nu}_{\nu_\mu+\bar\nu_\mu}(E_i, t_i) \approx 2.34 \int_{2.34E_i}^{m_\mathrm{X}/(N_\mathrm{q}+N_\mathrm{l})} \Phi_{\pi^++\pi^-}(E, t_i)\, \frac{\mathrm{d}E}{E} , \tag{4.8}$$

where $\Phi_{\pi^++\pi^-} = 2\Phi_{\pi^0}$. With the neutrinos from muon decays taken into account, the final muon neutrino spectrum from X-particle decays is twice (4.8):

$$\Phi_{\nu_\mu+\bar\nu_\mu}(E_i, t_i) = 2\Phi^{\pi\to\mu\nu}_{\nu_\mu+\bar\nu_\mu}(E_i, t_i) , \tag{4.9}$$

while the electron neutrino spectrum is the same as in (4.8).

Two independent methods are used in calculations of neutrino fluxes resulting from X-particle decays producing quarks and leptons. In the first, the hadron fragmentation functions are determined by the Monte Carlo method with the use of the QCD event generator JETSET and HERWIG [210]. The second method is based on an analytic approach involving an approximation in which the total fragmentation function into hadrons, $\mathrm{d}N_\mathrm{h}/\mathrm{d}x$, is proportional to the parton (quark and gluon) spectra in the parton cascade initiated by a quark [90]. The parton distributions are deduced from the solutions of the Dokshitzer – Gribov – Lipatov – Altarelli – Parisi (DGLAP) evolution equations of perturbative QCD [211 – 213]. Supersymmetry effects are also taken into account [216, 217]. In calculations based on accelerator data from LEP and HERA, the fraction of the jet energy transferred to hadrons is assumed to be between 3 and 10%, while the remaining energy is transferred to π^0, π^+, π^- in equal parts [217]. Therefore, in a hadron jet produced by a quark, pions are predominant, and hence

$$\frac{\Phi_{\pi^0}}{\Phi_\mathrm{N}} \approx \frac{1}{3}\, \frac{1-f_\mathrm{N}}{f_\mathrm{N}} = 10 , \qquad \frac{\Phi_{\pi^+\pi^-}}{\Phi_\mathrm{N}} \approx 20$$

for the value $f_\mathrm{N} \approx 0.03$. Thus, in top-down scenarios, a small part of the energy is liberated in the form of photons and neutrinos. Because neutrino spectrum (4.8) is determined by the fragmentation function into a hadron jet, $\mathrm{d}N_\mathrm{h}/\mathrm{d}x$ in (4.4), it also exhibits a power-law form like (4.5):

$$\Phi_{\nu_\mu+\bar\nu_\mu}(E_i, t_i) \propto E^{-1.5} . \tag{4.10}$$

In Ref. [218], the results of hadron spectrum calculations for decays of X-particles of masses $M_\mathrm{X} > 10^{21}$ eV are compared using the Monte Carlo method [210] and the DGLAP equations [90, 214 – 217]. The main conclusion of the work is that the hadron spectra thus calculated are in good agreement with each other. Consequently, the γ-quantum and neutrino spectra obtained on their basis exhibit quite a universal form, independent of the specific TD production processes, as well as the emission and decay of X-particles.

Neutrino fluxes calculated within the top-down decay scenario of X-particles of different masses are presented in Fig. 8. The fluxes have a common tendency of increasing with the X-particle mass and at $M_\mathrm{X} = 2\times10^{21} - 2\times10^{25}$ eV amount to [90, 107, 117, 214 – 217]

$$E_\nu^2 \Phi_\nu^{\text{top-down}}(E_\nu) \leqslant (1-5)\times10^2 \text{ eV cm}^{-2}\,\text{s}^{-1}\,\text{sr}^{-1}. \tag{4.11}$$

Neutrino fluxes produced in the decays of mirror X-particles were estimated in Ref. [203]. Such a scenario assumes the chain of decays $\mathrm{X}_\mathrm{mirror} \to \pi^\pm_\mathrm{mirror} \to \nu_\mathrm{mirror}$. The produced mirror neutrinos ν_mirror, while covering cosmological distances, oscillate into ordinary neutrinos: $\nu_\mathrm{mirror} \to \nu_i$. The resulting neutrino flux in the mirror top-down scenario may be very large. For example, for $M_\mathrm{X} \approx 10^{25}$ eV, oscillation probabilities $P_\mathrm{osc} \approx 1/2$, and energies $E_\nu \approx 10^{20}$ eV, this flux may exceed the value in (4.11) by nearly two orders of magnitude:

$$E_\nu^2 \Phi_\nu^{\text{top-down (mirror)}} \approx 10^4 \text{ eV cm}^{-2}\,\text{s}^{-1}\,\text{sr}^{-1}. \tag{4.12}$$

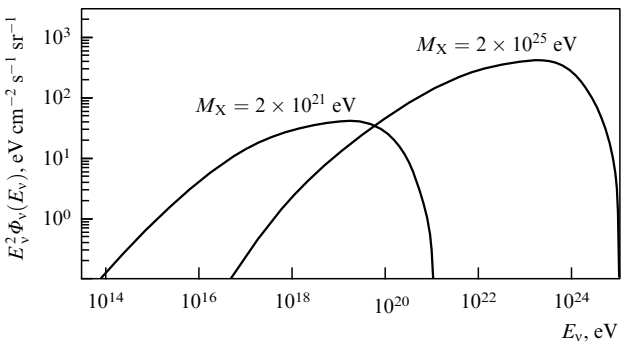

Figure 8. Neutrino fluxes in the top-down decay scenario of X-particles of different masses [215].

5. Background of atmospheric neutrinos at high energies

In experiments devoted to the observation of neutrinos of astrophysical origin, the main source of the background is high-energy atmospheric neutrino fluxes. Primary CR (mostly protons) interact in the upper layers of the earth's atmosphere, giving rise to cascades of elementary particles, a significant part of which consists of pions [219]. The decay chains of charged pions (2.37) determine the ratio of muon to electron neutrino fluxes:

$$\frac{\Phi^{\rm atm}(\nu_\mu+\bar\nu_\mu)}{\Phi^{\rm atm}(\nu_e+\bar\nu_e)}\approx 2:1\,. \tag{5.1}$$

For a more precise estimation of neutrino fluxes of atmospheric origin, kaon decay channels (the main mode is $K^+\to\mu^++\bar\nu_\mu$), charmed particle decays (of D-, $\bar{\rm D}$-mesons and of Λ_C-baryons) containing ν_μ, $\bar\nu_\mu$, ν_e, and $\bar\nu_e$ and the energy dependence of neutrino fluxes must be taken into account. As energy increases, a larger and larger part of muons reaches the earth's surface without undergoing interaction, thus enhancing ratio (5.1). The calculated value of this ratio is model dependent, because it contains the uncertainties in the primary CR fluxes and in processes of hadron production in the upper atmosphere. The absolute ν_μ and ν_e fluxes are known with the uncertainty 20–25% [220, 221]. The calculated value of the ratio between neutrino fluxes, Eqn (5.1), is ~ 2 for energies below 2 GeV [222], and reaches 8 for energies $E_\nu\approx 100$ GeV [223].

At energies around 100 TeV, the pion and kaon decay lengths become so large that these particles start interacting with nuclei in the atmosphere before having time to decay. This effect leads to a rapidly decreasing energy spectrum of the atmospheric neutrinos [219, 223]:

$$\Phi_\nu^{\rm atm}\propto E_\nu^{-2.7}\,. \tag{5.2}$$

At energies above 100 TeV, the decays of charmed hadrons (D^0-, $D^\pm$-, D_s-mesons and Λ_C-baryons) as well as B-particles start to contribute to the atmospheric neutrino fluxes significantly. The muons and neutrinos originating in such decays have been termed 'prompt.' All charmed and B-hadrons are short-lived with characteristic lifetimes $\sim 10^{-12}$ s, and up to energies of 10^{17} eV, they do not manage to interact before they decay. Thus, the spectrum of prompt neutrinos extends up to energies of 10^{17} eV.

Estimation of atmospheric neutrino fluxes at ultrahigh energies is performed on the basis of computed charmed and B-particle production cross sections, fragmentation functions of c- and b-quarks, and the fraction of decays proceeding via neutrino modes [224-231]. Figure 9 presents prompt ν_e and ν_μ fluxes calculated in Ref. [231]. It can be seen from the figure that the contributions of ν_e and ν_μ fluxes produced in the decays of charmed particles are comparable to the contributions of neutrinos from pion and kaon decays at energies $E_\nu\approx 3\times 10^{14}$ eV, while at higher energies, they become definitive. The main source of atmospheric ν_τ are lepton decays of D_s-mesons, $D_s\to\tau\nu_\tau$, with the subsequent decay $\tau\to\nu_\tau X$. The ν_τ fluxes extend up to 10^{17} eV — the limit energy above which the decay lengths of the relativistic D_s-meson and τ-lepton are greater than the vertical distance from the production point in the upper atmosphere to the earth's surface [229]. In Refs [228, 229], the ν_τ flux from decays of the $b\bar b$-quark system was also shown to provide an additional contribution to the total neutrino flux, amounting to about 30% of the flux due to decays of the charmed $c\bar c$-quark system.

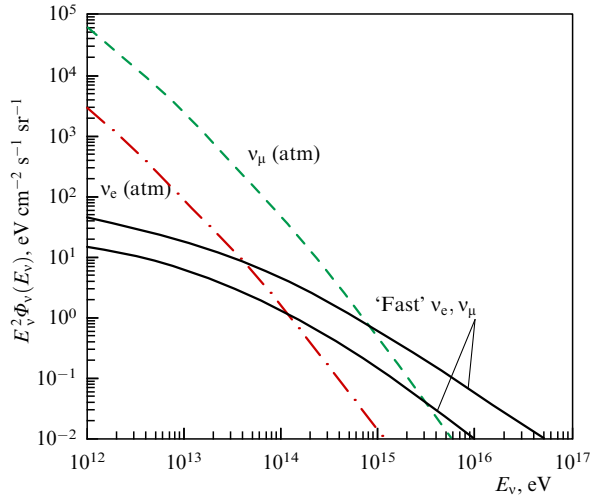

Figure 9. Fluxes of atmospheric 'prompt' ν_e and ν_μ neutrinos from charmed particle decays [231] are indicated by the region between the solid curves, which corresponds to uncertainties in the PDF behavior at small x values. The dashed and dashed-dotted lines show the atmospheric ν_μ and ν_e fluxes due to pion and kaon decays.

Astrophysical neutrino sources can be revealed only if the observed number of neutrino events significantly exceeds the computed amount of fast neutrinos. This condition must be satisfied within a broad range of energies. At $E_\nu\approx 10^{16}$ eV, the expected neutrino fluxes from GRBs and AGNs (see Figs 6 and 7) exceed the prompt neutrino flux by 2 and 4 orders of magnitude, respectively. For higher energies, where neutrino fluxes are the ones expected in top-down scenarios, the background of prompt neutrinos becomes negligible.

6. Deep-inelastic neutrino – nucleus interactions in the Standard Model at ultrahigh energies

To estimate the expected number of astrophysical neutrino interaction events to be registered by one detector or another, it is necessary to know, besides the neutrino spectra of various sources, the neutrino interaction cross sections with matter at different energies. The maximum neutrino energies for which neutrino – nucleus cross sections have been measured, were achieved in the NuTeV experiment at the FNAL accelerator and did not exceed ~ 400 GeV [43]. To determine the cross sections at higher energies, it is necessary to use calculations that involve various model assumptions and are consistent with Lorentz invariance, gauge invariance, and s-wave unitarity. First, we deal with the traditional computational schemes, based on the SM framework.

Neutrinos interact with the matter nucleons in charged current (CC) reactions

$$\nu_l(\bar\nu_l)+{\rm N}\to l^\mp(l^\pm)+{\rm X} \tag{6.1}$$

and neutral current (NC) reactions

$$\nu_l(\bar\nu_l)+{\rm N}\to\nu_l(\bar\nu_l)+{\rm X}\,, \tag{6.2}$$

where $l={\rm e},\mu,\tau$ and X represents all the hadrons produced as a result of the interaction.

The energy dependence of νN-interaction cross sections is different in different energy regions. At small energies $E_\nu \ll M_W^2/2M_N$ (where M_W and M_N are the W-boson and nucleon masses), the total cross section increases proportionally to the neutrino energy: $\sigma_{\nu N} \propto E_\nu$. The linear growth of the cross section is determined by the propagator of the W-boson and the parton distribution functions being nearly independent of Q at small Q^2 values. At energies $E_\nu \approx 10^4$ GeV, the exchange of a W-boson in interactions (6.1) leads to the growth of the cross section slowing down. In the high-energy region $E_\nu > 10^6$ GeV, the total cross section once again starts growing more rapidly. This is caused by enhancement of the PDF, due to the additional contributions from quarks with $x \ll 1$.

Deep-inelastic interaction processes of neutrinos with nuclei are traditionally described by the quark–parton model (QPM). Within the QPM framework, the differential inclusive neutrino interaction cross section with an isoscalar target can be expressed via the Bjorken scaling variables $x = Q^2/2M_N\nu$ and $y = \nu/E_\nu$ and the nucleon structure functions F_i as [232]

$$\frac{d^2\sigma_{\nu N,\,\bar\nu N}}{dx\,dy} = \frac{G_F M_N E_\nu}{\pi}\left(\frac{M_i^2}{Q^2+M_i^2}\right)^2 \times\left[\frac{1+(1-y)^2}{2}F_2^\nu(x,Q^2) - \frac{y^2}{2}F_L^\nu(x,Q^2) \pm y\left(1-\frac{y}{2}\right)xF_3^\nu(x,Q^2)\right], \quad (6.3)$$

where Q^2 is the squared momentum transferred from the incident neutrino to the secondary lepton, E_ν is the neutrino energy in the laboratory reference system, $\nu = E_\nu - E_l$, M_N is the nucleon mass, and M_i represents the mass M_W or M_Z of the W- or Z-boson, respectively, depending on the cross section of which reaction is being computed (CC or NC). The structure functions F_i are dimensionless and depend on two variables: the dimensionless ratio x and the quantity Q^2, which exhibits dimensionality.

The procedure for calculating the cross sections $\sigma_{\nu N}(E_\nu)$ starts with parameterization of the parton distribution functions. For this, data are used from experiments at the HERA and FNAL accelerators, obtained for maximum Q_0^2 values and minimum x values. Most calculations of cross sections in the high-energy region have been performed based on PDFs with Martin–Roberts–Stirling [233–237] and Glück–Reya–Vogt [48, 49] parameterizations, and that of the CTEQ group [238–243].

Then, applying one PDF parameterization or another with known Q_0^2 for extrapolation to large Q^2 values (not achievable in experiments), one proceeds to solve the set of integral DGLAP evolution equations of perturbative QCD [211–213]

$$Q^2\frac{dq(x,Q^2)}{dQ^2} = \frac{\alpha_S(Q^2)}{2\pi}\int_x^1\frac{dy}{y}\left[P_{qq}\left(\frac{x}{y}\right)q(y,Q^2) + P_{qG}\left(\frac{x}{y}\right)G(y,Q^2)\right],$$
$$Q^2\frac{dG(x,Q^2)}{dQ^2} = \frac{\alpha_S(Q^2)}{2\pi}\int_x^1\frac{dy}{y}\left[P_{Gq}\left(\frac{x}{y}\right)q(y,Q^2) + P_{GG}\left(\frac{x}{y}\right)G(y,Q^2)\right], \quad (6.4)$$

where $q(x,Q^2)$ and $G(x,Q^2)$ are the quark and gluon distributions and P_{qq}, P_{qG}, P_{Gq}, and P_{GG} are the so-called splitting functions describing the probabilities of the respective processes.

In Refs [50, 51], calculations of neutrino–nucleus cross sections at energies $E_\nu = 10^9 - 10^{21}$ eV were based on the CTEQ3 [238] and CTEQ4 [239] parton distributions and on the DGLAP equations. In the region of energies $10^{16} \leqslant E_\nu \leqslant 10^{21}$ eV, the cross sections obtained in Ref. [51] are approximated with a 10% precision by the expression

$$\sigma_i^j(E_\nu) = K_i^j \times 10^{-36}\ \text{cm}^2\left(\frac{E_\nu}{1\ \text{GeV}}\right)^{0.363}, \quad (6.5)$$

where $i = \nu N, \bar\nu N$; $j =$ tot, CC, NC, with $K_{\nu N}^{tot} = 7.84$, $K_{\nu N}^{CC} = 5.53$, $K_{\nu N}^{NC} = 2.31$, $K_{\bar\nu N}^{tot} = 7.80$, $K_{\bar\nu N}^{CC} = 5.52$, and $K_{\bar\nu N}^{NC} = 2.29$.

Solution of the DGLAP equations implies summation over powers of $\ln(Q^2/Q_0^2)$. However, besides the Q^2-dependence, an important new feature of neutrino cross section calculations at ultrahigh energies consists in contributions to PDFs from small values of

$$x = \frac{Q^2}{ys_{\nu N}} = 2\times10^{-4}\left(\frac{Q^2}{M_W^2}\right)\left(\frac{0.2}{y}\right)\left(\frac{10^{17}\ \text{eV}}{E_\nu}\right). \quad (6.6)$$

If at neutrino energies $E_\nu \approx 10^{15}$ eV the structure functions are sensitive to values of $x \approx 10^{-2}$, then at neutrino energies $E_\nu \approx 10^{19} - 10^{21}$ eV, they are sensitive to values of $x \leqslant 10^{-6} - 10^{-8}$. Thus, in calculations of cross sections in the energy region $E_\nu \approx 10^{19} - 10^{21}$ eV, there arise theoretical uncertainties related to the low-energy Q^2-parameterization and to the necessity of extrapolating parton distributions to large values of $Q^2 \approx M_W^2$, on the one hand, and to small x values, on the other.

A method for calculating νN cross sections based on the simultaneous solution of DGLAP equations and Balitsky–Fadin–Kuraev–Lipatov (BFKL) equations [244, 245] was proposed in Refs [52–54]. Such a unified approach permits taking important contributions proportional to $\ln(1/x)$ into account in addition to contributions proportional to $\ln(Q^2/Q_0^2)$. In this case, the cross sections are extrapolated to the region $x \leqslant 10^{-5}$, which cannot be achieved even in record measurements carried out at the HERA collider [44–46].

Table 1 presents the results of the neutrino cross section calculations in Refs [51, 53]. It can be seen that at ultrahigh energies, the cross sections $\sigma_{\nu N}^{CC}$ and $\sigma_{\bar\nu N}^{CC}$ calculated in these works practically coincide, while the difference between the cross sections $\sigma_{\nu N}^{NC}$ and $\sigma_{\bar\nu N}^{NC}$ is not above 30%. The cross sections presented are the same for the interactions of neutrinos of all flavors. The differences of $\nu_\tau N$ from $\nu_e N$ and $\nu_\mu N$ cross sections are revealed only at quite low energies and are discussed in Ref. [246]. To describe the $\nu_\tau N$ cross sections, two additional structure functions F_4 and F_5 are introduced, which are neglected in calculations of the $\nu_e N$ and $\nu_\mu N$ interactions because of a suppression factor depending on the square charged lepton mass, $m_l^2/M_N E_\nu$. The difference in the cross sections decreases as the energy increases and it is already less than 5% at $E_\nu \approx 10^3$ GeV. This is demonstrated in Fig. 10.

It is well known that enhancement of the inelastic cross section is restricted by unitarity, which in accordance with the optical theorem relates the total νN cross section and the imaginary part of the elastic amplitude of the forward νN scattering [247]. In the language of the parton model,

Table 1. Results of the νN cross section calculations from work by Gandhi, Quigg, Reno, and Sarcevic (GQRS) [51] based on the CTEQ4 distributions for DGLAP equations, and also from the work by Kwiecinski, Martin, and Stasto (KMS) [53] based on the unified DGLAP – BFKL formalism.

E_ν, GeV	$\sigma_{\nu N}^{CC}$, cm^2		$\sigma_{\nu N}^{NC}$, cm^2		$\sigma_{\bar\nu N}^{CC}$, cm^2		$\sigma_{\bar\nu N}^{NC}$, cm^2	
	GQRS	KMS	GQRS	KMS	GQRS	KMS	GQRS	KMS
10^5	2.02×10^{-34}	2.07×10^{-34}	7.66×10^{-35}	7.33×10^{-35}	1.68×10^{-34}	1.74×10^{-34}	6.52×10^{-35}	6.20×10^{-35}
10^6	6.34×10^{-34}	6.47×10^{-34}	2.60×10^{-34}	2.28×10^{-34}	6.05×10^{-34}	6.19×10^{-34}	2.49×10^{-34}	2.18×10^{-34}
10^7	1.75×10^{-33}	1.73×10^{-33}	7.48×10^{-34}	5.95×10^{-34}	1.73×10^{-33}	1.73×10^{-33}	7.42×10^{-34}	5.90×10^{-34}
10^8	4.43×10^{-33}	4.33×10^{-33}	1.93×10^{-33}	1.45×10^{-33}	4.43×10^{-33}	4.32×10^{-33}	1.94×10^{-33}	1.45×10^{-33}
10^9	1.05×10^{-32}	1.04×10^{-32}	4.64×10^{-33}	3.38×10^{-33}	1.05×10^{-32}	1.04×10^{-32}	4.64×10^{-33}	3.38×10^{-33}
10^{10}	2.38×10^{-32}	2.40×10^{-32}	1.06×10^{-32}	7.61×10^{-33}	2.41×10^{-32}	2.40×10^{-32}	1.07×10^{-32}	7.61×10^{-33}
10^{11}	5.36×10^{-32}	5.38×10^{-32}	2.38×10^{-32}	1.66×10^{-32}	5.36×10^{-32}	5.38×10^{-32}	2.38×10^{-32}	1.66×10^{-32}
10^{12}	1.18×10^{-31}	1.17×10^{-31}	5.20×10^{-32}	3.53×10^{-32}	1.17×10^{-31}	1.17×10^{-31}	5.20×10^{-32}	3.53×10^{-32}

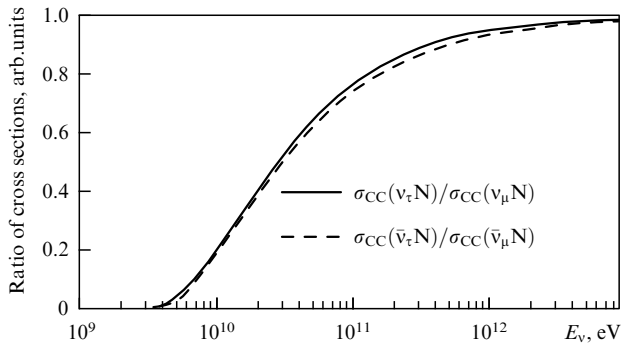

Figure 10. Ratio of charged current ν_τN to ν_μN cross sections for neutrinos and antineutrinos.

saturation of the cross section sets in owing to gluon recombination gg → g. In the case of large gluon densities, the contributions from these processes plays a screening role and restrict the growth of the νN cross section in accordance with the unitarity bound [248]. The contributions of gluon recombination can be described by nonlinear terms arising in the Balitsky – Kovchegov (BK) equations [249, 250]. As shown in Refs [251, 252], solutions of the BK equations exhibit properties of geometric scaling on the characteristic scale of saturation $Q_s^2(x) \propto x^{0.3}$. This is similar to the behavior of the dipole cross section in the saturation model [253, 254]

$$\sigma_{dip}(r,x) = \sigma_0\left[1-\exp\left(-\frac{r^2Q_s^2(x)}{4}\right)\right], \qquad (6.7)$$

which describes the interaction of a quark – antiquark pair (a color dipole of dimension r) with a nucleon. Saturation in this model is a manifestation of the dipole scattering amplitudes $A(r,x) = [1-\exp(-r^2Q_s^2(x)/4)]$ achieving the unitary limit A = 1 for dipole dimensions $r_0 > 1/Q_s(x)$ [255]. Cross section (6.7) saturates to the value σ_0, and hence $\sigma(r,x)/\sigma_0 \to 1$, and ceases to depend on either r or x. On the other hand, when $r_0 < 1/Q_s(x)$, cross section (6.7) is small and $\sigma(r,x)/\sigma_0 \propto\propto r^2Q_s^2(x)/4$. For a more precise description of the dipole cross section in the region of small dipole dimensions corresponding to large Q^2 values, the DGLAP equations [256] were introduced into the saturation model [253, 254].

Calculations of νN cross sections at ultrahigh energies, with the DGLAP – BFKL formalism supplemented by nonlinear contributions due to gluon recombination from the BK equations, were made in Ref. [55]. In the same work and also in Refs [257, 258], the calculations of neutrino cross sections were based on the model of a color quark – antiquark dipole with the addition of gluon contributions.

Figure 11 presents the results of νN cross section calculations at ultrahigh energies, obtained within the SM framework in Refs [48, 51, 53, 55]. It can be seen from this figure that the model cross sections obtained for various phenomenological realizations of linear and nonlinear QCD are in agreement with each other even in the energy region $E_\nu = 10^{10}-10^{12}$ eV. At the very highest energies, the maximum and minimum cross section values, $\sigma_{tot}^{\nu N}(E_\nu = 10^{12}\ \text{GeV}) \approx (1-2)\times10^{-31}$ cm^2 only differ by a factor of 2. Most likely, this points to the cross section estimation in the predicted energy region being reasonable.

In the works discussed above, the growth dynamics of the νN cross section with energy is determined by the PDF behavior at large Q^2 values and very small x. In the nearest future, new measurements of the PDF at the LHC collider will be sensitive to x values even smaller than at HERA. These measurements will permit determining the νN cross sections

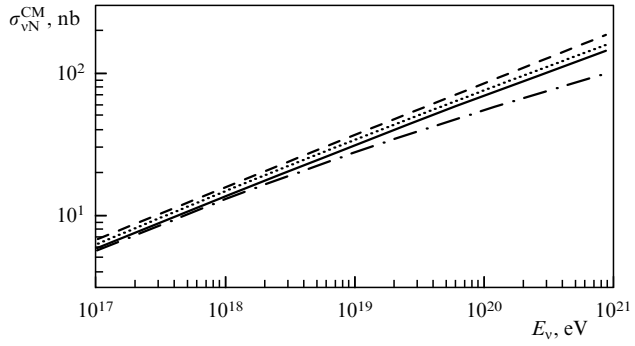

Figure 11. Total neutrino – nucleus cross sections $\sigma_{\nu N}^{CM}$ at ultrahigh neutrino energies, calculated within the SM framework for various phenomenological realizations of linear and nonlinear QCD: dashed line — DGLAP equations and PDF dynamic parameterization [48], dotted line — DGLAP equations and CTEQ4 parameterization [51], solid line — the unified DGLAP – BFKL formalism [53], dashed-dotted line — the model of the dipole cross section saturation [55].

with a high degree of reliability at least up to energies $E_\nu \approx 10^{17}$ eV. However, it is already evident that standard neutrino cross sections are lower than hadron cross sections approximately by 5–6 orders of magnitude, even at $E_\nu \approx 10^{21}$ eV (see Fig. 11). This is the main argument against assuming the neutrino to be a possible source of CR events of energies higher than the GZK-cutoff. Given such cross section values, even at ultrahigh energies the amount of registered atmospheric showers due to neutrinos should be extremely small, and they should originate with practically the same probability over the entire depth of the atmosphere. These assertions contradict observations of CR fluxes. On the other hand, the transparency of the universe to the neutrino, as well as indications of a certain clusterization of CR events with energies above the GZK threshold arriving from directions associated with distant astrophysical objects, is considered by a number of authors to be evidence in favor of precisely neutrinos being the possible source of such events. About 40 years ago, Berezinsky and Zatsepin considered [56] the idea of a strong increase in νN cross sections at energies above the GZK-cutoff as a possible solution. If the neutrino cross section is assumed to have a value of the order of a millibarn at energies $E_\nu \approx 10^{20}$ eV, then the observed UHECR flux and the absence of 'deeply penetrating' CR events is readily explained. To obtain νN cross section values significantly superior to the ones considered in this section is only possible in scenarios involving, to some extent, the New Physics beyond the SM.

7. Neutrino–nucleus cross sections and the new physics

7.1 Electroweak processes induced by instantons

Taking the contributions from instanton-induced nonperturbative electroweak processes into account allows obtaining neutrino cross sections reaching values of hadron interaction cross sections, even remaining within the SM framework [259]. In the SM, instantons describe fluctuations of non-Abelian gauge fields — tunneling between degenerate topologically nonequivalent vacua — and are associated with axial anomalies, violating the conservation of the sum of the baryon and lepton numbers, B + L. The corresponding tunnel barrier is determined by the energy of the sphaleron — an unstable static solution of the Yang–Mills equations — $E_{sp} \approx \pi M_W/\alpha_W \approx 10$ TeV. Below this energy, instanton processes are exponentially suppressed. If, on the contrary, energies above E_{sp} are achieved, then instanton-induced processes may not be suppressed, which leads to an increase in the parton–parton cross sections. Instanton processes may be observable in deep-inelastic interactions at ultrahigh energies and identified by a characteristic signature — the existence of hadron final states with anomalously high multiplicities [260, 261]. There are indications that such anomalous events are observed in the H1 [262] and ZEUS [263] experiments at the HERA collider.

The actual values of instanton contributions to the νN cross section are difficult to calculate unambiguously [264]. Two approaches are used for their estimation: the first is perturbative, involving an instanton background field [259], and the second is semiclassical [265, 266]. In both approaches, a very rapid enhancement is expected of the νN cross section above the threshold energy estimated as $E_\nu^{th} \approx 10^{18}$ eV in Ref. [259] and $E_\nu^{th} \geqslant 10^{19}$ eV, in accordance with calculations

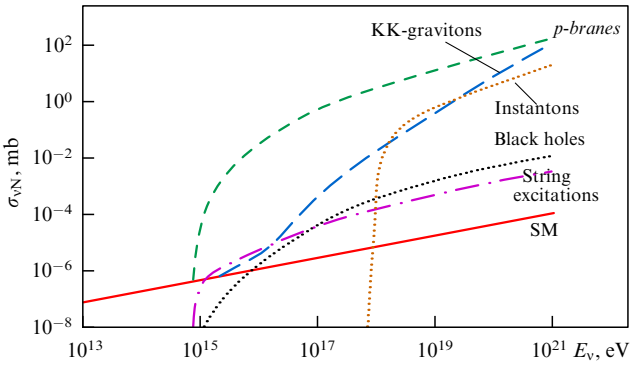

Figure 12. Neutrino–nucleus cross sections in nonstandard scenarios: if account is taken of the contributions due to instanton-induced processes [261]; due to the exchange of KK gravitons in the mode $\sigma_{\nu N}^{KK} \propto \log s$ with $M_{4+n} = 1$ TeV [63]; in the case of excitation of string resonances on the string scale $M_s = 1$ TeV with account of neutrino–quark interactions and neutrino–gluon scattering [291, 292]; in the case of microscopic black holes produced in νN interactions, with $M_{4+n} = 1$ TeV, $M_{BH,min}/M_{4+n} = 1$, $n = 7$ [66, 287]; and of p-branes on a scale $M_{4+n} = 1$ TeV, with the number of asymmetric extra dimensions $n = 7$, $p = 6$ [68]. The standard SM cross section in Ref. [51] is shown for comparison.

in the semiclassical approximation [265, 266]. At energies $E_\nu \approx 10^{20}$ eV, the neutrino–nucleus cross sections in the instanton mode, determined within these approaches, differ by three orders of magnitude, reaching the respective values $\sigma_{\nu N}^{inst} \approx 1$ mb [261] and $\sigma_{\nu N}^{inst} \approx 10^3$ mb [267]. The neutrino–nucleus cross section due to the contribution of instanton-induced processes, calculated perturbatively, is shown in Fig. 12.

7.2 New particles, interactions, and symmetries

In supersymmetric theories, new particles are introduced — supersymmetric partners of SM particles. The processes of the direct superpartner particle production in ordinary neutrino interactions may introduce additional contributions to the νN cross sections. However, the values actually added to the standard SM cross sections are not large. Estimations in [268] reveal the additional contribution to the $\nu_\mu N \to \mu^- X$ reaction cross section due to squark production in the s-channel of $\nu_\mu d_L \to \tilde{d}_R \to \mu_L^- u_L$, which involves valence quarks, and of the $\tilde{d}_R$ exchange u-channel in the reaction $\nu_\mu \bar{u} \to \bar{d}\mu^-$, involving only sea quarks, to increase the SM cross section by no more than 60 and 30% for the respective right squark masses $\tilde{m}_R = 200$ and 400 GeV.

In νN interactions at high energies, the production of bound states of leptons and quarks — leptoquarks (LQs) — may occur. Estimations in [269] reveal additional contributions from the processes $\nu_\mu q \to LQ \to \mu + q'$ and $\nu_\mu q \to LQ \to \nu_\mu + q$ to the νN cross section to be proportional to the mass of the leptoquark state, $M_{LQ}^{-0.5}$. If the leptoquark mass is $M_{LQ} \approx 200$ GeV, the addition to the SM cross section does not exceed 40% and becomes even smaller as M_{LQ} increases.

The possibility of increasing the νN cross section by introducing a new broken quark and lepton 'generation symmetry,' described by the SU(3) group, is considered in Ref. [270]. In this scheme, new color and gauge bosons without charge lead to interactions of the neutral current involving a change of flavor. Such gauge bosons must be very heavy (with masses in the 10–100 TeV range), such that at

energies below 100 TeV, interactions via exchanges by these gauge bosons play a negligibly small role compared to the standard neutrino interactions due to weak forces. But above 100 TeV, the new interactions may result in νN and nuclear cross sections being of the same order of magnitude.

7.3 Quantum gravity with large extra space – time dimensions

A radically new approach to the possibility of significantly enhancing the νN cross section is related to quantum gravity theories involving large extra space – time dimensions. Early Grand Unification theories were based on the idea that unification of all interactions occurs in the vicinity of the Planck scale, $M_{\rm Pl} \equiv G_4^{-1/2} \approx 10^{28}$ eV, where $G_4 = 6.707 \times 10^{-33}$ TeV^{-2} is the gravitational constant in a world of four-dimensional space – time. In a number of recent publications, unification on a new TeV scale is proposed for all interactions including gravity [59 – 62, 271, 272]. Such a 'premature' unification may take place owing to manifestation on this scale of extra dimensions, whose possible existence was first voiced by Kaluza and Klein [273]. For a long time, such extra dimensions were considered small, and hence they could not affect physics at relatively low energies. It has recently been shown within the framework of string models that some of these dimensions may be large (about a millimeter) without contradicting observational data, including the proton lifetime [274 – 277]. In this approach to gravity, space – time exhibits a *brane – bulk* structure. The *brane* space has a (3 + 1)-dimensionality of the ordinary space – time, in which all ordinary particles and SM fields exist. The *bulk* space, together with the (3 + 1)-dimensions of Minkowski space, also contains n extra dimensions, where gravity and, possibly, nonobservable gauge particles and SM singlets exist. In a world with n dimensions, the fundamental mass can be written as

$$M_{4+n} = G_{n+4}^{-1/(n+2)} . \tag{7.1}$$

There exist several models involving a TeV scale of quantum gravity. In the RS scenario [61, 62], the metric of the 4-dimensional space is additionally multiplied by a 'curving factor,' which is a function of one extra noncompactified dimension. In this case, gravity propagates along a slice of the anti-de Sitter (4 + 1)-space and the TeV scale of gravity exists at the same time as the Planck scale.

In the ADD scenario [59, 60], the existence of n extra space dimensions is assumed, with the gravitational potentials in 4- and $(n + 4)$-dimensions related by

$$G_4 = \frac{G_{n+4}}{V_n} . \tag{7.2}$$

The volume of space with n extra dimensions $V_n = R_1 \times R_2 \times \ldots \times R_n$ is determined by the compactification radii

$$R_n \approx 2 \times 10^{31/n-16} \text{ mm} \times \left(\frac{1 \text{ TeV}}{M_{4+n}} \right)^{1+2/n} . \tag{7.3}$$

It follows from (7.3) that for $M_{n+4} \approx 1$ TeV and $n = 2$, the characteristic size of the extra dimensions R amounts to millimeters. The relation between the fundamental interaction unification scale M_{4+n} and the macroscopic Planck scale is given by

$$M_{\rm Pl}^2 \approx M_{4+n}^{2+n} R_1 R_2 \ldots R_n . \tag{7.4}$$

The increase in the νN cross section in scenarios with a TeV scale of gravity, as compared with the SM cross section, is a consequence of the rapid growth of the density level of intermediate excited states — of Kaluza – Klein (KK) gravitons of spin 2 [278, 279]. High-energy neutrinos may exchange KK gravitons with quarks and gluons in the nucleon target, which leads to additional contributions to the cross section. As a result, in the vicinity of the scale $M_{4+n} \approx \sqrt{s} \approx 1$ TeV (which corresponds to an energy $E_\nu \approx 10^{15}$ eV in the nucleon rest frame), the νN cross section increases by several orders of magnitude compared to the standard cross section.

Estimates of additional contributions to the νN cross section due to the exchange by KK gravitons are quite ambiguous. For calculations in the energy region $\sqrt{s} \leqslant M_{4+n} \approx 1$ TeV, a perturbative approach was developed based on the Feynman sum rules [271, 280, 281]. But in the $\sqrt{s} \gg M_{4+n}$ mode, no reliable procedure for calculating gravitational scattering cross sections exists, and different authors apply three asymptotic forms for the cross section behavior: $\sigma_{\nu N}^{\rm KK}$ is proportional to $\log s$, s^1 and s^2 [63, 64, 278, 282 – 286]. The most realistic approximation, consistent with unitarity, assumes a linear growth of the cross section with energy [285],

$$\sigma_{\nu N}^{\rm KK} \approx \frac{4\pi s}{M_{4+n}^4} \approx 10^{-28} \left(\frac{1 \text{ TeV}}{M_{4+n}} \right)^4 \left(\frac{E_\nu}{10^{19} \text{ eV}} \right) \text{cm}^2 . \tag{7.5}$$

A follows from (7.5) and the results of calculations in [66, 87], presented in Fig. 12, the contribution to the νN cross section due to gravitational scattering on the quantum gravity scale $M_{4+n} \approx 1$ TeV may amount to approximately units of millibarns for of a neutrino of the energy $E_\nu \approx 10^{20}$ eV. A cross section of still another order of magnitude greater can be obtained if the growth mode is $\sigma_{\nu N}^{\rm KK} \propto s^2$ [63, 64, 284].

7.4 String resonance at the TeV scale of quantum gravity

Recent years have witnessed active development of string theories involving large extra dimensions and a TeV scale of quantum gravity. They are based on the assumption that the string scale at which unification of all interactions begins is far from the Planck scale and is related to the $(4 + n)$-dimensional quantum gravity scale by [288, 289]

$$M_{\rm s} = g_{\rm s}^{2/(n+1)} M_{4+n} , \tag{7.6}$$

where $g_{\rm s} \leqslant 1$ is the string unification constant.

String models predict that in the low-energy region, when $s < M_{\rm s}^2$, particles interact with cross sections in accordance with the SM. The cross section of the neutrino – quark (gluon) interaction in the vicinity of $s_0 \approx M_{\rm s}^2$ may rapidly increase owing to an increase in the density of states in the string excitation spectrum $\propto \exp(a\sqrt{s})$ [278, 279]. The unitary scattering amplitudes of an open string are constructed on the Veneziano amplitudes [290] and form resonances at the energies [281]

$$\sqrt{s} = \sqrt{n} M_{\rm s} . \tag{7.7}$$

The contributions of string resonances to the νN cross sections were calculated taking neutrino – quark interactions [291] and neutrino – gluon scattering [292] into account, and are shown in Fig.12. The energy dependence of the νN cross section due to contributions from string resonances is weaker

than in the case of contributions from KK gravitons. Taking string excitations into account permits increasing the total νN cross section as compared to the SM value, but even in the case of extremely high energies ($E_\nu \approx 10^{22}$ eV), not more than up to $\sigma_{\nu N}^{\rm string} \sim 10^{-2}$ mb [292].

7.5 Microscopic black holes

A most remarkable event on the TeV scale of quantum gravity is the possibility of producing black holes [65, 66, 287, 293–295]. In the ordinary 4-dimensional world, a black hole originates as the result of gravitational collapse. When the radii of extra dimensions R_n are much smaller than the Schwarzschild radius of the black hole R_S defined in $(4+n)$-dimensional space, then such a black hole represents an ordinary 4-dimensional object. If, on the contrary, $R_n \gg R_S$, there may arise microscopic black holes of spherical symmetry that are virtual $(4+n)$-dimensional objects of a characteristic size less than R_n. In a space with n large extra dimensions, microscopic holes can be produced in high-energy scattering processes at energies $\sqrt{s} \geqslant M_{n+4}$, resulting in an increase in the cross sections of the respective interaction processes.

The cross section of black hole production due to the interaction of partons i and j with a center-of-mass energy $\sqrt{\hat{s}} \approx M_{\rm BH}$ can be estimated on the basis of geometrical arguments for the impact parameter $b < R_S$ [65, 66] as

$$\hat{\sigma}_{ij}^{\rm BH}(\sqrt{\hat{s}}) \approx \pi R_S^2 = \frac{1}{M_{4+n}^2}\left[\frac{M_{\rm BH}}{M_{4+n}}\,\frac{1}{n+2}\,8\Gamma\left(\frac{n+3}{2}\right)\right]^{2/(n+1)}. \qquad (7.8)$$

The neutrino is an effective source of possible microscopic black hole production in the atmosphere. The total production cross section of black holes originating in neutrino scattering on nucleons is determined as [66, 292]

$$\sigma_{\nu N}^{\rm BH}(\sqrt{s}) = \sum_i \int_{M_{\rm BH,\,min}^2/s}^1 {\rm d}x\, \hat{\sigma}_i(xs)\, F_i(x, Q^2)\,, \qquad (7.9)$$

where $s = 2m_N E_\nu$, $F_i(x, Q^2)$ are parton distribution functions and $M_{\rm BH,\,min}$ is the minimum mass required for creating a black hole. Cross section (7.9) is calculated using one PDF parameterization or another for values $Q \approx M_{\rm BH} = \sqrt{s}$; summation is performed over all parton states in the nucleon [66, 287, 296]. Figure 12 shows the black hole production cross section calculated with use of the CTEQ6 PDF parameterization. It is seen that starting from energies $E_\nu \approx 10^{16}$ eV, the cross section exceeds the SM cross section and reaches values $\sigma_{\nu N}^{\rm BH}(E_\nu = 10^{21}\ {\rm eV}) = 10^{-2}$ mb at $E_\nu \approx 10^{21}$ eV. At energies $\sqrt{s} \geqslant M_{\rm BH} \approx 1$ TeV, black hole production may be the dominant phenomenon, because these processes are not suppressed by perturbative interactions, and enhancement of the cross section is a result of summation over all parton states, including gluons.

Estimates of microscopic black hole production cross sections [66, 287, 296] based on geometric cross section (7.8) assume the black hole mass to fully correspond to the energy $\sqrt{s}$. However, even in an idealized interaction with the impact parameter $b = 0$, part of the collision energy can dissipate in the form of gravitational waves. Taking the interaction inelasticity factor $y = M_{\rm BH}/\sqrt{s} = f(n, b)$ into account leads to a reduction in the mass of the black hole produced and in the cross section of the respective process [297–299].

7.6 *p*-branes

In quantum gravity theories with extra dimensions, the possibility arises of producing, together with black holes (spherically symmetric 0-branes), specific higher-dimensional states — p-branes [67, 300, 30]. For the creation of p-branes, the existence of asymmetric extra dimensions is especially important [302]. Such an asymmetry assumes the existence of m extra dimensions compactified on the fundamental TeV gravity scale $L \leqslant M_{4+n}^{-1}$, and of $(n-m)$ dimensions compactified on a significantly larger scale $L' \gg M_{4+n}^{-1}$ [67, 300, 301].

As in the case of black holes, the production of p-branes of a mass $M_{\rm p\text{-}brane}$ occurs when two partons i, j with a center-of-mass energy $\sqrt{\hat{s}} \approx M_{\rm p\text{-}brane}$ are scattered with an impact parameter $b \leqslant R_{\rm p\text{-}brane}$ [301]. This results in a geometric cross section of form (7.8),

$$\sigma_{ij}^{\rm p\text{-}brane}(\sqrt{s}) \approx \pi R_{\rm p\text{-}brane}^2\,. \qquad (7.10)$$

The physical radius $R_{\rm p\text{-}brane}$ is determined by the metric of the $(4+n)$-dimensional space–time and is essentially analogous to the Schwarzschild radius R_S.

The p-brane production cross section in νN scattering processes has the same form (7.9) as in the case of black hole production with the lower integration limit replaced by $M_{\rm p\text{-}brane,\,min}^2/s$. This cross section depends strongly on the number and compactification radii of the extra dimensions [68, 303]. If p-branes are wrapped around the compact m extra dimensions, then their production cross section at $E_\nu \approx 10^{11}$ GeV may reach the value $\sigma_{\nu N}^{\rm p\text{-}brane} \approx 100$ mb (see Fig. 12), which is four orders of magnitude greater than in the case of black hole production with the same mass. If, on the contrary, the p-branes are wrapped around the large $(n-m)$ dimensions, then their production is suppressed in proportion to the value of $M_{4+n}/M_{\rm Pl}$ [67, 300].

8. Registration of astrophysical neutrino fluxes with ground-based detectors

8.1 Neutrino propagation inside the earth and the detector material

The number of neutrinos that are absorbed in the atmosphere and by the earth is a function of the interaction cross section with matter. A definitive role is played by the neutrino–nucleus cross section, in which the relation between the contributions due to charged and neutral currents is [50, 51]

$$\sigma_{\nu N}^{\rm CC} : \sigma_{\nu N}^{\rm NC} \cong 0.7 : 0.3\,. \qquad (8.1)$$

The leptons produced in the final state, both in CC (l_i) and in NC (ν_i) reactions, carry on average about 75% of the intial neutrino energy [50, 51],

$$E_{l_i,\,\nu_i} \approx \left(1 - \langle y\rangle\right) E_\nu^0\,, \qquad (8.2)$$

where $\langle y\rangle$ is the inelasticity interaction coefficient characterizing the fraction of the initial neutrino energy E_ν^0 transferred to the secondary hadrons X.

The total cross section $\sigma_{\nu N}^{\rm tot}$ can be expressed through the neutrino–nucleus interaction length

$$L_{\nu N}^{\rm int}(E_\nu) = \left[\sigma_{\nu N}(E_\nu)\, N_A\right]^{-1}, \qquad (8.3)$$

where

$$N_A = 6.022 \times 10^{23}\ \text{mole}^{-1} = 6.022 \times 10^{23}\ \text{cm}^{-3}\ \text{water equiv.}$$

Figure 13 presents the energy dependence $L_{\nu N}^{\text{int}}(E_\nu)$ for cross sections of various types. It can be seen from the figure that for the νN cross section values calculated within the SM framework [51, 53], the diameter of the earth exceeds $L_{\nu N}^{\text{int}}$ for neutrinos of energies above 40 TeV. The earth becomes totally opaque to neutrinos when $E_\nu \geqslant 100$ TeV.

As was shown in the preceding section, the new physics may result in νN cross sections being significantly greater than their SM predictions. In this case, the earth becomes totally opaque to neutrinos of energies lower than the SM energies. Thus, for example, taking the contributions from the KK-graviton exchange into account [63] reduces the neutrino – nucleus interaction length such that for the scale $M_{4+n} = 1$ TeV, the earth's diameter exceeds $L_{\nu N}^{\text{int}}$ starting from the energies $E_\nu \geqslant 10$ TeV [285] (see Fig. 13).

The issue of neutrinos propagating through the earth was first raised in Ref. [304]. More detailed studies of the absorption of high-energy neutrino fluxes of astrophysical origin having passed through the earth at different angles are performed in Ref. [305]. At present, the dynamics of neutrino and charged lepton fluxes traversing dense media are being investigated in the general form on the basis of solutions of unified transport equations, a method for solving which was proposed in Ref. [306]. The complete set of such evolution equations,

$$\frac{\partial \Phi_\nu}{\partial x} = -N_A \sigma_{\nu N}^{\text{CC+NC}} \Phi_\nu + \frac{m_l}{c\tau_l^{\text{dec}}\rho} \int \mathrm{d}E_l \, \frac{1}{E_l} \, \frac{\mathrm{d}n_l^{\text{dec}}}{\mathrm{d}E_\nu} \, \Phi_l(E_l) + N_A \int \mathrm{d}E'_\nu \, \frac{\mathrm{d}\sigma_{\nu N}^{\text{NC}}}{\mathrm{d}E_\nu} \, \Phi_\nu(E'_\nu) + N_A \int \mathrm{d}E'_l \, \frac{\mathrm{d}\sigma_{lN}^{\text{CC}}}{\mathrm{d}E_\nu} \, \Phi_l(E'_l), \tag{8.4}$$

$$\frac{\partial \Phi_l}{\partial x} = -N_A \sigma_{lN} \Phi_l - \frac{m_l}{c\tau_l^{\text{dec}}\rho E_l} \, \Phi_l + N_A \int \mathrm{d}E'_\nu \, \frac{\mathrm{d}\sigma_{\nu N}^{\text{CC}}}{\mathrm{d}E_l} \, \Phi_\nu(E'_\nu) + N_A \int \mathrm{d}E'_l \, \frac{\mathrm{d}\sigma_{lN}}{\mathrm{d}E_l} \, \Phi_l(E'_l) + \frac{m_l}{c\tau_l^{\text{dec}}\rho} \int \mathrm{d}E'_l \, \frac{1}{E'_l} \, \frac{\mathrm{d}n_l^{\text{dec}}}{\mathrm{d}E_l} \, \Phi_l(E'_l) \tag{8.5}$$

allows describing all possible effects related to passage through and regeneration in the earth of neutrino fluxes from any kind of source [307 – 313]. In (8.4) and (8.5), $\Phi_\nu = \mathrm{d}N_\nu/\mathrm{d}E_\nu$ and $\Phi_l = \mathrm{d}N_l/\mathrm{d}E_l$ are the neutrino and charged lepton differential energy spectra, $x = \int_0^{L'} \rho(L)\,\mathrm{d}L$ is the depth at which a neutrino and a lepton pass through the earth's matter with a variable density $\rho(L)$, $\mathrm{d}n_l^{\text{dec}}/\mathrm{d}E$ is the energy distribution of lepton l decay products, and m_l and τ_l^{dec} are the lepton mass and the time it travels before decaying. Equation (8.4) describes the neutrino propagation: the first term is related to knockout of the flux due to neutrino interactions, the second corresponds to the contributions of neutrinos arising in lepton decays, the third determines the neutrino energy transfer in NC-reactions, and the fourth reproduces the origination of neutrinos in CC reactions such as $\mu N \to \nu_\mu X$. Equation (8.5) describes the propagation of muons and τ-leptons. It contains terms similar to those in (8.4) and an additional term related to the disappearance of leptons from the flux owing to their decays.

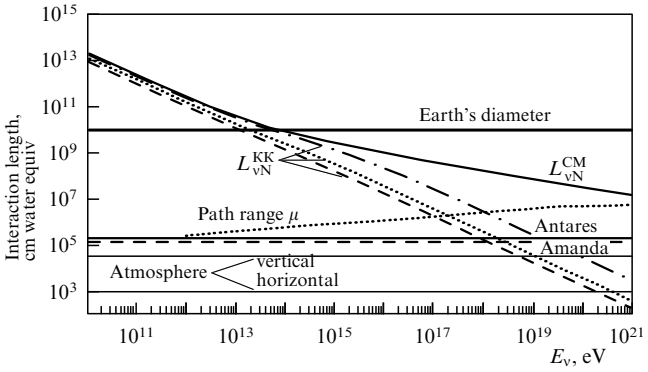

Figure 13. The νN interaction length in water or ice (8.3) for cross sections of various types [285]. The tilted lines correspond to: solid line — total νN cross section in the SM [51], dashed, dotted, and dashed-dotted lines — $\sigma_{\nu N}^{\text{KK}} \propto s$ cross section (7.5) due to KK-graviton exchange on quantum gravity scales $M_{4+n} = 1.0$, 1.2, and 2.0 TeV, respectively [63]. The horizontal lines corrspond (from top down) to: the earth's diameter, the depth of detectors ANTARES and AMANDA, and the depth of the horizontal and vertical atmospheres. The dotted curve corresponds to the muon path range.

8.2 Propagation of charged leptons and the regeneration of neutrino fluxes in the earth

In $\nu_e N$ – CC interactions, the electron originating in a dense medium rapidly loses energy in ionization processes and initiates an electromagnetic cascade.

Muons originating in $\nu_\mu N$ – CC interactions lose energy in ionization of the medium, in bremsstrahlung processes, in direct e^+e^--pair production, and in photonuclear reactions. Ionization losses play the main role for muons at energies $E_\mu \leqslant 10^{11}$ eV, while the e^+e^--pair production dominates at higher energies $\sim E_\mu \geqslant 10^{12}$ eV [309]. In the latter case, a muon passing through a thick layer of matter gives rise to secondary showers. As a result, even muons of energies $E_\mu \geqslant 10^{19}$ eV have path ranges in the earth that do not exceed 10 km, which is always less than the muon decay length (Fig. 14) [314].

A different situation arises in the case of a τ-lepton produced in a $\nu_\tau N$ – CC interaction. For a τ-lepton of energy

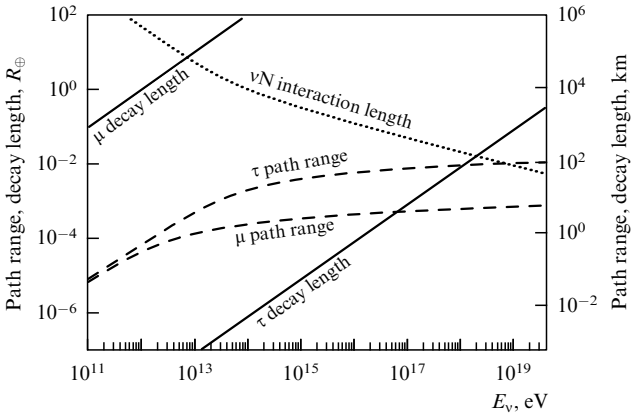

Figure 14. Propagation of muons and τ-leptons in the earth [314]. The νN interaction length (8.3) is shown for comparison.

10^{12} eV $\leqslant E_\tau \leqslant 10^{15}$ eV, energy losses due to pair production and photonuclear processes are equally important, while at $E_\tau \geqslant 10^{15}$ eV, the losses due to photonuclear reactions become dominant [309]. It can be seen from Fig. 14 that at energies $E_\tau < 10^{17}$ eV, the average decay length $\langle L_\tau^{\rm decay}(E)\rangle = \gamma c\tau\rho$ (where $c\tau = 86.93$ μm is the path range in the rest state and $\gamma = E_\tau/m_\tau$ is the Lorentz factor) is significantly smaller than the path range due to energy losses. Consequently, a τ-lepton of energy up to 10^{17} eV decays retaining a large part of its initial energy. τ-leptons with $E_\tau \geqslant 10^{17}$ eV lose a significant part of their energy before they decay. Thus, for a τ-lepton with the initial energy $E_\tau \approx 10^{21}$ eV traveling in ice, its average energy just before it decays is $E'_\tau \approx 10^8$ eV [310, 311].

The τ-lepton decay proceeds via many channels, but they all have a ν_τ in the final state. As was first shown in Ref. [315], unlike with high-energy (starting from 40 TeV) ν_e and ν_μ fluxes, the earth is always transparent to ν_τ fluxes. In other words, regeneration of the ν_τ flux occurs when for each primary ν_τ of an energy E_0 having interacted in a CC-reaction, there appears another ν_τ produced in the τ-lepton decay, but already with the energy $E_1 \approx 0.75 \times 0.4E_0 \approx (1/3)\,E_0$. Here, 0.75 and 0.4 are the respective average parts of energy transferred to the τ-lepton and to the secondary ν_τ resulting from the τ-decay [308]. The regeneration process continues until ν_τ reaches the opposite side of the earth, or until the energy of the newly produced ν_τ in the nth act, $E_n \approx (1/3)\,E_{n-1} \approx (1/3)^n E_0$, falls to the value at which the ν_τ-interaction length becomes equal to the subsequent path inside the earth.

The effect of ν_τ regeneration in the earth is well seen from the angular dependence of neutrino fluxes studied in Refs [307, 308, 310, 313]. In Fig. 15 from Ref. [310], the ratio $\Phi_{\nu_\tau}/\Phi^0_{\nu_\tau}$ is shown for the incidence angles $\theta = 80$, 85, and 89°. The primary cosmogenic neutrino fluxes are assumed [69] and then oscillations result in their having the same flavor composition at the earth's surface. The ratio $\Phi_{\nu_\tau}/\Phi^0_{\nu_\tau}$ reproduces the combination of ν_τ-regeneration processes due to τ-lepton decays and absorption of the neutrino fluxes of all flavors. For angles close to horizontal incidence ($\theta = 89°$), the absorption is small (the neutrinos pass through a thin layer of the earth's matter) and the final flux Φ_{ν_τ} is quite significant even at very high energies. In this case, the regeneration effect provides an additional contribution of about 25% to the flux having passed in the energy region of $E_{\nu_\tau} = 10^{16} - 10^{17}$ eV. As the angle θ decreases, the contributions due to regeneration increase, but the absorption also increases. At $\theta = 80°$, neutrinos of energies $E_{\nu_\tau} > 10^{17}$ eV are practically totally absorbed. On the other hand, if $E_{\nu_\tau} \approx 10^{15}$ eV, then the contributions from regeneration enhance the primary flux for these energies by a factor of 3.

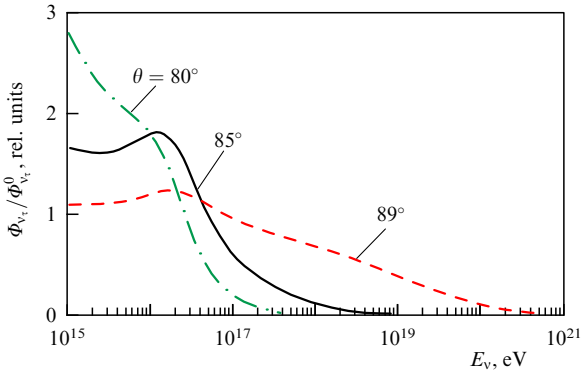

Figure 15. Ratio $\Phi_{\nu_\tau}/\Phi^0_{\nu_\tau}$ of the final flux to the primary flux for cosmogenic neutrinos for the incidence angles $\theta = 80$, 85, and 89° [310].

It is shown in Ref. [314] that at the same time as the regeneration of ν_τ fluxes occurs, purely leptonic decay modes $\tau \to \mu\nu_\tau\bar\nu_\mu$ and $\tau \to e\nu_\tau\bar\nu_e$ also lead to regeneration of $\bar\nu_\mu$ and $\bar\nu_e$ fluxes in the earth. The fraction of each of these leptonic modes amounts to 18% and, consequently, 0.18 of the ν_τ flux is to be attributed to the $\bar\nu_\mu$ and $\bar\nu_e$ fluxes. Energy transfer to the leptons in a decay, for example, via the $\tau \to \mu\nu_\tau\bar\nu_\mu$ mode, is on the average distributed as $\mu : \nu_\tau : \bar\nu_\mu = 4 : 4 : 2$ [308]. Similarly, in the case of a primary $\bar\nu_\tau$ flux, secondary ν_μ and ν_e fluxes are produced. The larger the number of regeneration steps undergone by the $\nu_\tau(\bar\nu_\tau)$, the more possibilities for the creation of secondary $\bar\nu_\mu(\nu_\mu)$ and $\bar\nu_e(\nu_e)$ arise. Secondary $\bar\nu_\mu(\nu_\mu)$- and $\bar\nu_e(\nu_e)$-neutrinos are detected when a respective μ-track and an electromagnetic cascade produced in CC-interactions are registered, which enhances the detectability of ν_τ. These arguments are valid for the model monoenergetic neutrino flux considered in Ref. [314].

The regeneration effect of $\bar\nu_\mu$- and $\bar\nu_e$-neutrinos from the lepton modes of the τ-decay was studied in Ref. [316] for the energy dependences of the primary fluxes $\Phi^0_\nu \propto E_\nu^{-1}$ and $\Phi^0_\nu \propto E_\nu^{-2}$. Calculations of the final neutrino fluxes Φ_ν that passed through the earth at the angle $\theta = 0°$ reveal that in the case of neutrinos of TeV energies with a primary spectrum proportional to E_ν^{-1}, the contributions due to regeneration amount to about 20%. The secondary $\bar\nu_\mu$ and $\bar\nu_e$ fluxes in the case of the power spectrum $\Phi^0_\nu \propto E_\nu^{-2}$ are suppressed more strongly.

8.3 The number of neutrino events in detectors and their specific topologies

The direction from which a neutrino arrives in a neutrino detector plays an important role for registration in the detector of a high-energy lepton produced in CC interactions (6.1). For 'downward' events, in which the neutrino lands in the detector having only crossed the vertical atmosphere, the number of CC interactions registered by the observation of a lepton l_α of flavor α is given by [50]

$$N_{\rm event} = A_{\rm eff}\,T \int_{E_{l_\alpha}^{\rm min}}^{E_{l_\alpha}^{\rm max}} \frac{{\rm d}\Phi_\nu}{{\rm d}E_\nu}\,(E_\nu)\,P_{\nu_\alpha\to l_\alpha}(E_{\nu_\alpha}, E_{l_\alpha}^{\rm min})\,{\rm d}E_\nu\,, \tag{8.6}$$

where the fluxes ${\rm d}\Phi_\nu/{\rm d}E_\nu$ correspond to a neutrino source of a definite type, with the effect of oscillations taken into account. The probability

$$P_{\nu_\alpha\to l_\alpha}(E_{\nu_\alpha}, E_{l_\alpha}^{\rm min}) = N_{\rm A}\int_0^{1-E_{l_\alpha}^{\rm min}/E_{\nu_\alpha}} {\rm d}y\,R_\alpha(E_{\nu_\alpha}, E_{l_\alpha}^{\rm min})\,\frac{{\rm d}\sigma^{\rm CC}_{\nu_\alpha N}(E_{\nu_\alpha}, y)}{{\rm d}y} \tag{8.7}$$

is calculated in accordance with one of the parameterizations of the νN cross section, and the path ranges R_α of leptons in matter are presented in Table 2.

A different situation occurs in the case of 'upward' neutrino fluxes undergoing absorption inside the earth.The loss of energy by a charged lepton with the initial energy E_l, crossing a layer of matter of thickness x, is characterized by

Table 2. Path ranges of electrons, muons, and τ-leptons in matter.

Lepton flavor α	R_α, cm of water equiv.	Reference
e	$40\left[\left(1-\langle y(E_{\nu_e})\rangle\right)\dfrac{E_{\nu_e}}{6.2\times10^4\ \text{GeV}}\right]$	[50]
μ	$\dfrac{1}{\beta}\ln\left[\dfrac{\alpha+\beta E_\mu}{\alpha+\beta E_\mu^{\min}}\right]$, $\alpha\approx2.0\times10^{-3}$ GeV (cm of water equiv.)$^{-1}$, $\beta\approx3.9\times10^{-6}$ (cm of water equiv.)$^{-1}$	[50]
τ	$\dfrac{E_{\nu_\tau}(1-y)\,\tau_c}{m_\tau c^2}$,	[317]

the mean value

$$-\left\langle\frac{\mathrm{d}E_l}{\mathrm{d}x}\right\rangle=\alpha+\beta E_l\,, \tag{8.8}$$

where $\alpha\approx2.0$ MeV g^{-1} cm^{-1} is a constant determining the energy loss by ionization,

$$\beta^i(E)=\frac{N_A}{A}\sum_i\int_{y_{\min}}^{y_{\max}}\mathrm{d}y\,y\,\frac{\mathrm{d}\sigma^i(y,E_l)}{\mathrm{d}y} \tag{8.9}$$

is a function weakly depending on energy, which characterizes the fraction of energy losses $y=E_l-E_l'/E_l$ in the processes of bremsstrahlung, electron – positron production, and inelastic interaction with nuclei, indicated by the index i, E_l' is the final lepton energy, and A is the target atomic number. In the first approximation, $\beta\approx10^{-6}$ cm^{-1} g^{-1}. A more precise approximation for the τ-lepton energy losses has been obtained in Ref. [318].

The final state of any ν_αN–CC interaction always contains a hadron cascade together with a charged lepton, and hence the total energy of the showers determines the primary ν_α energy. It is usually impossible to separate the electromagnetic and hadron cascades, and the ν_eN–CC interaction in the detector looks like a shower interaction. The final states of ν_αN–NC interactions also always contain a hadron cascade, and hence the registration probability of a shower event in a detector of length L is given by

$$P_{\nu\to\text{shower}}\approx\rho N_A\sigma_{\nu N}^{\text{tot}}\,L\,. \tag{8.10}$$

In ν_μN–CC interactions, there always exists a μ-track against the hadron background, which provides the clean event signature. The probability (8.7) of registering such an event is

$$P_{\nu_\mu\to\mu}\approx\rho N_A\sigma_{\nu N}^{\text{tot}}R_\mu\,, \tag{8.11}$$

where the value of R_μ is calculated by the formula in Table 2. The neutrino telescopes Baikal [319], Antares [320], and Amanda/IceCube [321] are sensitive to muons with PeV energies.

Owing to the short lifetime of the τ-lepton, registration of ν_τN–CC interactions presents a difficult experimental task. At energies $E_\tau\approx10^{15}$ eV, the τ-lepton path range before it decays in the detector is ∼ 100 m, which is comparable to the characteristic dimensions of neutrino telescopes. In Ref. [322], a method was proposed for registering ν_τ by the presence of double-bang events in the detector. The signature of such an event is the presence of a large hadron shower from the primary ν_τ interaction, of a τ-lepton track (similar to the muon track), and of a second large cascade of particles produced in the τ-decay (two or three times larger than the first cascade, which follows from the τ-lepton decay kinematics). However, such events can be observed only within a narrow interval of energies. If the neutrino energy is less than several PeV, then two showers cannot be separated using the above method. On the contrary, if $E_{\nu_\tau}>3\times10^{16}$ eV, then the τ-lepton path range becomes greater than 1 km and separating such τ from muons becomes quite difficult even in new-generation detectors with the characteristic diameter 1 km [317].

The identification of ν_τ is also possible even when only the second shower is registered in the detector, if its energy is not less than 10 PeV. Such a signature of the ν_τ interaction has been termed a lollipop event. It comprises part of the primary ν_τ interaction, which occurred outside, but close to, the fiducial volume, the final part of the τ-lepton track, registered in the detector, and the second cascade from the τ-lepton decay, which lies totally inside the detector. The inverse structure of such an event, when only the first cascade and the τ-lepton track leaving the fiducial volume are registered, is indistinguishable from a ν_μN–CC interaction with a registered hadron cascade and a muon track.

The results of calculations of the number of double-bang and lollipop events that can be registered in real detectors are quite pessimistic [141, 310, 312, 317]. Thus, according to calculations in Ref. [141], assuming the initial neutrino flux $E_{\nu_\mu}^2\,\mathrm{d}N_{\nu_\mu}/\mathrm{d}E_{\nu_\mu}=10^2$ eV cm^{-2} s^{-1} sr^{-1}, the total statistic of double-bang and lollipop events in the IceCube detector will only amount to ~0.5 year^{-1}. This is related to the small registration probability, which becomes

$$\begin{aligned}P_{\text{double-bang}}(E_{\nu_\tau})&\cong\rho N_A\int_0^1\mathrm{d}y\,\frac{\mathrm{d}\sigma}{\mathrm{d}y}\\&\times\left[(L-x_{\min}-R_\tau)\exp\left(-\frac{x_{\min}}{R_\tau}\right)+R_\tau\exp\left(-\frac{L}{R_\tau}\right)\right]\\&\approx\rho N_A\sigma\left[(L-x_{\min}-R_\tau)\exp\left(-\frac{x_{\min}}{R_\tau}\right)\right.\\&\left.+R_\tau\exp\left(-\frac{L}{R_\tau}\right)\right]_{y=\langle y\rangle},\end{aligned} \tag{8.12}$$

$$\begin{aligned}P_{\text{lollipop}}(E_{\nu_\tau})&\cong\rho N_A(L-x_{\min})\int_0^1\mathrm{d}y\,\frac{\mathrm{d}\sigma}{\mathrm{d}y}\exp\left(-\frac{x_{\min}}{R_\tau}\right)\\&\approx\rho N_A\,\sigma(L-x_{\min})\left[\exp\left(-\frac{x_{\min}}{R_\tau}\right)\right]_{y=\langle y\rangle}.\end{aligned} \tag{8.13}$$

In these expressions, L is the detector length and R_τ is the path range of the τ-lepton determined by the formula in Table 2. The integration limits in (8.12) assume the τ-track length to exceed $x_{\min}\approx200-400$ m (for separating showers) and to be less than L (for there to be sufficient place in the detector for both showers). The right-hand sides of (8.12) and (8.13) are obtained using the approximation where $\mathrm{d}\sigma/\mathrm{d}y=\sigma\delta(y-\langle y\rangle)$, with $\langle y\rangle=0.25$ at energies $\sim10^{15}$ eV. Probabilities (8.12) and (8.13) calculated in Ref. [141] are $P_{\text{double-bang}}(E_\nu=10^{18}\text{ eV})\leqslant10^{-5}$ and $P_{\text{lollipop}}(E_\nu=10^{18}\text{ eV})\leqslant5\times10^{-4}$. About 4–5 times more double-bang and lollipop events are expected to be registered in the IceCube detector according to estimates in Ref. [313].

This is mainly due to the smaller value of $x_{\min} = 70$ m, assumed in the calculations, as compared with $x_{\min} = 200-400$ m in Ref. [141]. Thus, even by the most optimistic estimates, it will be possible to register only several double-bang and lollipop events a year in detectors of the volume 1 km^3.

One more method for identifying ν_τ is the pile-up method proposed in Ref. [315]. At energies $E_{\nu_\tau} \approx 10-100$ TeV, when the ν_τ interaction length is comparable to the earth's diameter, the primary neutrino may undergo interaction near the detector and be registered in the $\tau^- \to \mu^-\nu_\tau\nu_\mu$ decay by observation of a muon track. However, the muons originating in the τ-lepton decay can be distinguished from the muons produced in ν_μN–CC reactions only statistically. All the neutrinos with energies $E_{\nu_\tau} > 100$ TeV undergo interaction inside the earth, but the detector is reached only by secondary ν_τ of reduced energy, which group on the average in the region of 100 TeV [315]. Registration in the detector of muons leaving the earth with a certain energy ~ 100 TeV may serve as the signature of a ν_τ-component present in the flux of astrophysical neutrinos.

Events initiated by high-energy neutrinos can be observed not only in neutrino telescopes but also in ground-based setups registering broad atmospheric showers (BASs) or fluorescent light in the atmosphere (AGASA, HiRes, Telescope Array, and AUGER), as well as in experiments on orbital space stations (EUSO, OWL). The idea of detecting high-energy neutrinos by observing deep horizontal showers in the atmosphere was put forward many years ago by Berezinsky and Smirnov [323]. The depth of the atmosphere in the horizontal direction is 36 times larger than in the vertical direction, and therefore, for a hadron falling at a small height in the horizontal direction, the probability of forming a shower is negligible. At energies above 10^{15} eV, the flux of atmospheric muons is also extremely small. Thus, only neutrinos can pass through thick layers of the atmosphere without undergoing absorption and form deep showers registered by detectors. Evidence in favor of neutrino interactions would be showers initiated at depths not less than 4000 g cm^{-2}, which is equivalent to zenith angles $\sim 75^\circ$.

The natural way of enhancing the statistics of registered events is to increase the sensitive volume of the detector. Another possibility is to separate the target from the detector. In this case, an enormous volume could be provided by a detector registering fluorescent or Cherenkov light in the atmosphere, while the layer near the surface of the earth or extended mountain ridges would play the role of the target. The concept of such a detection method, based on the possibility of natural filtration of quasihorizontal high-energy showers initiated by τ-leptons, was proposed in Refs [324, 325]. In the region $E_\tau \approx 10^{18}-10^{21}$ eV, the τ-lepton decay length is not much larger than its interaction length (see Fig. 14), and therefore τ-leptons of such energies produced in ν_τN–CC reactions close to the earth's surface have a chance to enter the atmosphere. A shower due to the decay of such a τ-lepton can be registered by fluorescence detectors [326–328]. The idea of such an experiment, in which extended mountain ridges simultaneously play the roles of the target and of the CR filter, is interesting. After leaving a mountain ridge, the horizontal shower from a τ-lepton should be observed in the large volume of air where the detector registering muons and γ-quanta is placed. Here, quite a clean signature of the separation of high-energy ν_μN and ν_τN interactions must appear. At neutrino energies ~ 10 PeV, a meson produced in a ν_μN–CC interaction is to be registered as a single track passing through the detector. On the other hand, the τ-lepton decays at distances ~ 100 m from the interaction vertex and the entire shower may happen to be in the detector volume. This ν_τ detection principle underlies the CRTNT project [329].

It was proposed in Refs [141, 308, 330] to analyze the ratio of the respective numbers of events containing a μ-track and a shower, instead of restoring the lepton's flavor (when identifying the μ-track and the τ-lepton signatures). If oscillations of astrophysical neutrinos result in identical fluxes of neutrinos of all flavors landing in the detector, then for fluxes arriving from the quasihorizontal directions, the ratio of the number of interaction events containing a μ-track to the number of purely shower events amounts to $N_{\mu\text{-track}}/N_{\text{shower}} \approx 8.5-9$ [141]. This quantity is very sensitive to the relation between neutrino fluxes of various flavors arriving on earth. Deviation from this value should point to a deviation from the canonical relation between astrophysical fluxes (2.54).

Finally, for detecting ultrahigh-energy neutrinos, one seemingly very promising method is based on the registration of coherent Cherenkov radioemission from electromagnetic cascades in condensed media. The idea of the method goes back to the works of Askarian [331, 332], where it was first claimed that the total charge of particles in a shower is different from zero. This is due to the existence in a shower of a significant number of particles with energies lower than the critical value ($E_{\text{cr}} \approx 73$ MeV for ice), for which an essential role is played not only by charge-symmetric processes and pair production and bremsstrahlung in the Coulomb field of atomic nuclei but also by interactions with atomic electrons:

$$\gamma + e^-_{\text{at}} \to \gamma + e^-\,, \quad e^+ + e^-_{\text{at}} \to e^+ + e^-,$$
$$e^- + e^-_{\text{at}} \to e^- + e^-. \tag{8.14}$$

This interaction leads to electrons being 'pulled out' from the surrounding material into the shower. Moreover, positrons in the shower annihilate just 'in passing,'

$$e^+ + e^-_{\text{at}} \to \gamma + \gamma\,. \tag{8.15}$$

The combination of processes (8.14) and (8.15) results in the BAS charge asymmetry: the excess of negative charges in the shower disk amounts to 20–30% of the total number of electrons. The fast electrons of this excess that have energies above the Cherenkov radiation threshold emit electromagnetic waves owing to the Cherenkov mechanism. The power of radioemission is then proportional to the squared energy of the shower.

There exist a number of computational works in which the characteristics were studied of the radio signal appearing when electromagnetic and hadron showers propagate in media transparent to radio signals [333–335]. Recently, the possibility of registering Cherenkov radio emission from electromagnetic cascades in condensed media was successfully confirmed in accelerator experiments [336, 337]. At present, the radio method underlies a number of experiments and projects for registration of ultrahigh-energy particles in natural media that are transparent to radio signals such as the earth's atmosphere (LOFAR [338]), salt domes (SalSA [78]), ice shields of the Antarctic (RICE [76], ANITA [80]), and Greenland (FORTE [77]). In a number of works, the

possibility is discussed of using the layer near the surface of the moon (regolith) as a target for the registration of cosmic particles by the radio method with the aid of ground-based radio telescopes (GLUE [79]) or radio receiving devices on satellites of the moon (LORD [81, 82]).

9. The possibilities to experimentally determine neutrino – nucleus cross sections at ultrahigh energies

The number of horizontal atmospheric showers registered in detectors can be used to impose an upper limit on the νN cross section. In principle, this is a model-independent approach in the sense that independently of the sources of additional contributions to the νN cross section, the excess of statistics over the calculated SM value can be revealed in experiments. On the basis of no horizontal showers having been observed in the AGASA and Fly's Eye setups in Ref. [285], an upper limit has been obtained for the neutrino cross section as

$$\sigma_{\nu N}(E_\nu) \leqslant 10^{-28} \left(\frac{10^{-18}\,\mathrm{cm^{-2}\,s^{-1}\,sr^{-1}}}{\Phi_\nu^{\mathrm{GZK}} E_\nu}\right)\left(\frac{10^{19}\,\mathrm{eV}}{\langle y_{\mathrm{sh}}\rangle E_\nu}\right)^{1/2} \mathrm{cm}^2, \tag{9.1}$$

where Φ_ν^{GZK} is the cosmogenic neutrino flux and $\langle y_{\mathrm{sh}}\rangle = E_{\mathrm{sh}}/E_\nu$ is the average fraction of the neutrino energy invested in the shower. For the minimum flux $E_\nu^2 \Phi_\nu^{\mathrm{GZK\text{-}min}}(E_\nu = 10^{19}\ \mathrm{eV}) \approx 3 \times 10^1\ \mathrm{eV\,cm^{-2}\,s^{-1}\,sr^{-1}}$ (2.44) [69], a bound on the total cross section follows from (9.1) as

$$\sigma_{\nu N}(E_\nu = 10^{19}\ \mathrm{eV}) \leqslant \frac{30}{\sqrt{\langle y_{\mathrm{sh}}\rangle}}\ \mu\mathrm{b}. \tag{9.2}$$

More rigorous estimates of the upper bound of the νN cross section were obtained in Refs [339, 340] and are presented in Fig. 16. In Ref. [339], calculations are based on the length of the run performed with Fly's Eye, which provided 9 times more than the observational statistics used in Ref. [285]. In Ref. [340], the upper bound for the cross section is obtained from restrictions on the cosmogenic neutrino flux established in the RICE experiment [76].

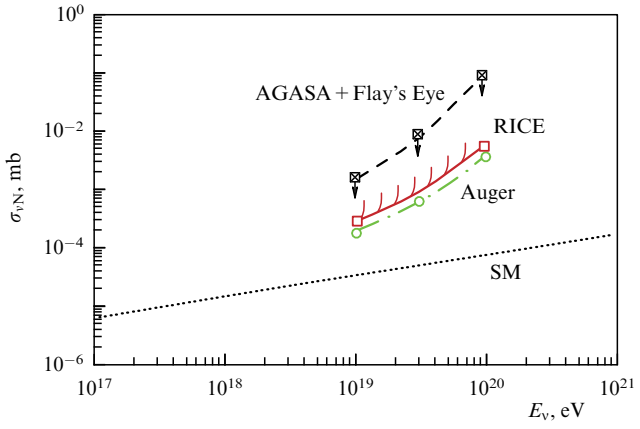

Figure 16. Upper bound for the inelastic neutrino – nucleus cross section [339, 340]. The solid line corresponds to restrictions on the cosmogenic neutrino flux obtained in the RICE experiment, the dashed line to results of horizontal showers not having been observed in the AGASA and Fly's Eye setups. The dashed-dotted line shows the sensitivity achievable in the Auger experiment, the dotted line shows the standard SM cross section.

As the authors of Ref. [340] note, all the restrictions on νN cross sections considered above are valid only if $\sigma_{\nu N}^{\mathrm{tot}} \leqslant 0.5$ mb. If, on the contrary, neutrinos interact more strongly, then the restrictions obtained from the absence of observed quasihorizontal showers are no longer applicable.

The registration of shower events initiated by neutrinos may turn out to be the sole experimental method for direct determination of the neutrino – nucleus cross section at ultrahigh energies. The idea of the method was first proposed in Ref. [341] and is based on comparison of the number of registered atmospheric showers arriving in the detector from directions close to horizontal and the number of 'upward' showers initiated by muons and τ-leptons produced in ν_μN and ν_τN interactions in the upper surface layer of the earth. The possibilities of applying the method for various neutrino detectors have been analyzed in Refs [310 – 313, 324 – 326]. The expected number of quasihorizontal atmospheric showers should be directly proportional to the cross section: $N_\nu^{\mathrm{hor}} \propto \sigma_{\nu N}$. On the other hand, screening of ultrahigh energy neutrinos by the earth, due to enhancement of the cross section, leads to the number of events with upward showers being inversely proportional to the cross section: $N_\nu^{\mathrm{up\text{-}going}} \propto \sigma_{\nu N}^{-1}$. It is important that the ratio of the number of quasihorizontal atmospheric showers to the number of upward showers from neutrino interactions in the earth's surface layer is independent of theoretical uncertainties in the cross section. The authors of Ref. [341] actually consider $\sigma_{\nu N}$ a free parameter. The results of calculations of the numbers of expected events containing horizontal and upward showers from the cosmogenic neutrino flux are shown in Fig. 17 as functions of the cross section $\sigma_{\nu N}$. It is seen that in the case of small cross sections, events with showers upward from the earth dominate, while in the case of large cross sections, events with horizontal showers dominate.

It was proposed in Ref. [342] that neutrino – nucleus cross sections at high energies can be determined using the ratio between the numbers of neutrino events with upward and downward showers (Fig. 18). Shower events occur in all ν_αN interactions within SM (CC + CC), and their number increases with the cross section owing to additional contributions from KK gravitons, the production of black holes, *p*-branes, etc. It can be seen that for cross sections smaller than $\sim 10^{-7}$ mb, the above ratio is of the order of unity and is revealed with difficulty. On the contrary, if $\sigma_{\nu N} \geqslant 10^{-4}$ mb,

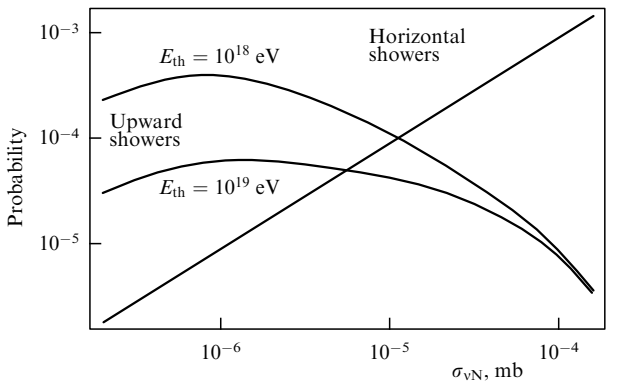

Figure 17. Formation probability of horizontal and upward showers per incident ν_τ versus the νN cross section. The neutrino energy $E_\nu = 10^{20}$ eV; the registration threshold energies of upward showers are $E_{\mathrm{th}} = 10^{18}$ and 10^{19} eV [341].

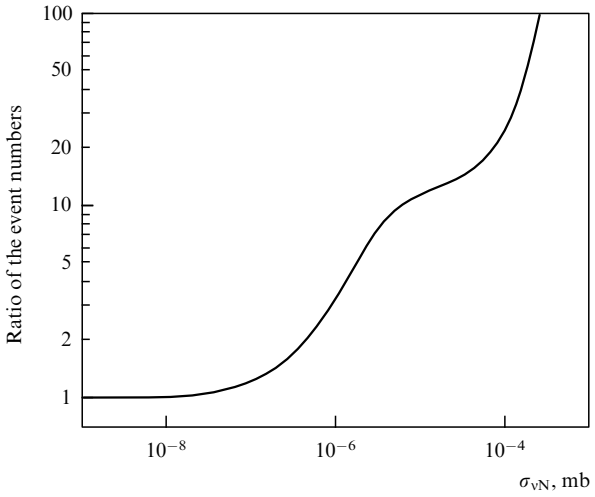

Figure 18. The ratio between the numbers of neutrino events with downward and upward showers registered in neutrino telescopes versus the νN cross section [342].

then the ratio increases rapidly, which permits determining the cross section, provided the statistic is sufficient.

To determine the $\sigma_{\nu N}$ cross section, one can also apply the method based on analysis of the angular distribution of neutrino events with upward showers, which should exhibit a maximum at $\cos\theta_{\rm peak} \approx L_{\nu N}^{\rm int}/2R_\oplus$ (where $R_\oplus$ is the earth's radius). The maximum in the angular distribution should correspond to the value $\sigma_{\nu N} \approx (2\langle\rho\rangle R_\oplus \cos\theta_{\rm peak})^{-1}$, where $\langle\rho\rangle$ is the average of the earth density along the neutrino's path length $L_{\nu N}^{\rm int}$ [341]. This method is independent of the calculated neutrino fluxes.

The upper bounds for the νN cross section can be applied for imposing restrictions on the fundamental scale M_{4+n} within the context of TeV gravity models [285, 339, 343]. Whatever happens in the vicinity of the scale M_{4+n} (the formation of black holes, p-branes, etc.), the decay of such objects should be observable, resulting in the development of cascades deep in the atmosphere [344–346]. Assuming parameterization (7.5) of the gravitational scattering cross section, the upper bound for the cross section in (9.1), and a conservative estimate of the cosmogenic neutrino flux $\Phi_\nu^{\rm GZK\text{-}min}(E_\nu)$ in (2.42), the following restriction used in Ref. [285] is independent of the number n of extra dimensions:

$$M_{4+n} \geqslant 1.2 \text{ TeV} \quad (E_\nu = 10^{18} \text{ eV},\ \langle y_{\rm sh}\rangle = 1)\,. \qquad (9.3)$$

Restrictions similar to (9.3) were obtained in Refs [339, 343] on the basis of horizontal showers not having been observed in the AGASA and Fly's Eye setups. The absence of any registered neutrino events of whatever origin during a 5-year period in the RICE experiment [76] is also consistent with (9.3) [347].

Enhancement of the νN interaction cross sections in theories involving the fundamental scale M_{4+n} as compared with its SM value should manifest itself at neutrino energies $E_\nu \approx 10^{15}-10^{16}$ eV. In this energy region, also, neutrino fluxes in GRB [165], the hidden-nucleus AGN [179], and blazar [184] models are close to the maximum (see Figs 6 and 7). As shown in Refs [348, 349], the registration in neutrino telescopes, such as IceCube, of upward and downward μ-, τ-, and shower events will permit determining the deviation from the SM cross section even for neutrinos with energies close to the detection threshold ($E_{\rm th} \approx 0.5$ PeV).

10. Conclusion

From the standpoint of propagation in the universe, the neutrino is an ideal candidate for the primary particle — the source of UHECRs with energies beyond the GZK cutoff of the CR spectrum. Since neutrinos are stable and can travel cosmological distances practically without undergoing absorption even with energies $E_\nu \gg E_{\rm GZK} \approx 7\times10^{19}$ eV, neutrino fluxes from different astrophysical sources can be regarded as a sensitive instrument in studying the universe right up to its observable boundaries.

On the other hand, neutrinos with SM cross sections should not produce vertical showers high up in the atmosphere, such as are observed in the case of UHECR events. For the neutrino to be a source of such events, the νN cross section at ultrahigh energies must be at least 5 orders of magnitude larger than the SM cross section. Such a possibility opens up, for example, in the light of quantum gravity theories involving the unification of interactions at a TeV scale and large extra space–time dimensions.

Studying UHEN fluxes allows determining inelastic νN cross sections at energies not available even at the future LHC accelerator. Any statistically reliable evidence in favor of an enhancement of the cross sections above SM values may be a manifestation of the new physics.

At the same time that the νN cross sections increase with energy, the neutrino fluxes produced in various sources rapidly decrease. Therefore, new large-scale experimental installations are being created for their registration, and new detection methods are being applied. A quantity used for comparison and characterizing the potentials of different experiments for UHEN registration is the product of the detector aperture A, the solid angle $\Delta\Omega$, and the exposure time Δt [350]. This quantity is shown in Fig. 19.

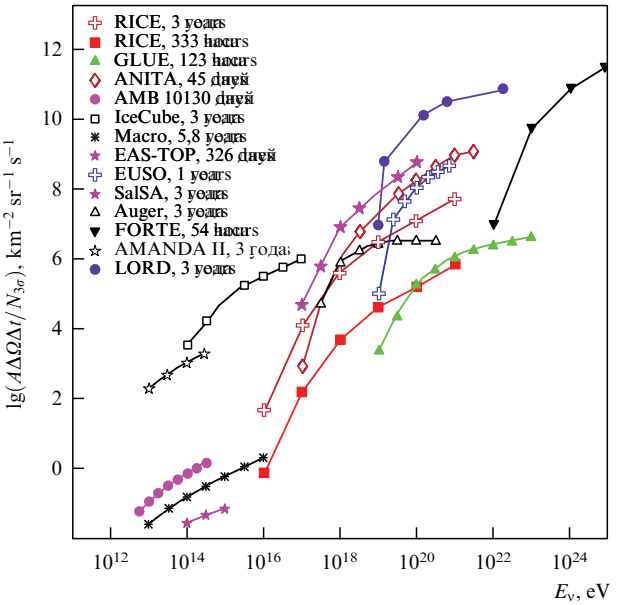

Figure 19. Product of detector aperture A, solid angle $\Delta\Omega$, and exposure time Δt for different experiments aimed at UHEN registration versus energy [350]. The LORD curves are taken from Ref. [82].

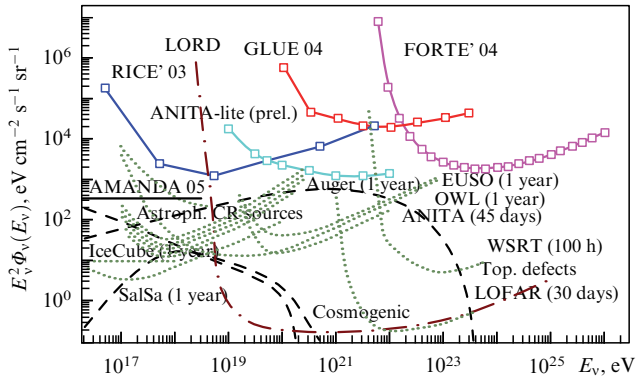

Figure 20. Restrictions on astrophysical neutrino fluxes [352] obtained in experiments AMANDA [72], ANITA-lite [351], FORTE [77], GLUE [79], and RICE [76], and, also, values expected from experiments in the nearest future, ANITA [80], Auger [84], IceCube [75], EUSO [85], OWL [86], LOFAR [338], LORD [81, 82], SalSA [78], and WSRT [338]. Also shown are cosmogenic neutrino fluxes [116]; fluxes predicted within the extended WB scenario of CR formation [144]; fluxes within the TD model [352].

At present, in the AMANDA [72], ANITA-lite [351], BAIKAL [319], FORTE [77], GLUE [79], and RICE [76] experiments, restrictions have been imposed on the fluxes of astrophysical neutrinos in the energy range $E_\nu = 10^{16} - 10^{26}$ eV (Fig. 20). The sensitivity of these experiments, however, is insufficient for the registration of cosmogenic neutrino fluxes or of neutrino fluxes generated in powerful cosmic 'accelerators,' such as GRBs and AGNs, and produced in TD decays. In the nearest future, this problem may be resolved in experiments using the neutrino telescopes ANTARES [74] and IceCube [75], the radio detector ANITA [80] and the ground-based CR detectors Auger [84], and Telescope Array [83]. The prospects for further enhancement of the sensitivity of experiments to the registration of astrophysical neutrino fluxes are related to the planned radio detectors SalSA [78], LOFAR [338], and LORD [81, 82] and the cosmic observatories EUSO [85] and OWL [86] (see Fig. 20).

Hope remains that in the next decade, new experiments for UHEN registration will shed light on many of the problems considered in this review.

The author is grateful to V A Tsarev for useful discussions of many of the issues raised in the review and for a number of valuable comments.

References

1. Swordy S P et al. *Astropart. Phys.* **18** 129 (2002); astro-ph/0202159
2. Nagano M, Watson A A *Rev. Mod. Phys.* **72** 689 (2000)
3. Gaisser T K, Stanev T *Nucl. Phys. A* (in press); astro-ph/0510321
4. Poincaré *La Science et l'hypothèse* (Paris: Flammarion, 1968) [Translated into English: *Science and Hypothesis* (New York: Dover Publ., 1952) translated into Russian: in *O nauke* (On Science) (Ed. L S Pontryagin) (Moscow: Nauka, 1983) p. 97]
5. Ave M et al. *Phys. Rev. D* **65** 063007 (2002); astro-ph/0110613
6. Anchordoqui L, Goldberg H *Phys. Lett. B* **583** 213 (2004); hep-ph/0310054
7. Antonov E E et al. *Pis'ma Zh. Eksp. Theor. Fiz.* **69** 614 (1999) [*JETP Lett.* **69** 650 (1999)]
8. Takeda M et al. *Astrophys. J.* **522** 225 (1999); Hayashida N et al. astro-ph/0008102
9. Takeda M et al. *Astropart. Phys.* **19** 447 (2003); astro-ph/0209422
10. Bird D J et al. *Astrophys. J.* **441** 144 (1995)
11. Abbasi R U et al. (High Resolution Fly's Eye Collab.) *Phys. Rev. Lett.* **92** 151101 (2004); astro-ph/0208243
12. Abbasi R U et al. (High Resolution Fly's Eye Collab.) *Astropart. Phys.* **23** 157 (2005); astro-ph/0208301
13. Greisen K *Phys. Rev. Lett.* **16** 748 (1966)
14. Zatsepin G T, Kuz'min V A *Pis'ma Zh. Eksp. Theor. Fiz.* **4** 114 (1966) [*JETP Lett.* **4** 78 (1978)]
15. Yoshida S, Dai H *J. Phys. G: Nucl. Part. Phys.* **24** 905 (1998); astro-ph/9802294
16. Arons J *Astrophys. J.* **589** 871 (2003); astro-ph/0208444
17. Singh S, Ma C-P, Arons J *Phys. Rev. D* **69** 063003 (2004); astro-ph/0308257
18. Elbert J W, Sommers P *Astrophys. J.* **441** 151 (1995); astro-ph/9410069
19. Protheroe R J, Meyer H *Phys. Lett. B* **493** 1 (2000); astro-ph/0005349
20. Fagrion D, Mele B, Salis A *Astrophys. J.* **517** 725 (1999); astro-ph/9710029
21. Weiler T J *Astropart. Phys.* **11** 303 (1999); hep-ph/9710431
22. Biermann P L *J. Phys. G: Nucl. Part. Phys.* **23** 1 (1997)
23. Blandford R D *Phys. Scripta* **T85** 191 (2000); astro-ph/9906026
24. Gatanese M, Weekes T C *Publ. Astron. Soc. Pacif.* **111** 1193 (1999); astro-ph/9906501
25. Piran T *Rev. Mod. Phys.* **76** 1143 (2004); astro-ph/0405503
26. Maraschi L, Tavecchio F *Astrophys. J.* **593** 667 (2003); astro-ph/0205252
27. Rachen J P, Mészáros P *Phys. Rev. D* **58** 123005 (1998); astro-ph/9802280
28. Bhattacharjee P, Rana N C *Phys. Lett. B* **246** 365 (1990)
29. Hill C T, Schramm D N, Walker T P *Phys. Rev. D* **36** 1007 (1987)
30. Bhattacharjee P, Sigl G *Phys. Rev. D* **51** 4079 (1995); astro-ph/9412053
31. Berezinsky V, Martin X, Vilenkin A *Phys. Rev. D* **56** 2024 (1997); astro-ph/9703077
32. Berezinsky V, Vilenkin A *Phys. Rev. Lett.* **79** 5202 (1997); astro-ph/9704257
33. Masperi L, Silva G *Astropart. Phys.* **8** 173 (1998)
34. Berezinsky V, Blasi P, Vilenkin A *Phys. Rev. D* **58** 103515 (1998); astro-ph/9803271
35. Zel'dovich Ya B, Starobinsky A A *Zh. Eksp. Theor. Fiz.* **61** 2161 (1971) [*Sov. Phys. JETP* **34** 1159 (1972)]
36. Kuzmin V A, Rubakov V A *Yad. Fiz.* **61** 1122 (1998) [*Phys. At. Nucl.* **61** 1028 (1998)]; astro-ph/9709187
37. Kuzmin V A, Tkachev I I *Phys. Rep.* **320** 199 (1999); hep-ph/9903542
38. Bhattacharjee P, Hill C T, Schramm D N *Phys. Rev. Lett.* **69** 567 (1992)
39. Athar H, Ježabek M, Yasuda O *Phys. Rev. D* **62** 103007 (2000); hep-ph/0005104
40. Athar H *Astropart. Phys.* **14** 217 (2000); hep-ph/0004191
41. Gershteĭn S S, Kuznetsov E P, Ryabov V A *Usp. Fiz. Nauk* **167** 811 (1997) [*Phys. Usp.* **40** 773 (1997)]
42. Ryabov V A *Fiz. Elem. Chastits At. Yad.* **34** 1256 (2003) [*Phys. Part. Nucl.* **34** 651 (2003)]
43. Tzanov M et al., hep-ex/0509010
44. Adloff C et al. (The H1 Collab.) *Eur. Phys. J. C* **30** 1 (2003); hep-ex/0304003
45. Chekanov S et al. (ZEUS Collab.) *Nucl. Phys. B* **713** 3 (2005); hep-ex/0501060
46. Chekanov S et al. (ZEUS Collab.) *Eur. Phys. J. C* **42** 1 (2005); hep-ph/0503274
47. Frichter G M, McKay D W, Ralston J P *Phys. Rev. Lett.* **74** 1508 (1995); hep-ph/9409433
48. Glück M, Kretzer S, Reya E *Astropart. Phys.* **11** 327 (1999); astro-ph/9809273
49. Glück M, Reya E, Vogt A *Eur. Phys. J. C* **5** 461 (1998); hep-ph/9806404
50. Gandhi R et al. *Astropart. Phys.* **5** 81 (1996); hep-ph/9512364
51. Gandhi R et al. *Phys. Rev. D* **58** 093009 (1998); hep-ph/9807264
52. Kwiecinski J, Martin A D, Stasto A M *Phys. Rev. D* **56** 3991 (1997); hep-ph/9703445
53. Kwiecinski J, Martin A D, Stasto A M *Phys. Rev. D* **59** 093002 (1999); astro-ph/9812262

54. Kwiecinski J, Martin A D, Stasto A M *Acta Phys. Polon. B* **31** 1273 (2000); hep-ph/0004109
55. Kutak K, Kwiecinski J *Eur. Phys. J. C* **29** 521 (2003); hep-ph/0303209
56. Beresinsky V S, Zatsepin G T *Phys. Lett. B* **28** 423 (1969)
57. Ringwald A *Phys. Lett. B* **555** 227 (2003); hep-ph/0212099
58. Fodor Z et al. *Phys. Lett. B* **561** 191 (2003); hep-ph/0303080
59. Arkani-Hamed N, Dimopoulos S, Dvali G *Phys. Lett. B* **429** 263 (1998); hep-ph/9803315
60. Arkani-Hamed N, Dimopoulos S, Dvali G *Phys. Rev. D* **59** 086004 (1999); hep-ph/9807344
61. Randall L, Sundrum R *Phys. Rev. Lett.* **83** 3370 (1999); hep-ph/9905221
62. Randall L, Sundrum R *Phys. Rev. Lett.* **83** 4690 (1999); hep-th/9906064
63. Jain P et al. *Phys. Lett. B* **484** 267 (2000); hep-ph/0001031
64. Kachelriess M, Plümacher M *Phys. Rev. D* **62** 103006 (2000); astro-ph/0005309
65. Argyres P C, Dimopoulos S, March-Russell J *Phys. Lett. B* **441** 96 (1998); hep-th/9808138
66. Feng J L, Shapere A D *Phys. Rev. Lett.* **88** 021303 (2002); hep-ph/0109106
67. Ahn E-J, Cavaglià M, Olinto A V *Phys. Lett. B* **551** 1 (2003); hep-th/0201042
68. Jain P, Kar S, Panda S *Int. J. Mod. Phys. D* **12** 1593 (2003); hep-ph/0201232
69. Engel R, Seckel D, Stanev T *Phys. Rev. D* **64** 093010 (2001); astro-ph/0101216
70. Markov M A, in *Proc. of the 10th Annual Intern. Conf. on High-Energy Physics, Rochester 1960* (Eds E C G Sudarshan, J H Tinlot, A C Melissionos) (New York: Interscience Publ., 1960) p. 579
71. Balkanov V A et al. (BAIKAL Collab.) *Yad. Fiz.* **63** 1027 (2000) [*Phys. At. Nucl.* **63** 951 (2000)]; astro-ph/0001151
72. Ahrens J et al. (AMANDA Collab.) *Phys. Rev. Lett.* **90** 251101 (2003); astro-ph/0303218
73. Aggouras G et al. (NESTOR Collab.) *Astropart. Phys.* **23** 377 (2005)
74. Montaruli T (for the ANTARES Collab.) *Acta Phys. Polon. B* **36** 509 (2005); hep-ex/0410079
75. Ahrens J et al. (IceCube Collab.) *Astropart. Phys.* **20** 507 (2004); astro-ph/0305196
76. Kravchenko I et al. *Astropart. Phys.* **20** 195 (2003); astro-ph/0206371
77. Lehtinen N G et al. *Phys. Rev. D* **69** 013008 (2004); astro-ph/0309656
78. Gorham P et al. *Nucl. Instrum. Meth. A* **490** 476 (2002); hep-ex/0108027
79. Gorham P W et al. *Phys. Rev. Lett.* **93** 041101 (2004); astro-ph/0310232
80. Miocinovic P et al., in *22nd Texas Symp. on Relativistic Astrophysics at Stanford, Palo Alto, 13–17 December 2004*, TSRA04-2516; astro-ph/0503304
81. Gusev G A et al. *Kosmich. Issled.* **44** (1) 22 (2006) [*Cosmic Res.* **44** 19 (2006)]
82. Gusev G A et al. *Dokl. Ross. Akad. Nauk* **406** 327 (2006) [*Dokl. Phys.* **51** 22 (2006)]
83. Sasaki M, Asaoka Y, Jobashi M *Astropart. Phys.* **19** 37 (2003); astro-ph/0204167
84. Cronin J W *Nucl. Phys. B*: *Proc. Suppl.* **138** 465 (2005); astro-ph/0402487
85. Teshima M, Lipari P, Santangelo A, in *Proc. of the 28th Intern. Cosmic Ray Conf., ICRC, Tsukuba, Japan, 2003*, p. 1069; http://www-rccn.icrr.u-tokyo.ac.jp/icrc2003/PROCEEDINGS/PDF/268.pdf
86. Stecker F W et al. *Nucl. Phys. B*: *Proc. Suppl.* **136** 433 (2004); astro-ph/0408162
87. Dicus D A, Repko W W *Phys. Rev. Lett.* **79** 569 (1997); hep-ph/9703210
88. Massó E, Rota F *Phys. Lett. B* **488** 326 (2000); hep-ph/0006228
89. Seckel D *Phys. Rev. Lett.* **80** 900 (1998); hep-ph/9709290
90. Bhattacharjee P, Sigl G *Phys. Rep.* **327** 109 (2000); astro-ph/9811011
91. Abbasabadi A et al. *Phys. Rev. D* **59** 013012 (1999); hep-ph/9808211
92. Yoshida S et al. *Astrophys. J.* **479** 547 (1997); astro-ph/9608186
93. Enqvist K, Kainulainen K, Maalampi J *Nucl. Phys. B* **317** 647 (1989)
94. Dolgov A D *Phys. Rep.* **370** 333 (2002); hep-ph/0202122
95. Dicus D A, Kovner K, Repco W W *Phys. Rev. D* **62** 053013 (2000); hep-ph/0003152
96. Goyal A, Gupta A, Mahajan N *Phys. Rev. D* **63** 043003 (2001); hep-ph/0005030
97. 'Review of Particle Physics' *Eur. Phys. J. C* **15** 266 (2000)
98. Päs H, Weiler T J *Phys. Rev. D* **63** 113015 (2001); hep-ph/0101091
99. Fodor Z, Katz S D, Ringwald A *Phys. Rev. Lett.* **88** 171101 (2002); hep-ph/0105064
100. Fodor Z, Katz S, Ringwald A *J. High Energy Phys.* (JHEP06) 046 (2002); hep-ph/0203198
101. Gelmini G, Varieschi G, Weiler T *Phys. Rev. D* **70** 113005 (2004); hep-ph/0404272
102. Eberle B et al. *Phys. Rev. D* **70** 023007 (2004); hep-ph/0401203
103. Barenboim G, Mena Requejo O, Quigg C *Phys. Rev. D* **71** 083002 (2005); hep-ph/0412122
104. Blanco-Pillado J J, Vázquez R A, Zas E *Phys. Rev. D* **61** 123003 (2000); astro-ph/9902266
105. Yoshida S, Sigl G, Lee S *Phys. Rev. Lett.* **81** 5505 (1998); hep-ph/9808324
106. Kalashev O E et al. *Phys. Rev. D* **65** 103003 (2002); hep-ph/0112351
107. Kalashev O E et al. *Phys. Rev. D* **66** 063004 (2002); hep-ph/0205050
108. Singh S, Ma C-P *Phys. Rev. D* **67** 023506 (2003); astro-ph/0208419
109. Ringwald A, Wong Y Y Y *J. Cosmol. Astropart. Phys.* (JCAP12) 005 (2004); hep-ph/0408241
110. McKellar B H J et al., in *Proc. of Intern. Europhysics Conf. on High Energy Physics, Budapest, Hungary, July 12–18, 2001*; hep-ph/0106123
111. Gelmini G, Kusenko A *Phys. Rev. Lett.* **82** 5202 (1999); hep-ph/9902354
112. Gelmini G, Kusenko A *Phys. Rev. Lett.* **84** 1378 (2000); hep-ph/9908276
113. Sreekumar P et al. *Astrophys. J.* **494** 523 (1998); astro-ph/9709257
114. Protheroe P J, Johnson P A *Astropart. Phys.* **4** 253 (1996); astro-ph/9506119
115. Stanev T et al. *Phys. Rev. D* **62** 093005 (2000); astro-ph/0003484
116. Fodor Z et al. *J. Cosmol. Astropart. Phys.* (JCAP11) 015 (2003); hep-ph/0309171
117. Semikoz D V, Sigl G *J. Cosmol. Astropart. Phys.* (JCAP04) 003 (2004); hep-ph/0309328
118. Stanev T *Phys. Lett. B* **595** 50 (2004); astro-ph/0404535
119. Bugaev E V, Misaki A, Mitsui K *Astropart. Phys.* **24** 345 (2005); astro-ph/0405109
120. Bilenky S, Giunti C, Grimus W *Phys. Rev. D* **58** 033001 (1998); hep-ph/9712537
121. Lunardini C, Smirnov A Yu *Nucl. Phys. B* **583** 260 (2000); hep-ph/0002152
122. Fukuda Y et al. (Super-Kamiokande Collab.) *Phys. Rev. Lett.* **81** 1562 (1998); hep-ex/9807003
123. Fukuda S et al. (Super-Kamiokande Collab.) *Phys. Rev. Lett.* **85** 3999 (2000); hep-ex/0009001
124. Ashie Y et al. (Super-Kamiokande Collab.) *Phys. Rev. Lett.* **93** 101801 (2004); hep-ex/0404034
125. Ashie Y et al. (Super-Kamiokande Collab.) *Phys. Rev. D* **71** 112005 (2005); hep-ex/0501064
126. Aliu E et al. (K2K Collab.) *Phys. Rev. Lett.* **94** 081802 (2005); hep-ex/0411038
127. Apollonio M et al. *Eur. Phys. J. C* **27** 331 (2003); hep-ex/0301017
128. Berezinsky V, Narayan M, Vissani F *Nucl. Phys. B* **658** 254 (2003); hep-ph/0210204
129. Keränen P et al. *Phys. Lett. B* **574** 162 (2003); hep-ph/0307041
130. Beacom J F et al. *Phys. Rev. Lett.* **92** 011101 (2004); hep-ph/0307151
131. Horvat R *Phys. Rev. D* **64** 067302 (2001); hep-ph/0103200
132. Farzan Y, Smirnov A Yu *Phys. Rev. D* **65** 113001 (2002); hep-ph/0201105
133. Beacom J F, Bell N F *Phys. Rev. D* **65** 113009 (2002); hep-ph/0204111
134. Beacom J F et al. *Phys. Rev. Lett.* **90** 181301 (2003); hep-ph/0211305
135. Beacom J F et al. *Phys. Rev. D* **69** 017303 (2004); hep-ph/0309267
136. Barenboim G et al. *J. High Energy Phys.* (JHEP10) 001 (2002); hep-ph/0108199
137. Barenboim G, Borissov L, Lykken J *Phys. Lett. B* **534** 106 (2002); hep-ph/0201080

138. Barenboim G, Lykken J *Phys. Lett. B* **554** 73 (2003); hep-ph/0210411
139. Barenboim G, Quigg C *Phys. Rev. D* **67** 073024 (2003); hep-ph/0301220
140. Kashti T, Waxman E *Phys. Rev. Lett.* **95** 181101 (2005); astro-ph/0507599
141. Beacom J F et al. *Phys. Rev. D* **68** 093005 (2003); hep-ph/0307025
142. Waxman E, Bahcall J *Phys. Rev. D* **59** 023002 (1999); hep-ph/9807282
143. Waxman E, Bahcall J *Phys. Rev. D* **64** 023002 (2001); hep-ph/9902383
144. Ahlers M et al. *Phys. Rev. D* **72** 023001 (2005); astro-ph/0503229
145. Mannheim K, Protheroe R J, Rachen J P *Phys. Rev. D* **63** 023003 (2001); astro-ph/9812398
146. Rachen J P, Protheroe R J, Mannheim K, in *19th Texas Symp. on Relativistic Astrophysics and Cosmology, Paris, France, 14–18 December, 1998*; *Nucl. Phys. B*: *Proc. Suppl.* **80** 240 (2000); astro-ph/9908031
147. Mannheim K *J. Phys. G*: *Nucl. Part. Phys.* **27** 1691 (2001); astro-ph/0104165
148. Piran T *Phys. Rep.* **314** 575 (1999)
149. Zhang B, Mészáros P *Int. J. Mod. Phys. A* **19** 2385 (2004); astro-ph/0311321
150. Atkins R et al. (Milagro Collab.) *Astrophys. J.* **604** L25 (2004); astro-ph/0311389
151. Waxman E *Phys. Rev. Lett.* **75** 386 (1995); astro-ph/9505082
152. Vietri M *Astrophys. J.* **453** 883 (1995); astro-ph/9506081
153. Waxman E, Bahcall J *Phys. Rev. Lett.* **78** 2292 (1997); astro-ph/9701231
154. Waxman E *Astrophys. J.* **452** L1 (1995); astro-ph/9508037
155. Vietri M, De Marco D, Guetta D *Astrophys. J.* **592** 378 (2003); astro-ph/0302144
156. Halzen F, Zas E *Astrophys. J.* **488** 669 (1997); astro-ph/9702193
157. Waxman E *Nucl. Phys. B*: *Proc. Suppl.* **118** 353 (2003); astro-ph/0211358
158. Vietri M *Phys. Rev. Lett.* **80** 3690 (1998); astro-ph/9802241
159. Waxman E, Bahcall J N *Astrophys. J.* **541** 707 (2000); hep-ph/9909286
160. Paczynski B *Astrophys. J.* **494** L45 (1998)
161. MacFadyen A I, Woodsley S E *Astrophys. J.* **524** 262 (1999); astro-ph/9810274
162. Vietri M, Stella L *Astrophys. J.* **507** L45 (1998); astro-ph/9808355
163. Mészáros P, Waxman E *Phys. Rev. Lett.* **87** 171102 (2001); astro-ph/0103275
164. Granot J, Guetta D *Phys. Rev. Lett.* **90** 191102 (2003); astro-ph/0211433
165. Razzaque S, Mészáros P, Waxman E *Phys. Rev. Lett.* **90** 241103 (2003); astro-ph/0212536
166. Razzaque S, Mészáros P, Waxman E *Phys. Rev. D* **69** 023001 (2004); astro-ph/0308239
167. Dermer C D, Atoyan A *Phys. Rev. Lett.* **91** 071102 (2003); astro-ph/0301030
168. Halzen F, Hooper D W *Astrophys. J. Lett.* **527** L93 (1999); astro-ph/9908138
169. Alvarez-Muñiz J, Halzen F, Hooper D W *Phys. Rev. D* **62** 093015 (2000); astro-ph/0006027
170. Guetta D et al. *Astropart. Phys.* **20** 429 (2004); astro-ph/0302524
171. Alvarez-Muñiz J, Halzen F, Hooper D *Astrophys. J.* **604** L85 (2004); astro-ph/0310417
172. Wick S D, Dermer C D, Atoyan A *Astropart. Phys.* **21** 125 (2004); astro-ph/0310667
173. Sreekumar P et al. *Astropart. Phys.* **11** 221 (1999); astro-ph/9901277
174. Tavecchio F et al. *Astrophys. J.* **575** 137 (2002); astro-ph/0207157
175. Aharonian F et al. (HEGRA Collab.) *Astron. Astrophys.* **421** 529 (2004); astro-ph/0401301
176. Horan D et al. (VERITAS Collab.) *Astrophys. J.* **603** 51 (2004); astro-ph/0311397
177. Falcone A D et al. (VERITAS Collab.) *Astrophys. J.* **613** 710 (2004); astro-ph/0408365
178. Aharonian F et al. (H.E.S.S. Collab.) *Astron. Astrophys.* **441** 465 (2005); astro-ph/0507207
179. Stecker F W et al. *Phys. Rev. Lett.* **66** 2697 (1991)
180. Stecker F W, Salamon M H *Space Sci. Rev.* **75** 341 (1996); astro-ph/9501064
181. Stecker F W *Phys. Rev. D* **72** 107301 (2005); astro-ph/0510537
182. Mannheim K *Astron. Astrophys.* **269** 67 (1993); astro-ph/9302006
183. Mannheim K *Astropart. Phys.* **3** 295 (1995)
184. Protheroe R J, in *Accretion Phenomena and Related Out Flows*: *IAU Colloq. 163* (Astron. Soc. of the Pacific Conf. Ser., Vol. 121, Eds D T Wickramasinghe, G V Bicknell, L Ferrario) (San Francisco, Calif.: Astron. Soc. of the Pacific, 1997) p. 585; astro-ph/9607165
185. Mücke A, Protheroe R J *Astropart. Phys.* **15** 121 (2001); astro-ph/0004052
186. Bednarek W, Burgio G F, Montaruli T *New Astron. Rev.* **49** 1 (2005); astro-ph/0404534
187. Waxman E, Loeb A *Phys. Rev. Lett.* **87** 071101 (2001); astro-ph/0102317
188. Aharonian F A et al. (HEGRA Collab.) *Astrophys. J.* **539** 317 (2000); astro-ph/0003182
189. Atkins R et al. (Milagro Collab.) *Astrophys. J.* **595** 803 (2003); astro-ph/0305308
190. Aharonian F et al. (HEGRA Collab.) *Astron. Astrophys.* **370** 112 (2001); astro-ph/0102391
191. Enomoto R et al. (CANGAROO-II Collab.) *Nature* **416** 823 (2002); astro-ph/0204422
192. Enomoto R et al. (CANGAROO-II Collab.) *Astrophys. J.* **591** L25 (2003); astro-ph/0304356
193. Alvarez-Muñiz J, Halzen F *Astrophys. J.* **576** L33 (2002); astro-ph/0205408
194. Zhang B et al. *Astrophys. J.* **595** 346 (2003); astro-ph/0210382
195. Anchordoqui L A et al. *Astrophys. J.* **589** 481 (2003); hep-ph/0211231
196. Levinson A, Waxman E *Phys. Rev. Lett.* **87** 171101 (2001); hep-ph/0106102
197. Distefano C et al. *Astrophys. J.* **575** 378 (2002); astro-ph/0202200
198. Itoh C et al. *Astron. Astrophys.* **402** 443 (2003); astro-ph/0304295
199. Romero G E, Torres D F *Astrophys. J.* **586** L33 (2003); astro-ph/0302149
200. Sigl G, Schramm D N, Bhattacharjee P *Astropart. Phys.* **2** 401 (1994); astro-ph/9403039
201. Brandenberger R et al. *Phys. Rev. D* **54** 6059 (1996); hep-ph/9605382
202. Martins C J A P, Shellard E P S *Phys. Lett. B* **445** 43 (1998); hep-ph/9806480
203. Berezinsky V, Vilenkin A *Phys. Rev. D* **62** 083512 (2000); hep-ph/9908257
204. Chung D J H, Kolb E W, Riotto A *Phys. Rev. Lett.* **81** 4048 (1998); hep-ph/9805473
205. Chung D J H, Kolb E W, Riotto A *Phys. Rev. D* **59** 023501 (1999); hep-ph/9802238;
206. Chung D J H, Kolb E W, Riotto A *Phys. Rev. D* **60** 063504 (1999); hep-ph/9809453
207. Blasi P, Dick R, Kolb R W *Astropart. Phys.* **18** 57 (2002); astro-ph/0105232
208. Albuquerque I F M, Hui L, Kolb E W *Phys. Rev. D* **64** 083504 (2001); hep-ph/0009017
209. Hill C T *Nucl. Phys. B* **224** 469 (1983)
210. Birkel M, Sarkar S *Astropart. Phys.* **9** 297 (1998); hep-ph/9804285
211. Gribov V N, Lipatov L N *Yad. Fiz.* **15** 781 (1972) [*Sov. J. Nucl. Phys.* **15** 438 (1972)]
212. Altarelli G, Parisi G *Nucl. Phys. B* **126** 298 (1977)
213. Dokshitser Yu L *Zh. Eksp. Theor. Fiz.* **73** 1216 (1977) [*Sov. Phys. JETP* **46** 641 (1977)]
214. Berezinsky V, Kachelrieß M, Vilenkin A *Phys. Rev. Lett.* **79** 4302 (1997); astro-ph/9708217
215. Barbot C et al. *Phys. Lett. B* **555** 22 (2003); hep-ph/0205230
216. Sigl G et al. *Phys. Rev. D* **59** 043504 (1999); hep-ph/9809242
217. Berezinsky V, Kachelriess M *Phys. Rev. D* **63** 034007 (2001); hep-ph/0009053
218. Aloisio R, Berezinsky V, Kachelriess M *Phys. Rev. D* **69** 094023 (2004); hep-ph/0307279
219. Gaisser T K *Cosmic Rays and Particle Physics* (Cambridge: Cambridge Univ. Press, 1990)
220. Gaisser T K et al. *Phys. Rev. D* **54** 5578 (1996)
221. Gaisser T K, Honda M *Annu. Rev. Nucl. Part. Sci.* **52** 153 (2002); hep-ph/0203272

222. Barr G, Gaisser T K, Stanev T *Phys. Rev. D* **39** 3532 (1989)
223. Volkova L V *Yad. Fiz.* **31** 1510 (1980) [*Sov. J. Nucl. Phys.* **31** 784 (1980)]
224. Gelmini G, Gondolo P, Varieschi G *Phys. Rev. D* **61** 056011 (2000); hep-ph/9905377
225. Gelmini G, Gondolo P, Varieschi G *Phys. Rev. D* **63** 036006 (2001); hep-ph/0003307
226. Pasquali L, Reno M H, Sarcevic I *Astropart. Phys.* **9** 193 (1998); hep-ph/9710363
227. Pasquali L, Reno M H, Sarcevic I *Phys. Rev. D* **59** 034020 (1999); hep-ph/9806428
228. Martin A D, Ryskin M G, Stasto A M *Acta Phys. Polon. B* **34** 3273 (2003); hep-ph/0302140
229. Stasto A M *Int. J. Mod. Phys. A* **19** 317 (2004); astro-ph/0310636
230. Volkova L V, Zatsepin G T *Yad. Fiz.* **64** 313 (2001) [*Phys. At. Nucl.* **64** 266 (2001)]
231. Beacom J F, Candia J *J. Cosmol. Astropart. Phys.* (JCAP11) 009 (2004); hep-ph/0409046
232. Llewellyn Smith C H *Phys. Rep.* **3** 261 (1972)
233. Martin A D, Stirling W J, Roberts R G *Phys. Lett. B* **354** 155 (1995)
234. Martin A D et al. *Eur. Phys. J. C* **28** 455 (2003); hep-ph/0211080
235. Martin A D et al. *Eur. Phys. J. C* **35** 325 (2004); hep-ph/0308087
236. Martin A D et al. *Phys. Lett. B* **604** 61 (2004); hep-ph/0410230
237. Martin A D et al. *Eur. Phys. J. C* **39** 155 (2005); hep-ph/0411040
238. Lai H L et al. *Phys. Rev. D* **51** 4763 (1995); hep-ph/9410404
239. Lai H L et al. *Phys. Rev. D* **55** 1280 (1997); hep-ph/9606399
240. Lai H L et al. *Eur. Phys. J. C* **12** 375 (2000); hep-ph/9903282
241. Pumplin J et al. *J. High Energy Phys.* (JHEP07) 012 (2002); hep-ph/0201195
242. Stump D et al. *J. High Energy Phys.* (JHEP10) 046 (2003); hep-ph/0303013
243. Kretzer S et al. *Phys. Rev. D* **69** 114005 (2004); hep-ph/0307022
244. Fadin V S, Kuraev E A, Lipatov L N *Phys. Lett. B* **60** 50 (1975)
245. Balitsky YaYa, Lipatov L N *Yad. Fiz.* **28** 1597 (1978) [*Sov. J. Nucl. Phys.* **28** 822 (1978)]
246. Kretzer S, Reno M H *Phys. Rev. D* **66** 113007 (2002); hep-ph/0208187
247. Gribov L V, Levin E M, Ryskin M G *Phys. Rep.* **100** 1 (1983)
248. Jalilian-Marian J *Phys. Rev. D* **68** 054005 (2003); hep-ph/0301238
249. Balitsky I *Nucl. Phys. B* **463** 99 (1996); hep-ph/9509348
250. Kovchegov Yu V *Phys. Rev. D* **61** 074018 (2000); hep-ph/9905214
251. Kutak K, Stasto A M *Eur. Phys. J. C* **41** 343 (2005); hep-ph/0408117
252. Stasto A M *Acta Phys. Polon. B* **35** 3069 (2004); hep-ph/0412084
253. Golec-Biernat K, Wüsthoff M *Phys. Rev. D* **59** 014017 (1999); hep-ph/9807513
254. Golec-Biernat K, Wüsthoff M *Phys. Rev. D* **60** 114023 (1999); hep-ph/9903358
255. Iancu E, Itakura K, Munier S *Phys. Lett. B* **590** 199 (2004); hep-ph/0310338
256. Bartels J, Golec-Biernat K, Kowalski H *Phys. Rev. D* **66** 014001 (2002); hep-ph/0203258
257. Machado M V T *Phys. Rev. D* **70** 053008 (2004); hep-ph/0311281
258. Machado M V T *Phys. Rev. D* **71** 114009 (2005); hep-ph/0503058
259. Ringwald A *Phys. Lett. B* **555** 227 (2003); hep-ph/0212099
260. Khoze V V, Ringwald A *Phys. Lett. B* **259** 106 (1991)
261. Fodor Z et al. *Phys. Lett. B* **561** 191 (2003); hep-ph/0303080
262. Adloff C et al. (H1 Collab.) *Eur. Phys. J. C* **25** 495 (2002); hep-ex/0205078
263. Chekanov S et al. (ZEUS Collab.) *Eur. Phys. J. C* **34** 255 (2004); hep-ex/0312048
264. Rubakov V A, Shaposhnikov M E *Usp. Fiz. Nauk* **166** 493 (1996) [*Phys. Usp.* **39** 461 (1996)]
265. Bezrukov F et al. *Phys. Lett. B* **574** 75 (2003); hep-ph/0305300
266. Bezrukov F et al. *Phys. Rev. D* **68** 036005 (2003); hep-ph/0304180
267. Han T, Hooper D *Phys. Lett. B* **582** 21 (2004); hep-ph/0307120
268. Carena M et al. *Phys. Rev. D* **58** 095003 (1998); hep-ph/9804380
269. Doncheski M A, Robinett R W *Phys. Rev. D* **56** 7412 (1997); hep-ph/9707328
270. Bordes J et al. *Astropart. Phys.* **8** 135 (1998); astro-ph/9707031
271. Han T, Lykken J D, Zhang R-J *Phys. Rev. D* **59** 105006 (1999); hep-ph/9811350
272. Benakli K *Phys. Rev. D* **60** 104002 (1999); hep-ph/9809582
273. Klein O *Z. Phys.* **37** 895 (1926)
274. Witten E *Nucl. Phys. B* **471** 135 (1996); hep-th/9602070
275. Lykken J D *Phys. Rev. D* **54** R3693 (1996); hep-th/9603133
276. Antoniadis I, Dimopoulos S, Dvali G *Nucl. Phys. B* **516** 70 (1998); hep-ph/9710204
277. Dienes K R, Dudas E, Gherghetta T *Phys. Lett. B* **436** 55 (1998); hep-ph/9803466
278. Domokos G, Kovesi-Domokos S *Phys. Rev. Lett.* **82** 1366 (1999); hep-ph/9812260
279. Domokos G et al. *J. High Energy Phys.* (JHEP07) 017 (2001); hep-ph/0011156
280. Giudice G F, Rattazzi R, Wells J D *Nucl. Phys. B* **544** 3 (1999); hep-ph/9811291
281. Cullen S, Perelstein M, Peskin M E *Phys. Rev. D* **62** 055012 (2000); hep-ph/0001166
282. Nussinov S, Shrock R *Phys. Rev. D* **59** 105002 (1999); hep-ph/9811323
283. Nussinov S, Shrock R *Phys. Rev. D* **64** 047702 (2001); hep-ph/0103043
284. Jain A et al. *Int. J. Mod. Phys. A* **17** 533 (2002); hep-ph/0011310
285. Tyler C, Olinto A V, Sigl G *Phys. Rev. D* **63** 055001 (2001); hep-ph/0002257
286. Alvarez-Muñiz J et al. *Phys. Rev. Lett.* **88** 021301 (2002); hep-ph/0107057
287. Anchordoqui L A et al. *Phys. Rev. D* **65** 124027 (2002); hep-ph/0112247
288. Antoniadis I et al. *Phys. Lett. B* **436** 257 (1998); hep-ph/9804398
289. Antoniadis I, Dimopoulos S, Giveon A *J. High Energy Phys.* (JHEP05) 055 (2001); hep-th/0103033
290. Veneziano G *Nuovo Cimento A* **57** 190 (1968)
291. Cornet F, Illana J I, Masip M *Phys. Rev. Lett.* **86** 4235 (2001); hep-ph/0102065
292. Friess J J, Han T, Hooper D *Phys. Lett. B* **547** 31 (2002); hep-ph/0204112
293. Anchordoqui L A, Goldberg H, Shapere A D *Phys. Rev. D* **66** 024033 (2002); hep-ph/0204228
294. Giddings S B, Thomas S *Phys. Rev. D* **65** 056010 (2002); hep-ph/0106219
295. Kanti P *Int. J. Mod. Phys. A* **19** 4899 (2004); hep-ph/0402168
296. Emparan R, Masip M, Rattazzi R *Phys. Rev. D* **65** 064023 (2002); hep-ph/0109287
297. Eardley D M, Giddings S B *Phys. Rev. D* **66** 044011 (2002); gr-qc/0201034
298. Yoshino H, Nambu Y *Phys. Rev. D* **67** 024009 (2003); gr-qc/0209003
299. Anchordoqui L A et al. *Phys. Lett. B* **594** 363 (2004); hep-ph/0311365
300. Cheung K, Chou C-H *Phys. Rev. D* **66** 036008 (2002); hep-ph/0205284
301. Cavaglia M *Int. J. Mod. Phys. A* **18** 1843 (2003); hep-ph/0210296
302. Lykken J, Nandi S *Phys. Lett. B* **485** 224 (2000); hep-ph/9908505
303. Anchordoqui L A, Feng J L, Goldberg H *Phys. Lett. B* **535** 302 (2002); hep-ph/0202124
304. Volkova L V, Zatsepin G T *Izv. Akad. Nauk SSSR, Ser. Fiz.* **38** 1060 (1974)
305. Berezinsky V S et al. *Yad. Fiz.* **43** 637 (1986)
306. Naumov V A, Perrone L *Astropart. Phys.* **10** 239 (1999); hep-ph/9804301
307. Iyer S, Reno M H, Sarcevic I *Phys. Rev. D* **61** 053003 (2000); hep-ph/9909393
308. Iyer Dutta S, Reno M H, Sarcevic I *Phys. Rev. D* **62** 123001 (2000); hep-ph/0005310
309. Iyer Dutta S et al. *Phys. Rev. D* **63** 094020 (2001); hep-ph/0012350
310. Jones J et al. *Phys. Rev. D* **69** 033004 (2004); hep-ph/0308042
311. Jones J et al. *Int. J. Mod. Phys. A* **20** 1204 (2005); hep-ph/0408060
312. Yoshida S, Ishibashi R, Miyamoto H *Phys. Rev. D* **69** 103004 (2004); astro-ph/0312078
313. Bugaev E et al. *Astropart. Phys.* **21** 491 (2004); hep-ph/0312295
314. Beacom J F, Crotty P, Kolb E W *Phys. Rev. D* **66** 021302 (2002); astro-ph/0111482
315. Halzen F, Saltzberg D *Phys. Rev. Lett.* **81** 4305 (1998); hep-ph/9804354
316. Iyer Dutta S, Reno M H, Sarcevic I *Phys. Rev. D* **66** 077302 (2002); hep-ph/0207344

317. Athar H, Parente G, Zas E *Phys. Rev. D* **62** 093010 (2000); hep-ph/0006123
318. Iyer Dutta S, Huang Y, Reno M H *Phys. Rev. D* **72** 013005 (2005); hep-ph/0504208
319. Aynutdinov V et al. (BAIKAL Collab.) *Astropart. Phys.* **25** 140 (2006); astro-ph/0508675
320. Aguilar J A et al. (The ANTARES Collab.) *Astropart. Phys.* **23** 131 (2005); astro-ph/0412126
321. The IceCube Collab. "The IceCube Collaboration: Contributions to the 29th Intern. Cosmic Ray Conf. (ICRC 2005), Pune, India, Aug. 2005", astro-ph/0509330
322. Learned J G, Pakvasa S *Astropart. Phys.* **3** 267 (1995); hep-ph/9405296
323. Berezinsky V S, Smirnov A Yu *Astrophys. Space Sci.* **32** 461 (1975)
324. Fargion D *Astrophys. J.* **570** 909 (2002); astro-ph/0002453
325. Feng J L et al. *Phys. Rev. Lett.* **88** 161102 (2002); hep-ph/0105067
326. Fargion D et al. *Astrophys. J.* **613** 1285 (2004); hep-ph/0305128
327. Aramo C et al. *Astropart. Phys.* **23** 65 (2005); astro-ph/0407638
328. Fargion D et al. *Nucl. Phys. B*: *Proc. Suppl.* **136** 119 (2004); astro-ph/0409460
329. Cao Z et al. *J. Phys. G*: *Nucl. Part. Phys.* **31** 571 (2005); astro-ph/0411677
330. Iyer Dutta S, Reno M H, Sarcevic I *Phys. Rev. D* **64** 113015 (2001); hep-ph/0104275
331. Askar'yan G A *Zh. Eksp. Theor. Fiz.* **41** 616 (1961) [*Sov. Phys. JETP* **14** 441 (1962)]
332. Askar'yan G A *Zh. Eksp. Theor. Fiz.* **48** 988 (1965) [*Sov. Phys. JETP* **21** 658 (1965)]
333. Zas E, Halzen F, Stanev T *Phys. Rev. D* **45** 362 (1992)
334. Alvarez-Muñiz J, Vázquez R A, Zas E *Phys. Rev. D* **61** 023001 (2000); astro-ph/9901278
335. Alvarez-Muñiz J, Vázquez R A, Zas E *Phys. Rev. D* **62** 063001 (2000); astro-ph/0003315
336. Saltzberg D et al. *Phys. Rev. Lett.* **86** 2802 (2001); hep-ex/0011001
337. Gorham P W et al. *Phys. Rev. D* **72** 023002 (2005); astro-ph/0412128
338. Scholten O et al. *Astropart. Phys.* (submitted); astro-ph/0508580
339. Anchordoqui L A et al. *Phys. Rev. D* **66** 103002 (2002); hep-ph/0207139
340. Anchordoqui L A et al. *J. Cosmol. Astropart. Phys.* (JCAP06) 013 (2005); hep-ph/0410136
341. Kusenko A, Weiler T J *Phys. Rev. Lett.* **88** 161101 (2002); hep-ph/0106071
342. Hooper D *Phys. Rev. D* **65** 097303 (2002); hep-ph/0203239
343. Anchordoqui L A et al. *Phys. Rev. D* **68** 104025 (2003); hep-ph/0307228
344. Ahn E-J, Cavaglià M, Olinto A V *Phys. Lett. B* **551** 1 (2003); hep-th/0201042
345. Ahn E-J et al. *Phys. Rev. D* **68** 043004 (2003); hep-ph/0306008
346. Illana J I, Masip M, Meloni D *Phys. Rev. Lett.* **93** 151102 (2004); hep-ph/0402279
347. Hussain S, McKay D W *Phys. Lett. B* **634** 130 (2006); hep-ph/0510083
348. Jain P et al. *Phys. Rev. D* **66** 065018 (2002); hep-ph/0205052
349. Hussain S, McKay D W *Phys. Rev. D* **69** 085004 (2004); hep-ph/0310091
350. Saltzberg D, in *Proc. of Nobel Symp. 129* (*Neutrino Physics*); *Phys. Scripta* **T121** 119 (2005); astro-ph/0501364
351. Barwick S W et al. (ANITA Collab.) *Phys. Rev. Lett.* **96** 171101 (2006); astro-ph/0512265
352. Ringwald A, in *Acoustic and Radio EeV Neutrino Detection Activities, DESY, Zeuthen, Germany, 17–19 May 2005* (Eds R Nahnhauer, S Böser) (Singapore: World Scientific, 2006) p. 12; hep-ph/0510341